Journal of Environmental Chemical Engineering 13 (2025) 116921

Contents lists available at ScienceDirect

Journal of Environmental Chemical Engineering

journal homepage: www.elsevier.com/locate/jece

Sustainable green synthesis of metallic nanoparticle using plants and microorganisms: A review of biosynthesis methods, mechanisms, toxicity, and applications

Beatriz Cardoso [a,*], Glauco Nobrega [a,b], Inês S. Afonso [a,b,c], João E. Ribeiro [b,d], Rui A. Lima [a,e,f]

[a] Mechanical Engineering and Resource Sustainability Center (MEtRICs), Mechanical Engineering Department, University of Minho, Campus de Azurém, Guimarães 4800-058, Portugal
[b] Centro de Investigação de Montanha (CIMO), Instituto Politécnico de Bragança, Campus de Santa, Apolónia, Bragança 5300253, Portugal
[c] International Iberian Nanotechnology Laboratory, Braga 4715-330, Portugal
[d] Instituto Politécnico de Bragança, Campus de Santa Apolónia, Bragança 5300-253, Portugal
[e] Transport Phenomena Research Center (CEFT), Faculdade de Engenharia da Universidade do Porto (FEUP), Rua Roberto Frias, Porto 4200-465, Portugal
[f] Faculty of Engineering, Associate Laboratory in Chemical Engineering (ALiCE), University of Porto, Porto 4200-465, Portugal

ARTICLE INFO

Keywords:
Green-synthesis
Metallic nanoparticles
Green chemistry
Biosynthesis
Biore- duction

ABSTRACT

Green synthesis provides a sustainable approach to producing metallic nanoparticles (MNPs) using biological entities such as plants, algae, bacteria, yeast, and fungi. While extensive research has explored these biosynthetic processes, an integrated review is needed to systematically consolidate knowledge on biosynthesis mechanisms, key synthesis parameters, and the comparative advantages and limitations of green versus chemical synthesis methods. This review addresses these gaps by examining the roles of biological entities and their metabolites in reducing and stabilizing MNPs. Plants use polyphenols and sugars to reduce metal ions, while algae utilize compounds such as chlorophylls and carotenoids. Bacteria produce enzymes like nitrate reductase to reduce metal ions inside and outside the cell. Yeast, for instance, employs nitrate reductase for extracellular synthesis and metallothioneins for intracellular synthesis while fungi use enzymes like laccase and reductase to reduce metal ions and stabilize MNPs. It also examines how reaction factors—such as solvent type, pH, precursor concentration, and temperature—affect size, shape, and stability. The comparative analysis highlights the structural, functional, and environmental differences between green and chemical synthesis, emphasizing that green-synthesized MNPs exhibit improved biocompatibility and biological activity. While green synthesis avoids toxic chemicals and harsh conditions, reducing environmental impact, it may result in broader size distributions and less precise shape control compared to chemical methods. This review also addresses current limitations, including batch variability, differences in biological extracts, and challenges in maintaining consistent MNP properties. It emphasizes the need for advanced characterization techniques for reproducibility and quality control, proposing solutions such as bioprocess engineering, real-time monitoring, and lifecycle assessments to improve industrial scalability. In summary, this review provides a comprehensive resource for researchers and industries seeking to use green synthesis for sustainable, large-scale applications in medical, environmental, and biotechnological fields, supporting global sustainability goals and green chemistry principles.

1. Introduction

Nanoparticles (NPs) are an assorted class of materials represented by particulate substances whose, according to the International Organization for Standardization, all three cartesian dimensions are less than 100 nm. The literature demonstrates several types of NPs, including metal [1–4], lipid-based [5–8], carbon-based [9–11], ceramics [12–14], and polymeric [15–17]. The NPs' different shapes, sizes, and compositions confers these nanomaterials with unique properties that can be exploited for various applications. As a result, several industries benefit from nanotechnology, particularly from metallic NPs (MNPs), including the medical, electronics, agricultural, and environmental sectors.

There are several well-established techniques widely described in the literature for the synthesis of MNPs, which can generally be classified into three main approaches: chemical, physical, and green synthesis

* Corresponding author.
E-mail address: b13510@uminho.pt (B. Cardoso).

https://doi.org/10.1016/j.jece.2025.116921
Received 14 October 2024; Received in revised form 19 April 2025; Accepted 2 May 2025
Available online 6 May 2025

Nomenclature

99mTc	Technetium-99m
$AgNO_3$	Silver Nitrate
ALP	Alkaline Phosphatase
ALT	Alanine Aminotransferase
AST	Aspartate Aminotransferase
Au_0	Neutral Gold Atom
B.W.	Body Weight
BHI	Brain Heart Infusion
BNPs	Bimetallic Nanoparticles
$CdCl_2$	Cadmium Chloride
CdO	Cadmium Oxide
CdS	Cadmium Sulfide
C_m	Cystoseira myrica
C_p	Caulerpa prolifera
Cr(VI)	Hexavalent Chromium
Ct	Cystoseira trinodis
CuO	Copper Oxide
DPPH	2,2-Diphenyl-1-Picrylhydrazyl
e^-	Electron
eV	Electron Volt
DLS	Dynamic Light Scattering
Fe_3O_4	Magnetite
FeO	Iron(II) Oxide
FTIR	Fourier-Transform Infrared Spectroscopy
g	Gram
GO	Graphene Oxide
$HAuCl_4$	Tetrachloroaurate
h	Hour
HeLa	Human Cervical Carcinoma Cells
IC_{50}	Half Maximal Inhibitory Concentration
L	Liter
LD_{50}	Median Lethal Dose
mL	Milliliter
MIC	Minimum Inhibitory Concentration
MNPs	Metallic Nanoparticles
$NADP^+$	Nicotinamide Adenine Dinucleotide Phosphate (oxidized form)
NADPH	Nicotinamide Adenine Dinucleotide Phosphate
NaOH	Sodium Hydroxide
NiO	Nickel Oxide
nm	Nanometer
NPs	Nanoparticles
PCEs	Polychromatic Erythrocytes
PDI	Polydispersity Index
PBMCs	Peripheral Blood Mononuclear Cells
ppm	Parts Per Million
PVA	Polyvinyl Alcohol
RhB dye	Rhodamine B Dye
rGO/CHS/AuNPs	Reduced Graphene Oxide/Chitosan/Gold Nanoparticles
ROS	Reactive Oxygen Species
SEM	Scanning Electron Microscopy
SnO_2	Tin Dioxide
SPECT	Single Photon Emission Computed Tomography
SPR	Surface Plasmon Resonance
TEM	Transmission Electron Microscopy
TiO_2	Titanium Dioxide
UV-Vis	Ultraviolet-Visible Spectroscopy
v/v	Volume/Volume Ratio
XRD	X-ray Diffraction
$Zn(CH_3CO_2)_2$	Zinc Acetate Dehydrate
$Zn(OH)_2$	Zinc Hydroxide
ZnO	Zinc Oxide
°C	Degrees Celsius
µg	Microgram
γ-GT	Gamma-Glutamyl Transferase

methods. The first two are the most prevalent and are therefore considered traditional or conventional approaches, associated with high production yields, high purity levels, and precise control over structural characteristics [18,19]. For more detailed information on the technical aspects of these approaches, see references [2,20,21]. Despite their undeniable potential as disruptive technologies, discussions about their application must extend beyond the functionality of nanomaterials to encompass their impact on human health, economics, and the environment. In fact, both physical and chemical synthesis methods present significant challenges at the production level, including substantial energy consumption, the need for expensive high-grade resources, and the use of toxic materials (such as organic solvents, reducing agents, and

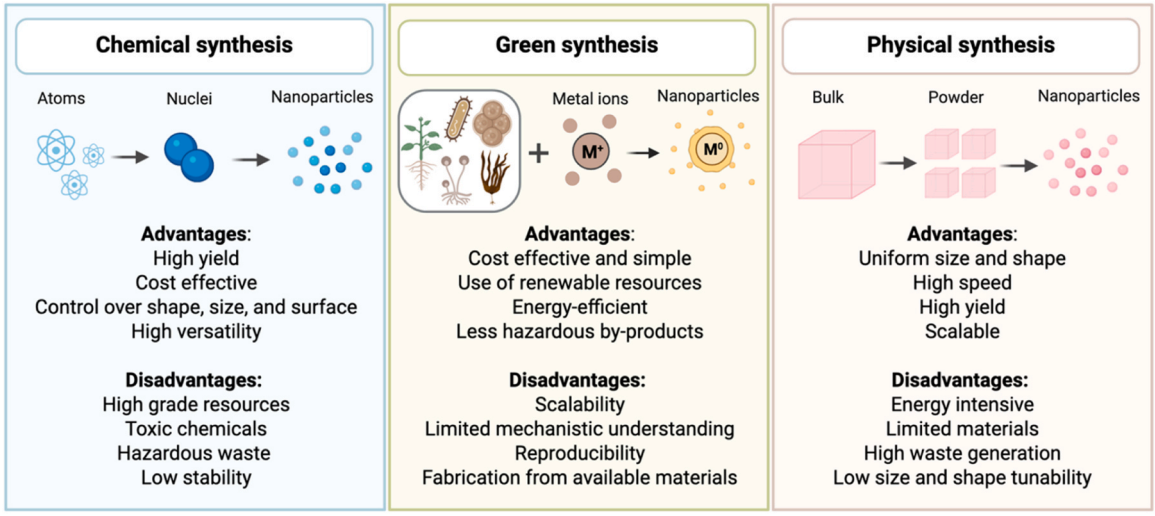

Fig. 1. Overview of metallic nanoparticle synthesis using chemical, green, and physical methods, along with their respective advantages and disadvantages.

stabilizers), which may lead to potential cytotoxicity, carcinogenicity, and environmental toxicity (Fig. 1) [22,23].

Thus, given the growing and cumulative impact of conventional synthesis processes, research and development must comply with sustainability principles, ensuring environmental and public health well-being. In fact, according to the 2030 Agenda for Sustainable Development, 14 of the 17 Sustainable Development Goals concern the application of green chemistry principles in the development of more sustainable models [24]. The concept of green chemistry was introduced by Paul Anastas and John C. Warner in 1998 and emerged because of the adverse effects of industrial development [25]. The 12 principles that govern it, aim to establish more sustainable, efficient, and safer chemical processes. Applying green chemistry involves, for instance, using biological synthesis methods - also known as green synthesis - as alternatives to produce MNPs. For this type of synthesis, plants, or microorganisms (algae, yeast, bacteria, and fungi) are used, ensuring the processes' sustainability by being substrates for the synthesis reaction itself.

Although the concept and potential of green synthesis have been recognized for decades, this approach has gained significant attention in the last decade as a biologically appropriate, clean, and environmentally friendly alternative [26]. Recent advances show that green synthesis involves simple, energy-efficient processes that reduce production costs by avoiding expensive precursors and complex equipment [27–29]. The use of non-toxic materials minimizes environmental impact and reduces hazardous by-products, while eliminating harmful chemicals like organic solvents and harsh reducing agents lowers the ecological footprint of nanomaterial manufacturing [30].

Despite extensive research on green MNP synthesis, key gaps persist, including the lack of an integrated analysis of biosynthesis mechanisms, synthesis parameters, direct comparisons with other synthesis approaches, a comprehensive biocompatibility assessment *in vitro* and *in vivo* and biocompatibility and degradation pathways. In this review, we explore the latest advances in detail, compiling findings on plant-based and microorganism-mediated (algae, yeast, fungi, and bacteria) synthesis into a single, cohesive manuscript. We thoroughly examine the biosynthesis mechanisms and active molecules involved in producing various types of MNPs, followed by an in-depth analysis of the influence of reaction factors — including extraction and reaction solvents, extraction concentration, metallic salt molarity, temperature, pH, and reaction time — on MNPs synthesis, stability, and properties. Additionally, we compare green and chemical synthesis, highlighting studies that directly contrast both methods' effects on structural, physical, stability, and activity profiles. Finally, we address the biocompatibility, toxicity, and biodistribution of green-synthesized MNPs through evidence from both in vitro and in vivo assays. The review concludes with a critical, integrated analysis of the current limitations of green synthesis and proposes strategic solutions to enhance reproducibility, scalability, and industrial feasibility.

2. Green approaches for metallic nanoparticle synthesis

2.1. From conventional to eco-friendly synthesis approaches of metallic nanoparticles

MNPs are a class made by metallic precursors (e.g., Fe, Zn, Cu, Au, Ag, Co, and Ni) individually or in groups of atoms. Their constitution has three distinct layers: core, shell, and surface layers [31–33]. The core layer is the central part of the particle (inner material), the particle itself; the shell layer is chemically different from the core layer, which influences the properties of the core particle. This layer allows, for instance, the modification and improvement of the dispersibility and thermal stability of the core particle; and the surface layer allows to be functionalized with various molecules like polymers, surfactants, and metal ions. More details about merits and demerits of MNP can be found at the Table 1.

Table 1
Merits and demerits of MNP.

MNP	Merits	Demerits	Ref
Ag	– High antimicrobial activity against various bacterial strains, including multidrug-resistant ones – Low toxicity	– High production cost	[34]
Cu	– Catalytic efficiency – Good antifungal and antibacterial activity	– Oxidation instability	[35,36]
ZnO	– Efficient in water treatment – Antibacterial properties – Non-toxic	– Potential toxicity when accumulated in cells – Impacts on photosynthesis	[37–39]
Au	– Low toxicity and high biocompatibility – Unique optical properties	– High production cost	[27]
Ni	– Application in catalysis – Good magnetic properties	– Risk of toxicity and allergenicity	[40–42]
Ti	– Exceptional photocatalytic activity – Chemical stability, – Nontoxicity – Low cost	– Low efficiency under visible light	[43,44]
Fe	– Application in magnetic resonance imaging, magnetic recording, hyperthermia, drug delivery, separation and recovery processes – Low cost – Low toxicity	– Tendency to aggregate due to magnetic characteristics	[45–47]
Se	– Antioxidant and anticancer properties	– Highly toxic	[48]
Mg	– Odorless – Antimicrobial properties – Low toxicity	– Highly reactive with air and water	[49]
Cd	– Photocatalysts, anticancer and antimicrobial activities	– Hardly be used in the *in vivo* studies with adverse effects for more than one year	[50,51]
Si	– Less hazardous to the environment compared to other nanomaterials – NPs can be easily modified	– Potentially carcinogenic – Poor biodegradation – Organ retention	[52]
Pd	– High catalytic activity – Thermal and chemically stability – cost-effectiveness	– Often need to be immobilized on solid supports or stabilized with specific ligands	[53]

The considerable reduction in the size of the NPs compared to the bulk material increases the number of atoms on the surface that are more active [54]. This activity is attributed to the diminished number of neighbouring coordinating atoms and unsaturated sites [54]. Besides, MNPs can show electric and magnetic resonance creating a quantum effect [55], are optically active [56], enhanced surface Raman [57,58] and Rayleigh scattering [59,60], have anti-friction effect in nanolubrifiaction [61], and higher surface energy which decreases the melting point [62]. These properties that MNPs exhibit have encouraged their exploration over the last century, having already shown potential in multiple application areas, ranging from nanomedicine to engineering.

According to the starting material, categories of NPs preparation are divided into: i) Top-Down approach, where synthesis of materials is done by the reduction of size of the starting material through different chemical and physical processes, and ii) Bottom-up approach, where atoms and molecules are assembled into larger stable structures through physical and chemical reactions [63]. Top-down techniques include ion sputtering, ball milling, laser ablation, electro-explosion, and mechanochemical synthesis. Bottom-up techniques include hydrothermal, chemical vapour deposition, physical vapour deposition, sol-gel, chemical reduction, solvothermal, spray pyrolysis, laser pyrolysis, and

flame pyrolysis. For detailed information see [2,64–67].

These physical and chemical methods are vastly described in the literature. The scientific community can synthesize controlled-sized NPs with distinct compositions, shapes, and properties [46,68–72]. Some of the limitations regarding such synthesis methods and processes are their environmental and economic impacts. Other limitations include: instability, costly analysis requirements, application of toxic precursors and organic solvents, generation of large amounts of waste, contamination of the product, low yield, necessity for skilled labour, lack of fundamental mechanisms, production of impurities, high-pressure necessities, and high energy losses [29,73–78]. Seeing the drawbacks, the scientific community felt the need to explore new and eco-friendly synthesis methods. The premise of using the palette of the natural resources of the planet initiated a new era of NPs synthesis known today, with a more common terminology, as "green synthesis".

2.2. *Principles of green synthesis*

Green synthesis refers to processes that use the organic parts of natural products to synthesize nanostructured materials through biological pathways (oxidation/reduction, chelation, and precipitation). Several biological systems can reduce metal ions to metal NPs, including various plants, algae, yeast, fungi, microbes, bacteria, actinomycetes, viruses, and biowaste (Fig. 2). The term “green” is implicitly associated with simple, cost-effective, and, above all, environmentally friendly approaches.

This eco-friendly feature is brought by (i) the use of less hazardous chemicals and solvents, (ii) performance at atmospheric pressure and temperature, (iii) requirement of low energy input, (iii) no toxic waste production [79–82].

The NPs synthesis process, in general, encompasses four distinct phases [83,84]:

(1) Initial phase: reaction solution containing biological systems and the metal salt precursor.
(2) Activation phase: This process involves the chemical reduction of metal ions, forming nucleation centers from which NPs gradually develop and expand.
(3) Growth phase: In this phase, small NPs coalesce, forming larger aggregates in several different shapes. This process involves heterogeneous nucleation, growth, and ongoing reduction of metal ions, known as Ostwald ripening. This phase is marked by a concurrent rise in the thermodynamic stability of the MNPS and is influenced by physicochemical variables (for instance, concentration, pH, temperature, and reaction time).
(4) Termination phase: in the final stage, the NPs assume their most energetically favourable conformation—also, the compounds involved in the reaction play a pivotal role in NPs’ stabilization.

Due to the difference in metabolic and chemical composition of each of the biological entities, the interaction of metal ions with these molecules also differs, thus resulting in different kinds of MNPs formations. Therefore, the synthesis route and biological entity used determine the type of MNPs that would be formed.

3. Biological routes and mechanisms for metallic nanoparticles synthesis

This section will explore recent advances in the biosynthesis processes of several MNPs using various biological entities, including

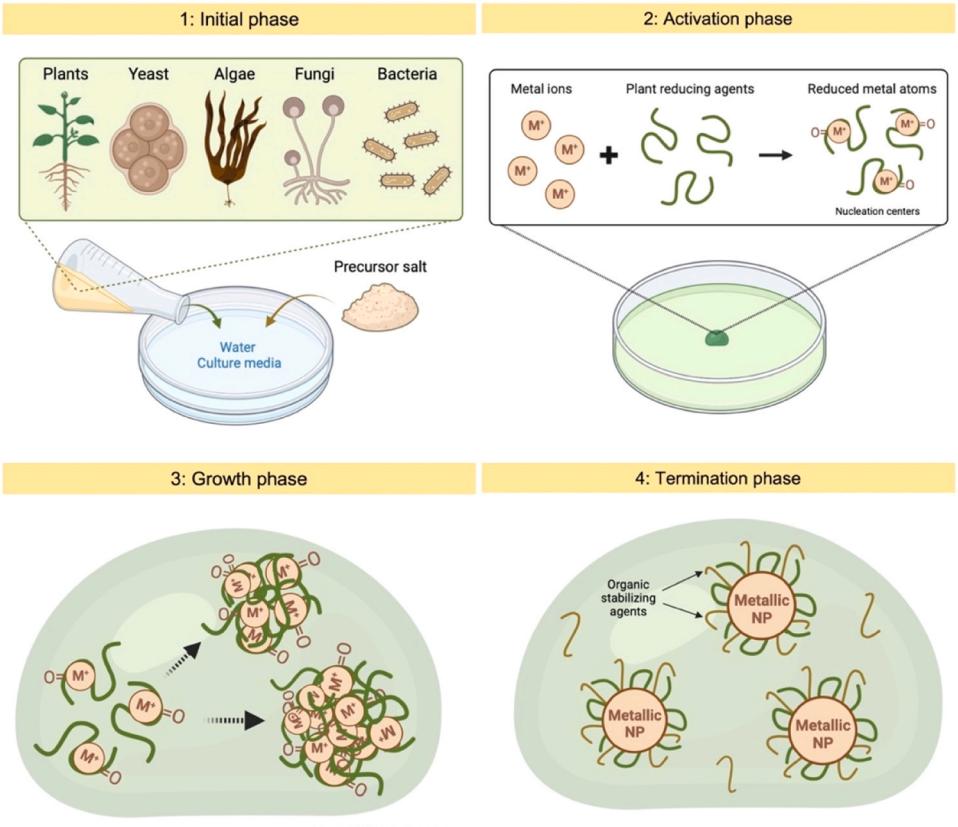

Fig. 2. Schematic representation of metallic nanoparticle synthesis using biological systems. In the initial phase, a solution with the biological systems and a metal precursor salt is added to the water/culture media. Then, in the activation phase, the metal ions are reduced, forming nucleation centers, which, in turn, coalesce, forming larger aggregates with different shapes and sizes (growth phase). In the termination phase, the formed NPs assume a more energetically favourable shape and size by interacting with organic stabilizing agents.

plants, algae, bacteria, yeast, and fungi. The main physical-chemical characteristics of MNPs are also explored according to the synthesis method and the main results of their applicability.

3.1. Plant-mediated synthesis

3.1.1. Overview of plant biosynthesis mechanisms and advantages

Due to their sustainable and renewable nature, plants and their parts are considered the leading factories for greenly synthesizing MNPs. In addition to the abundant resources, they are rich in phytochemicals, which play a preponderant role in the bioreduction of metal ions and the consequent synthesis and stabilization of NPs. Based on wide diversity, phytochemicals are broadly divided into primary and secondary metabolites [85]. Primary metabolites are naturally occurring in the plant and have a direct role in the growth of the plant, while secondary metabolites are formed due to the response of the plant to environmental stress, consisting of terpenoids, polyphenols, antioxidants, citric acid, saponins, heterocyclic compounds, peptides, tannins, and sugars [86–89]. In addition, the superiority of plant-mediated biosynthesis compared with that mediated by microorganisms is due to water-soluble phytochemicals [90,91]. Besides being environmentally friendly, the extracts are biodegradable, biocompatible, and cheap [92]. Several advantages have been pointed out on account of phyto-manufacturing, and therefore they include synergistic effects such as antibacterial and antioxidant effects arising from the functionalization at the surface of the NPs. Consequently, many parts of plants such as seeds, roots, stems, barks, leaves, flowers, and fruits have been used to take an extract out of it, which eventually becomes a driving solvent for the synthesis of several metallic NPs.

The general plant-mediated biosynthesis of metallic NPs is described in Fig. 3. The first step concerns selecting the plant species and the tissue/organ or other parts of the plant. The sample is then milled to obtain a powder to which distilled water is generally added. Then, the solution is boiled and filtered to obtain the plant extract, to which the specific salt precursor is added according to the required final concentration. The colour change of the solution is the first evidence of the reduction of metal ions to metal NPs [93,94].

3.1.2. Plant-mediated metallic nanoparticle synthesis and applications

Table 2 gives an overview of several plant-synthesizing MNPs and some of their key associated elements. The pioneering study on synthesizing silver NPs (Ag NPs) using *Medicago sativa* [95] has stirred up several subsequent studies using various plant species. Application interest for Ag NPs is mainly due to their antimicrobial and antibacterial activity. This results from the high bioavailability of bioactive compounds in plant extracts that play multiple and synergistic roles, ensuring the reduction, capping, and stabilization of NPs [96]. The process underlying the synthesis of Ag NPs typically entails the reaction in Eq. 1 [97]:

$$Ag^{2+}NO_3^{2-} + Plant\ extract(-C=O,\ -OH, etc) \rightarrow\ Ag^0\ \ NPs + by\ product \quad (1)$$

Recently, Yousefzadeh-Valendeh *et al.* [94] synthesized Ag NPs (Ag NPs) through a green method using a hydroalcoholic extract from Taraxacum officinale, commonly known as the dandelion flower. Silver nitrate ($AgNO_3$) was used as the precursor salt, and a distinct color change in the solution accompanied its reduction to Ag NPs. Capping agents included carotenoids, flavonoids, and phenolics responsible for the stabilization of the synthesized NPs. The Ag NPs exhibited outstanding antidiabetic, antioxidant, antibacterial, and photocatalytic properties. Ag NPs were also successfully biosynthesized using the leaf extract of *Catharanthus roseus*, with demonstrated antibacterial and heavy metal removal activity. The same NPs were synthesized using the aerial parts of *Zataria multiflora*, where the action of the reductant phytochemicals is potentiated by higher pH [98]. This results from the influence of pH on the dissociation, interfacial free energy, and net charge of a complexing agent [98]. Other reported species for Ag NPs biosynthesis include, for instance, *Origanum majorana* [34], *Echinacea purpurea* [99], *Catharanthus roseus* [100], *Phoenix dactylifera* [101], *Phyllanthus emblica*, *Psidium guajava* [102] and *Phyllanthus emblica* [103].

Gold NPs (Au NPs) are extensively documented in the literature on plant-mediated synthesis and have been associated with production with a good synthesis yield [104]. The process underlying the synthesis of Au NPs typically entails the reaction in Eq. 2 [97].

$$HAu^{3+}Cl_4^{-4} \bullet 4H_2O + Plant\ extract \rightarrow\ \ Au^0 NPs + by\ product \quad (2)$$

Like what was described for Ag NPs, several parts of the plant or even the entire plant can synthesize this type of NPs. In a study by Kaur *et al.* [105], the seed extract of *Bryonia laciniosa* was combined with an aqueous solution of tetrachloroaurate ($HAuCl_4$), leading to the formation of spherical Au NPs with sizes ranging from 20 to 40 nm. Also, *Leucophyllum frutescens* leaves allowed the synthesis of Au NPs of various geometries (triangular, spherical, rods) with an average size of ~22

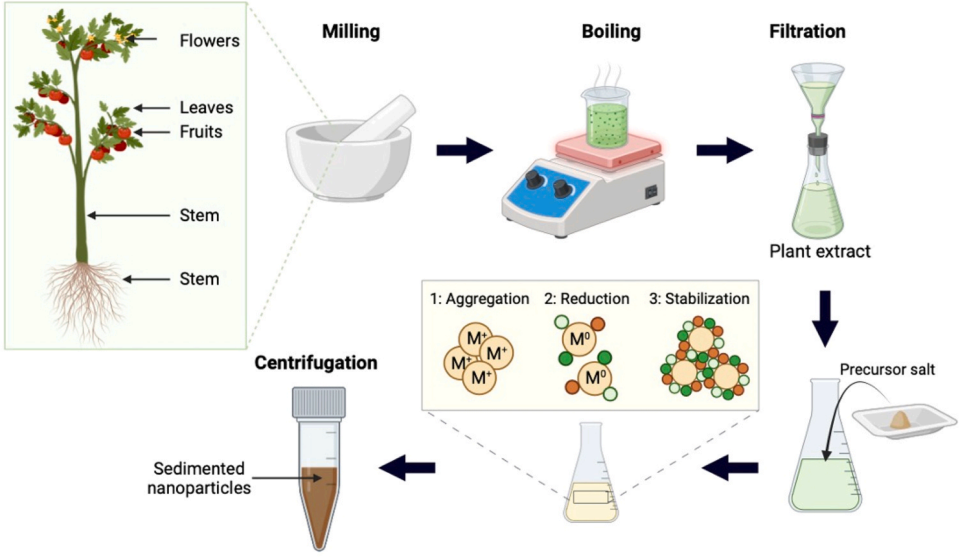

Fig. 3. Schematic representation of plant-mediated biosynthesis of metallic nanoparticles.

Table 2
Representative list of recent advances in the green synthesis of several types of MNPs using plants.

Plant	Extract	NP	Size (nm)	Shape	Application	Ref
Taraxacum officinale	Flowers	Ag	45–55	Spherical	Antioxidant Antimicrobial Antidiabetic Photocatalytic	[94]
Zataria multiflora	Total aerial parts	Ag	25.5	Spherical	Antibacterial Biofilm inhibitory activity	[98]
Origanum majorana	Leaf	Ag	10–60	Spherical	Antibacterial	[34]
Echinacea purpurea	Aerial part	Ag	68	Spherical	Antioxidant	[99]
Catharanthus roseus	Flower	Ag	5–20	Spherical	Photocatalytic reduction Antioxidant	[100]
Phoenix dactylifera	Seed	Ag	15–80	Spherical	Antibacterial Antibiofilm Cytotoxic	[101]
Psidium guajava	Stem Bark	Ag	20–80	cubic and hexagonal	Antimicrobial	[102]
Phyllanthus emblica	Fruit	Ag	60–80	Spherical	-	[103]
Bryonia laciniosa	Seeds	Au	20–40	Spherical	Catalytic Antimicrobial	[105]
Leucophyllum frutescens	Leaves	Au	~22	Triangular, spherical, rod	Catalytic	[106]
Physalis minima	Whole plant	Au	15	Spherical	Antidiabetic Antioxidant Antimicrobial	[107]
Vitis vinífera *Juglandaceae* *Buchananialanzan* *Phoenix dactylifera*	Fruits	Au		-	Antimicrobial	[108]
Sageretia thea	Leaves	Au	32	Spherical and rod	Antibacterial Antioxidant Antileishmanial Analgesic	[109]
Haplophyllum	Leaves	Au	4–4	Spherical	Anticancer	[110]
Verbascum speciosum	Leaves	Au	118	Polygonal and round	Anticancer	[111]
Ricinus communis L	Seeds	Au	> 100	Spherical	Antibacterial	[112]
Hypericum perforatum L	Flower Stem Leaf	Au	10.5 9.2 11.5	Spherical	Antioxidant	[113]
S. rechingeri Jamzad	Aerial parts	Au	15.1	Spherical	Anticancer	[114]
Heliotropium eichwaldi L	Whole plant	Au	20	Rod	Anti-acetylcholinesterase	[115]
Stevia rebaudiana	Leaves	NiO	2–16	Spherical	Antibacterial	[117]
Salvadora persica	Root	Ni	18–45	Spherical	Antibacterial	[118]
Alhagi maurorum	Leaves	Ni	20–36	Spherical	Anticancer	[119]
Berberis balochistanica	Stem	NiO	~31	Rhombohedral	Antioxidant	[120]
Lactuca serriola	Seed	Ni NiO	> 100	Spherical	Antibacterial Catalytic	[121]
Opuntia ficus indica	Leaves	NiO	20–35	Spherical	Energy storage	[122]
Avicennia marina	Leaves	NiO	30–100	Flacks	Electrochemical	[123]
Sesbania grandiflora	Flower	NiO	19–60	Rod	Anticancer	[124]
Portulaca oleracea	Leaf	Ni	40	Flake	-	[125]
Acacia nilotica	Leaves	Ni	16 18	Spherical Tetragonal	Antibacterial	[126]
Evolvulus alsinoides	Leaves	NiO	~11	Spherical	Photocatalytic Anticancer	[127]
Eichhornia crassipes	Whole plant	Ni	~10	Cubic	Hydrogen production	[128]
Phragmanthera austroarabica	Leaves	Cu	~44	Spherical	Anticancer Antibacterial Catalytic	[35]
Hipphophae rhamnoides L	Stem	Cu	38–94	Spherical	Anticancer	[36]
Moringa oleifera	Seeds	Cu	7.3	Spherical	Remediation Antimicrobial	[132]
Hyptis suaveolens	Leaves	Cu	7.2	Spherical	Antibacterial	[135]
Cynodon dactylon	Leaves	Cu	183	Spherical	Antibacterial Photocatalityc	[136]
Foeniculum vulgare	Leaves	Cu	33–74	Spherical	Anticancer Antioxidant	[137]
Carum carvi	Seeds	Cu	12.4	Spherical	Seedlings	[138]
Ocimum sanctum	Leaves	Cu	80–100	Spherical	Antibacterial	[139]
Tinospora Cordifolia	Leaves	Cu	500–1500	Irregular	Photocatalytic	[140]
Malva parviflora	Leaves	ZnO	15–53	Hexagonal Irregular	Shelf-life improvement	[143]
Syzygium cumini	Leaves	ZnO	64–78	Spherical	Fertilizer Photocatalytic	[144]
Thymbra spicata L.	Leaves	ZnO	6.5–7.5	Irregular	Antimicrobial	[145]
Bergenia ciliata	Rhizome	ZnO	30	Flower	Antimicrobial Anticancer	[146]
Solanum nigrum	Leaves	ZnO	30–86	Rectangular	Anticancer	[147]

(*continued on next page*)

Table 2 (*continued*)

Plant	Extract	NP	Size (nm)	Shape	Application	Ref
Salix tetrasperma	Leaves	ZnO	5–43	Spherical	Antimicrobial Anticancer Antioxidant	[148]
Caesalpinia crista	Seeds	ZnO	34.67	Irregular	Antimicrobial Anticancer Antioxidant	[149]
Callicarpa tomentosa	Leaves	ZnO	30–60	Hexagonal	Bactericidal	[150]
Areca catechu	Nut	ZnO	20	Spherical	Photocatalytic Antibacterial	[37]
Dysphania ambrosioides	Leaves	ZnO	7–130	Spherical	Antibacterial	[38]
Nigella sativa	Seed	Cu	~98	-	Antibacterial Antiobesity	[151]
Acer pentapomicum	Leaf	Ag	19–25	Multiple	Antimicrobial Antioxidant	[152]
Ferula pseudolliacea	Root	Ag	-	Multiple	Antibacterial Antimicrobial Antioxidant	[153]
Olea europaea	Leaf	Ag	35–40	Multiple	Antibacterial	[154]
Camellia sinensis	Leaf	Ag	25–30	Multiple	Antibacterial	[154]
Rosa damascena	Flowers	Au	-	Spherical	Anticancer	[155]
Camellia sinensis	Leaf	Fe	30–120	-	Catalysts in biodiesel production	[156]

± 20 nm [106]. In turn, *Physalis minima* (whole plant) allowed the synthesis of NPs (15 nm) with antidiabetic, antioxidant, and antimicrobial properties [107]. Patil *et al.* synthesized Au NPs using extracts from *Vitis vinífera*, *Juglandaceae, Buchananialanzan* and *Phoenix dactylifera* [108]. The extract from each plant has its own identity as a natural product, resulting in different patterns of formation of adducts and coordination bonds between Au and the compounds. *Sageretia thea* leaves extract (naturally enriched with phenols, flavonoids, and flavonoids-O-glycosides) produced Au NPs showing antibacterial, antioxidant, antileishmanial, and analgesic activities [109].

Other reported species for Au NPs biosynthesis include, for instance, *Haplophyllum* [110], *Verbascum speciosum* [111], *Ricinus communis L* [112], *Hypericum perforatum L* [113], *S. rechingeri* Jamzad [114] and *Heliotropium eichwaldi L* [115].

Despite the significant prevalence of Ag and Au NPs in the literature regarding plant-mediated green synthesis, nickel (Ni), copper (Cu), and zinc (Zn) NPs have also gained the interest of the scientific community. Ni and Ni oxide NPs (NiO NPs) present exciting properties for use in multiple applications, such as bad gap stability and high surface area, and they are reusable [116]. Moghadam *et al.* [117] reported the synthesis of Ni NPs using *Stevia rebaudiana* leaves (2–16 nm). These Ni NPs demonstrate a dose-dependent growth inhibition of *Streptococcus mutans* with a minimum inhibitory concentration of 250 μg/mL. The phytoconstituents (steroids, flavonoids, ester, and fatty acids) of *Salvadora persica* root were also used as reducing and capping agents of spherical Ni NPs with a size range of 18.20–45.12 nm [118]. In addition to demonstrating good antioxidant activity, these NPs have good antibacterial activity for several microbial strains, presenting the highest antibacterial activity for *Enterobacter cloacae* [118]. In turn, *Alhagi maurorum* leaves extract synthesized Ni NPs with sizes between 20.56–36.63 nm [119]. The NPs demonstrated anti-human ovarian cancer properties, revealing half maximal inhibitory concentration (IC_{50}) values of 191, 312, 250, 396, and 241 μg/mL against OVCAR-3, ES-2, TOV-21G, OV-90, and UWB1.289 cell lines respectively. Other reported species for Ni NPs biosynthesis include, for instance, *Berberis balochistanica* [120], *Lactuca serriola* [121], *Opuntia ficus indica* [122], *Avicennia marina* [123], *Sesbania grandiflora* [124], *Portulaca oleracea* [125], *Acacia nilótica* [126], *Evolvulus alsinoides* [127], *and Eichhornia crassipes* [128].

Even though not fully known yet, the biosynthesis of Cu NPs is associated with the free carboxylic and amino groups of phenolic, flavonoids, and other molecules as reducing agents of Cu ions [129]. In turn, the MNPs stabilization is ensured by the $C = C$, $C = O - C$, and $C = O$ groups of heterocyclic compounds [130,131].

Phragmanthera austroarabica was used to mediate the synthesis of Cu NPs, and the authors studied several biosynthesis parameters (metal concentration, incubation period, and pH) [35]. It was found that 10 mM of Cu sulfate was the ideal concentration, and higher concentrations lead to increased instability and MNPs size, harming the NPs synthesis. Furthermore, pH 10 was ideal for the synthesis, while an acidic medium does not allow NPs synthesis [35]. In turn, Dadhwal *et al.* [36] used the stem extract of *Hippophae rhamnoides L.* in the synthesis process, and the solution colour changed from pale yellow to dark brown, indicating the reduction of Cu (iii) to cupric ion (Cu^{+}). The spherical NPs (38–94 nm) revealed concentration-dependent activity with an IC_{50} value at 48 μg/mL towards HeLa (human cervical carcinoma cells) cancer cell lines. Furthermore, the seed extract of *Moringa oleifera* mediated the synthesis of Cu NPs, which showed a dose-dependent removal of the water pollutant hexavalent chromium [Cr(VI)] [132]. The removal of pollutants using green-synthesized NPs has also been demonstrated with other systems, highlighting the versatility of this approach. For example, a nano-MgO carbon nanocomposite synthesized from cashew nut shells and rose petal extract effectively adsorbed the dye Rhodamine B due to the presence of uniformly distributed MgO nanoparticles and surface functional groups introduced during the green synthesis process [133]. Similarly, chitosan–MgO nanocomposites efficiently removed acenaphthene via electrostatic interactions and physisorption [134].

Other reported species for Cu NPs biosynthesis include, for instance, *Hyptis suaveolens* [135], *Cynodon dactylon* [136], *Foeniculum vulgare* [137], *Carum carvi* [138], *Ocimum sanctum* [139], and *Zataria multiflora* [140].

Zinc oxide (ZnO) NPs are another class of metallic NPs that physical, chemical, or biological routes can synthesize. This type of NPs has gained importance due to their pyroelectric and piezoelectric properties, high band gap, and structure-dependent thermal properties [141]. Its plant-mediated synthesis process is similar to the NPs discussed previously, based on adding precursor salts (Zn nitrate or Zn acetate) to plant extracts. The aromatic OH groups of bioactive components extracted from plants or parts thereof adhere to Zn^{+}, reducing it to ZnO NPs [142]. Iqbal *et al.* [143] described the process in two steps. The first one involved the reduction of Zn acetate dehydrate ($Zn(CH_3CO_2)_2$) to Zn hydroxide ($Zn(OH)_2$) by the flavonoids present in the plant extract. The next step is promoted by adding a basic solution (sodium hydroxide (NaOH)), which reduces Zn hydroxide to ZnO NPs. Eq. 3 summarizes the processes [143].

$$Zn(CH_3CO_2)_2 \bullet 2H_2O \longrightarrow Zn(OH)_2 + 2CH_3COOH$$

$$Zn(OH)_2 \longrightarrow ZnO + H_2O \quad (3)$$

For instance, ZnO NPs can be used as a fertilizer for wastewater purification. Rafique *et al.* [144] used *Syzygium cumini* extract to synthesize ZnO and found that by increasing the amount of extract (from 10 to 25 mL), the size of the NPs decreased from 78 to 64 nm. This effect is associated with an increase in the concentration of phytochemicals, which, in turn, increases the capping ability during the nucleation, aggregation, and formation of NPs. The NPs demonstrated dual functionality by enhancing the germination of *Pennisetum glaucum* seeds by 60 % and degrading 98 % of Rhodamine B (RhB) dye from contaminated water. This type of MNPs also has antibacterial properties. For example, Gur *et al.* [145] synthesized ZnO NPs from *Thymbra Spicata L.* plant leaves, demonstrating activity against *Escherichia coli, Bacillus subtilis, Pseudomonas aeruginosa,* and *Candida albicans*. The anticancer potential of green synthesized ZnO mediated by *Bergenia ciliata* was explored [146]. The synthesized NPs demonstrated anticancer ability towards HeLa cells (IC_{50}= 101.7 μg/mL) and HT-29 cancer cells (IC_{50}=124.3 μg/mL). The same type of NPs, this time synthesized from the leaves of *Solanum nigrum*, was also demonstrated to induce apoptosis in HeLa cell lines [147]. The significant anticancer activity was associated with inhibition of β-catenin and increased caspase-3, caspase-9, and p53 levels. The ZnO NPs synthesized from *Salix tetrasperma* demonstrated promising results in multiple applications [148]. The authors demonstrated their antioxidant potential, antimicrobial activity (confirmed for *Staphylococcus aureus, Salmonella typhimurium, Pseudomonas aeruginosa, Bacillus subtilis, Klebsiella pneumonia,* and *Escherichia coli*) and anticancer activity against prostate cancer cells. Other reported species for ZnO NPs biosynthesis include, for instance, *Caesalpinia crista* [149], *Callicarpa tomentosa* [150], *Areca catechu* [37], and *Dysphania ambrosioides* [38].

3.2. Algae-mediated synthesis

3.2.1. Overview of algae biosynthesis mechanisms and advantages

Algae are eukaryotic organisms that make photosynthesis and inhabit the water [157]. Algae-microalgae and seaweed have been used as food and medicinal resources for the last 14,000 years ago in Asia beyond the old register of seaweed culture in Chile and some islands around the world [158]. Macroalgae are primarily applied in nori and other foods known worldwide as *wakame* and *kombu.* In contrast, microalgae such as *Chlorella vulgaris* have been used as protein, amino acids, and vitamin B12 sources [157]. Micro and macroalgae have pigments such as Lutein, Fucoxanthin, Astaxanthin, and Zeaxanthin that have biological activities as anti-cancer, antioxidant, anti-inflammatory, anti-cancer, anti-obesity, neuroprotective, and cardioprotective that can be applied in functional food, pharmaceuticals, and cosmeceuticals industry with a expect market of US$452 million by 2025 [159]. Furthermore, the algae are rich in soluble fibres, proteins, carbohydrates, lipids, oils, fats, polyunsaturated fatty acids, minerals, and vitamins, being, therefore, an indispensable source of food [157,159,160]. Despite algae usually having taste and smell undesired by the majority of people, some modifications to improve the sensory perspectives and increase their use have been made [157]. They can also be used in wastewater treatment when living algae or biomass make the biosorption of heavy metal ions during the growth algae process [161]. Algae can efficiently remove nitrogen, phosphorus, and cod from water while producing biomass, that can be used as biofuel [161]. In addition to the examples above, algae can also be used for greenhouse gas reduction, medicine [161,162], bioactive pigments [159], bioplastic [160], bio-fertilizer [163], and NPs synthesis [164].

Algae extracts have various bioactive compounds such as chlorophylls, phycobilins, carotenoids, and antioxidants that work as reducing and stabilizing agents [165]. The synthesis mostly reports the process of NPs mediated by algae as extracellular that occurs almost in the same as what is previously mentioned in the plant section where the extract is made usually in aqueous and/or alcoholic with heat and stirring. Then, it is mixed with metallic salt under determinate temperature, stirring, time and, sometimes, pH control. The general algae-mediated biosynthesis of metallic NPs is described in Fig. 4.

The biosynthesis mediated by algae can also be intracellular, where natural metabolic processes such as respiration, photosynthesis, or nitrogen fixation are utilized for the synthesis. The enzyme that carries the electrons in cells, nicotinamide adenine dinucleotide phosphate (NADPH), and their dependence are probably responsible for the NPs synthesis when the cells are in contact with metallic ions [165]. Although biomolecules play an unequivocal role in the synthesis, stabilization, and capping of NPs, the complete process is not yet fully understood by the scientific community. To gain a deeper understanding of this topic, some researchers have employed atomic-scale simulations. For instance, Les *et al.* [166] investigated the interaction of gallic acid molecules with magnetite nanoparticles to enhance biocompatibility. Gallic acid, a molecule commonly found in plants, algae, and fruits, was analysed using the molecular modelling software Spartan'18. The study aimed to evaluate how gallic acid contributes to improving the dispersion of nanoparticles in water. TEM images confirmed the good interaction between the molecules and the nanoparticles, showing a coating of the biomolecule on the nanoparticle surface. Simulation results demonstrated that hydration of the gallic acid molecule increased its dipole moment, facilitating water interaction. The authors also observed that dipole-dipole interactions and hydrogen bonds coexisted and varied in influence depending on the solvent concentrations of ethanol or dimethyl sulfoxide.

In another study, Kim *et al.* [167] explored the growth mechanism of AuNPs in the presence of caffeic acid. Caffeic acid, which is found in microalgae and plants, served as a reducing agent for AuNP synthesis. Oxidized caffeic acid, resulting from the reduction of gold ions, was used in molecular dynamics simulations conducted with the LAMMPS software. TEM analysis revealed that a concentration of 0.008 mM caffeic acid had no significant effect on the size of the AuNPs. However, at concentrations ranging from 0.04 mM to 0.24 mM, the particle shape became increasingly spherical. Beyond this range, the shape stabilized in a more spherical form. Simulations showed that at low concentrations, the shape of the AuNPs was primarily controlled by the surface free energy of specific facets. As the concentration increased, caffeic acid molecules were adsorbed onto the surfaces, acting as stabilizing agents during particle formation.

3.2.2. Algae-mediated metallic nanoparticle synthesis and applications

Most recent studies involving the application of algae for NPs synthesis are focused on biomedical applications, followed by water treatment, particularly for dye removal, as seen in Table 3. In this context, Ag is one of the most extensively investigated metals. Pekkon *et al.* [168] used the algae *Sargassum spp.*, which harms the local ecosystem and impacts human activities and the economy during excessive bloom events. The obtained extract contained polysaccharides, proteins, and a small amount of phenols, contributing to reducing Ag^+ ions to form NPs (Fig. 5). In addition to conventional preparation techniques (involving stirring and heating), the authors conducted the synthesis using a microwave for 0–4 min. The results demonstrated that microwaves facilitated the formation of NPs, reduced the synthesis time, reduced energy consumption, and improved the uniform dispersion of Ag NPs. The authors hypothesise that microwaves may promote the degradation of polysaccharides and release sugars that favour the synthesis process, although the exact mechanism remains unspecified [168]. Although the Ag NPs were relatively uniform, they were likely aggregated due to hydrogen bonding, revealing a zeta potential of −9.4 mV. Besides the demonstrated antioxidant potential, Ag NPs also exhibited toxicity to cancer cells while harmless to healthy cells. Additionally, Vinayagam *et al.* [169] obtained a more stable Ag NPs solution with a zeta potential

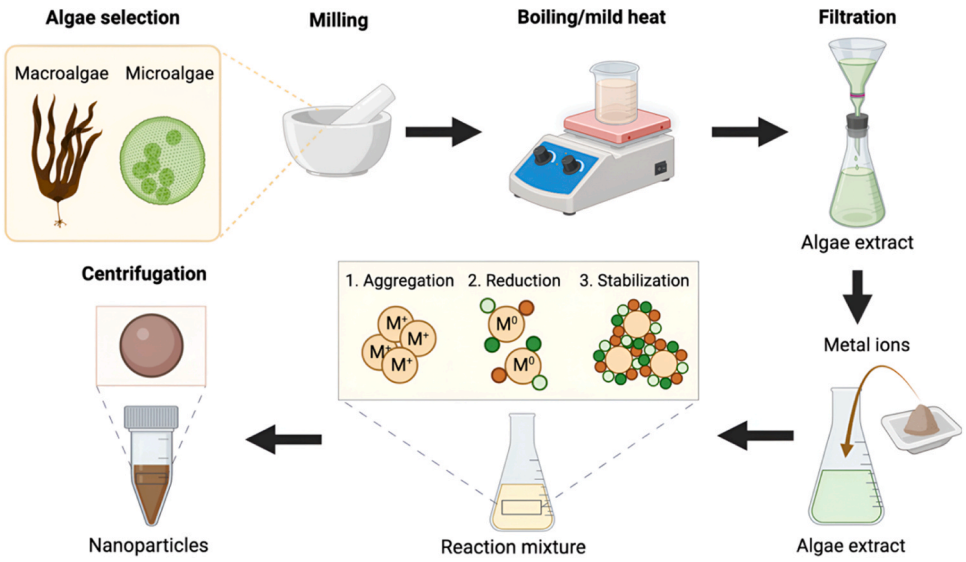

Fig. 4. Schematic representation of algae-mediated biosynthesis of metallic nanoparticles.

of −22.6 mV using the same algae. The XRD results revealed the presence of organic components from the algal extract on the surface of the nanoparticles, which acted as a capping agent.

The red algae *Calliblepharis fimbriata* was used to obtain an extract containing starches, alcohols, ethers, carboxylic acids, and anhydrides to synthesise Ag NPs [170]. The reaction resulted in spherical-shaped NPs ranging from 25 to 30 nm (using scanning electron microscopy (SEM) and transmission electron microscopy (TEM)), while dynamic light scattering (DLS) studies indicated an average size of 198 nm and a polydispersity index (PDI) of 0.305. The fourier-transform infrared spectroscopy (FTIR) results demonstrated the reduction of silver ions and the oxidation of carbonyl and hydroxyl groups, proving that secondary metabolites played a role in the synthesis and stabilization of the NPs.

Caulerpa racemosa was used by Thanigaivel *et al.* [171] in ethanolic extract to collect polysaccharides to work as a reducing agent, and the resulting NPs were applied against the bacterium *P. aeruginosa*, achieving an efficacy rate above 80 % in tilapia in a contaminated tank. Biomolecules extracted in ethanolic extract from *Ulva fasciata* with ultrasound were used to synthesise Ag NPs of ~50 nm, possibly reduced with the assistance of O-H groups. These particles demonstrated antifungal, antioxidant, and anticancer activities [172]. Recently, other studies have synthesised Ag NPs using algae such as *Chlorococcum humicola* and *Chlorella vulgaris* [173,174], *Porphyra yezoensis* [175], *Sargassum horneri* [176], *Sargassum polycystum* [177], *Turbinaria ornata* [178], *Sargassum tenerrimum* [179], *Cheatomorpha antennia* [180], *Capsosiphon fulvescens* [181], *Ulva lactuca* [182], and *Eisenia bicyclis* [183].

AuNPs have been the focus of numerous recent studies. Govindaraj [184] used the algae *Spatoglossum asperum* to synthesise Au NPs for the treatment of brain cancer (glioblastoma), which is challenging to treat due to its resistance to chemotherapeutic drugs, their side effects, and the challenge of delivering medications to the brain. Spectroscopy studies revealed increased intensity peaks at 530 nm (characteristic of Au NPs) along the reaction time, followed by colour changes. FTIR results indicated a significant presence of phenolic and carboxylic groups, while mass spectrometry identified a substantial peak of $C_{16}H_{11}F_6N_3O_4$, a flavonoid present in vitamin P. The Au NPs revealed an average size of 20 nm NPs with cubic shape (Fig. 6) and to be efficient against free radicals in a dose-dependent manner, with an efficacy close to that of vitamin C, when varying the concentration between 10 and 50 μg/mL. Furthermore, concentrations between 3 and 50 μg/mL were revealed to reduce the viability of cancer cells, causing damage, and preventing their spread while showing no significant action against healthy fibroblast cells. This efficacy is attributed to the combined action of gold atoms and the biomolecules from the algae.

Au NPs synthesis was also performed using ethanolic extracts of *Cystoseira trinodis* (Ct), *Cystoseira myrica* (Cm), and *Caulerpa prolifera* (Cp) [185], which contained various biomolecules such as alcohols, phenols, hydroxyl groups, polysaccharides, and carboxylate groups. Upon the reaction, assays indicated slightly spaced peaks for each NPs: Au NP (Cm) had 545 nm, Au NP (Ct) 540 nm, and Au NP (Cp) 555 nm, with zeta-potentials of −20 mV, −40.3 mV, and −47.2 mV, respectively. The diameter ranged from 12.6 to 15.5 nm, with spherical, hexagonal, and triangular shapes. Microorganism tests showed that Au NP (Cm) performed equal to or better than control antibiotics against *S. aureus, E. coli, Salmonella enterica, Candida albicans,* and *Aspergillus niger*. Moreover, Au NP (Ct) also performed better against *S.s aureus, E. coli, Salmonella enterica, Candida albicans*, and *Aspergillus niger*. Regarding anti-inflammatory activity, Au NP (Cm) performed almost identically to sodium diclofenac at the same concentrations, while the other NPs showed slightly inferior performance. Against the larvae of *S. mansoni* (cercariae), all NPs achieved 100 % mortality, with times ranging from 7 minutes for Au NP (Cm) to 30 minutes for Au NP (Ct). AuNPs were also extracted using algae extracts from *Digenea simplex* [186] *Undaria pinnatifida* [187], *Padina tetrastromatica* [188], and *Sargassum horneri* [176].

In a study diverging from the majority of the algae-based synthesis, Žvab *et al.* [189] used biosynthesis to convert metals and ions into non-toxic waste, potentially reducing the cost of cleaning water contaminated by Cu on a large scale. The above contamination is responsible for decreased biodiversity, increased bacterial antibiotic resistance, and risk to human health. The research was conducted with genetically confirmed clone sequences of *Chlamydomonas reinhardtii* cultivated in a controlled environment with added Cu^{2+}. Samples were collected on the first day and over the next three days, confirming the synthesis of Cu NPs with a diameter of less than 10 nm and spherical shape. Cu NPs were also the subject of the Alsalamah *et al.* [190] study, which used the *Padina boergesenii* algae, rich in daidzein, ellagic acid, and chlorogenic acid. A control solution containing Cu acetate, but no extract exhibited no colour change after 5 hours and showed no effect. The CuO NPs have shown spherical shape with an average size between 5 and 17 nm with crystalline structures. The antifungal assays indicated a concentration-dependent inhibition of growth, with inhibition zones of 26 mm for *B. subtilis*, 23 mm for *E. coli*, 25 mm for *K. pneumoniae*, and 22 mm for S. aureus, support the potential of using CuONPs as effective antibacterial agents to combat various bacterial pathogens.

Table 3
Representative list of recent advances in the green synthesis of several types of MNPs using algae.

Algae	NP	Size (nm)	Shape	Application	Reference
Sargassum spp	Ag/AgCl	10–175	Spherical	Anticancer Antioxidant	[168]
Sargassum spp.	Ag	~11.99	Spherical	Detection of H_2O_2	[169]
Calliblepharis fimbriata	Ag	25–30	Spherical	Nanopesticide production	[170]
Caulerpa racemosa	Ag	88 ± 0.5	Spherical	Ant-pathogenic fish bacteria	[171]
Ulva fasciata	Ag/AgCl	~50	Spherical	Antifungal Antioxidant Anti-cancer	[172]
Chlorococcum humicola and Chlorella vulgaris	Ag	10–13	Spherical	Antimicrobial	[173]
Porphyra yezoensis	Ag	100–200	Spherical	Antioxidant	[175]
Sargassum horneri	Ag and Au	22.7(Ag) 13.2(Au)	Spherical	Prevent water pollution and to treat wastewater	[176]
Sargassum polycystum	Ag	< 100	Spherical	Antimicrobial	[177]
Turbinaria ornata	Ag	~74	Spherical	Antioxidant Anti-uropathogenic	[178]
Sargassum tenerrimum	Ag	13–46	Spherical	Antimicrobial	[179]
Cheatomorpha antennia	Ag	24 ± 2.4	Spherical	Antibacterial	[180]
Capsosiphon fulvescens	Ag	20–22	Spherical	Anti-cancer	[181]
Ulva lactuca	Ag	39	-	Biohydrogen production	[182]
Eisenia bicyclis	Ag	18.5 ± 1.2	Spherical	Antimicrobial Anticancer	[183]
Spatoglossum asperum	Au	20	Cubic	Anticancer Antioxidant	[184]
Cystoseira trinodis, Cystoseira myryca, and Caulerpa profilera	Au	~15	Spherical, triangle, and hexagonal	Antimicrobial Anti-inflammatory Schistolarvicidal activity	[185]
Digenea simplex	Au, ZnO and ZnO-Au	5–40	Spherical, rods, triangles. and hexagonal	Antioxidant Antitoxicity Anti-inflammatory wound healing activities	[186]
Undaria pinnatifida	Au	17.36 ± 2.49	Spherical	Obesity control	[187]
padina tetrastromatica	Au	10–70	Multiples	Anticancer	[188]
Chlamydomonas reinhardtii	Cu	< 10	Spherical	-	[189]
Padina boergesenii	CuO	5–17	Spherical	Control of fungal Bacterial growth Photocatalytic degradations of dyes	[190]
Padina tetrastromatica	CuO	~83	Lamellar	Antibacterial Anticancer	[191]
Ulva lactuca	Cu	-	-	Antioxidant	[192]
Padina pavonica	Fe3O4	10–21	Spherical	Remove dye Antioxidant	[193]
Spatoglossum asperum	Fe3O4	~16	Spherical	Antioxidant Anticancer	[194]
Spirulina	Fe3O4	~28.5	Multiples	Remove CV dye from wastewater	[195]
Pterocladia capillacea	Zn and ZnO	1000	-	Elimination of Organic Toxic Dye (absorption)	[196]
Tetraselmis indica	ZnO	27	Spherical	Antibacterial Antioxidant Hemolytic assays.	[197]
Kappaphycus alvarezii	ZnO	100–200	Spherical	Antimicrobial Anticancer	[198]
Elodea canadensis	Co	~14	Multiples	Antimicrobial	[199]
Padina gymnospora and Turbinaria ornata	SnO_2	3–25	Spherical	Antioxidant Antibacterial	[200]
Caulerpa racemosa, Codium fragile, and Cystoseira myrica	TiO_2	20–30	Tetragonal	Antibacterial	[201]
Bostrychia tenella and Laurencia obtusa, Halimeda tuna, Sargassum filipendula)	TiO_2	8–23	Spherical	Antifouling	[202]

Furthermore, the algae alone proved almost inoffensive, except for the maximum concentration of 200 mg (Fig. 7.A). The dye degradation assays with methyl green and methyl orange, showed an increased degradation over time when exposed to CuO NPs, with methyl orange continuously degrading less than methyl green. Other algae, such as *Padina tetrastromatica* [191], and *Ulva lactuca* [192] were also used for CuO or Cu NPs synthesis.

The seaweed *Padina pavonica*, containing significant amounts of carbohydrates, lipids, minerals, and vitamins, was used by Caf [193] to prepare Fe_3O_4 NPs for dye adsorption applications and neurotoxicity and antioxidant activity evaluation. Fe_3O_4 NPs with diameters within 10 and 20 nm and a zeta potential of −8.53 mV were produced; the zeta value indicates anionicity, as is usual with algae, but also low colloidal suspension stability. Concerning the removal of the dye, the outcome demonstrated that when the NPs concentrations were higher, the potential removal of dyes was significant and within a short period. In addition, the adsorption was faster under acidic conditions where the dye was cations and reacted with cations over the NPs surfaces. Human cells were used for *in vitro* evaluation of the toxicity of NPs, which indicated its toxicity only with high doses since the IC_{50} was at a concentration of 400 μg/mL (Fig. 7.B). Then, the antioxidant activity towards 2,2-diphenyl-1-picrylhydrazyl (DPPH) was measured, and it was found that they had an antioxidant activity of 39.6 %, whereas the extract had 70.96 %. *Spatoglossum asperum* [194] and *Spirulina* [195] were also utilised to synthesise Fe_3O_4 NPs.

Other than these metals, some different metals have been used in algae-assisted synthesis, such as Zn [186,196–198], cobalt [199], tin [200], and titanium [201,202]. Cobalt (Co) is one of the significant

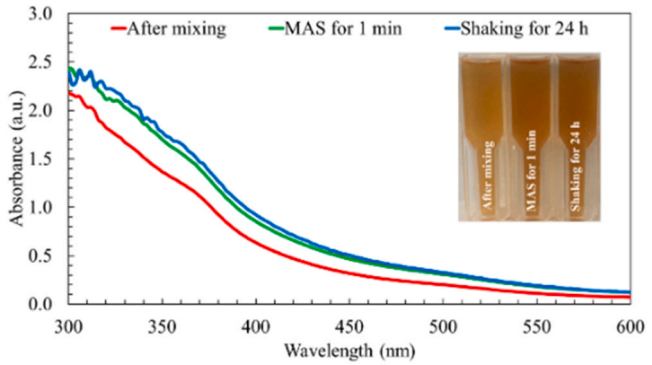

Fig. 5. Ultraviolet-visible spectroscopy (UV-Vis) absorption spectra of *Sargassum spp*. extract and Ag salt immediately after mixing, after 1 minute in the microwave, and after stirring for 24 hours. Adapted from [168].

materials with heat-resistant and magnetic properties. In biomedicine, Co NPs may be used in magnetic resonance imaging, drug delivery, and hyperthermia, besides having antibacterial, optical, and catalytic properties. Shu-Hua *et al.* [199] extracted from *Elodea canadensis* algae for Co NPs synthesis. For the extract, 5 g of algae was placed in 100 mL of distilled water, left overnight, and then heated at 80°C for 35 min, cooled, and microfiltered. The synthesis was done by mixing 10 mM of cobalt (II) nitrate with 30 mL algae extract, which showed a colour change after 90 min. FTIR results showed the presence of polyphenolic groups of O-H bonding aromatic C═O groups and carbonyl groups of proteins or amino acids possibly encapsulated the NPs, preventing their aggregation and growth.

Furthermore, Thirumoorthy *et al.* [197] used *Tetraselmis indica* algae as a precursor to obtain ZnO NPs. X-ray Diffraction (XRD) confirmed the wurtzite (HCP) crystalline structure in a spherical shape with an average diameter of 27 nm. SEM images showed diameters between 20 and 40 nm and 10–20 nm in TEM. The ZnO NP demonstrated antibacterial properties against *S. aureus* and *E. coli*. Other recent works synthesised Zn NPs using *Kappaphycus alvarezii* [198], *Pterocladia capillacea* [196], *Digenea simplex* [186], de Tin oxide with *Padina gymnospora* and *Turbinaria ornata* [200] and Titanium oxide using *Caulerpa racemosa, Codium fragile*, *Cystoseira myrica* [201] *Bostrychia tenella, Laurencia obtusa, Halimeda tuna, and Sargassum filipendula* [202].

3.3. Bacteria-mediated synthesis

3.3.1. Overview of bacteria biosynthesis mechanisms and advantages

Bacteria are no-nucleus, single-celled prokaryotic microorganisms whose forms are: rod-shaped, bacilli; spherical, cocci; spiral-shaped, spirilla; and helical, spirochetes, and some may attain several millimetres in length whilst others reach only several micrometres [203, 204]. The cell is simple while containing a cell wall, plasma membrane and cytoplasm, where all the metabolic activities take place [205]. Other bacterial components are flagella, providing them mobility; pili-adhesiveness; and plasmids-small fragments of DNA that can be passed from one bacterium to another and can transmit resistance to antibiotics [206]. Despite their simplicity, bacteria play a significant role in a series of ecological processes: they cycle nutrients, degrade organic matter, and fix nitrogen in soil [207]. Bacteria are applied from an ecological standpoint because they range through almost all possible ecological niches and could be capable of metabolizing a high number and variety of substances from environment control through food technology to biotechnology and onward [208].

Bacteria can synthesise NPs intracellularly, within the cytoplasm, or

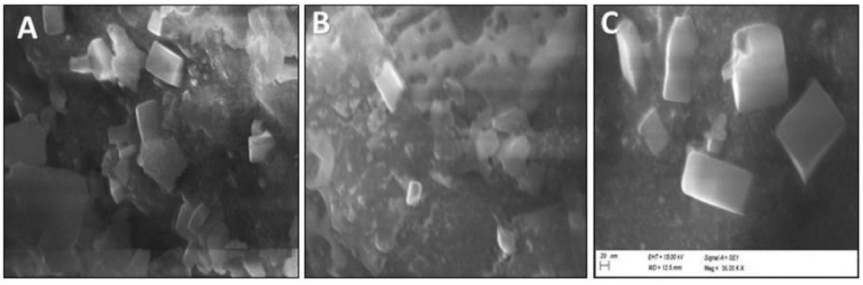

Fig. 6. (A-C) SEM images demonstrating the cubic shape of Au NPs at different magnifications.
Adapted from [184].

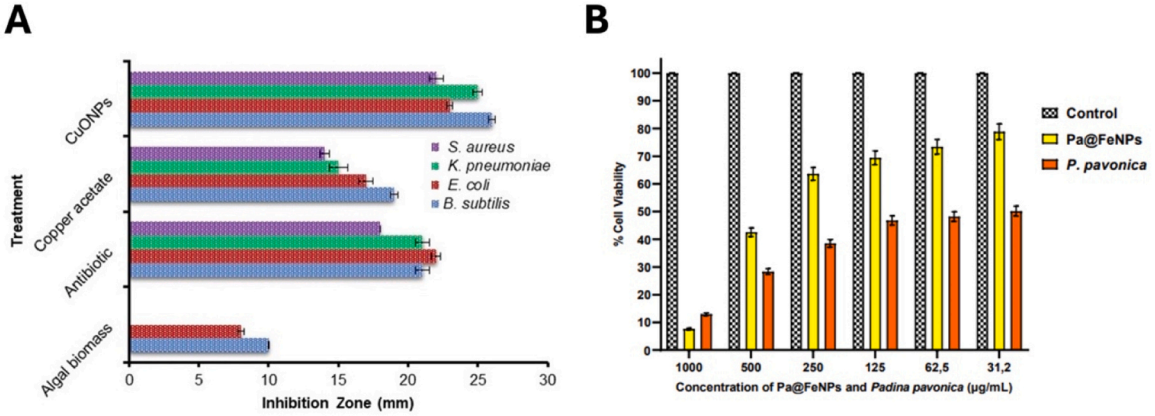

Fig. 7. (A) Inhibition zone of *S. aureus, K. pneumoniae, E. coli,* and *B. subtilis* bacteria subjected to algal biomass, antibiotics Cu acetate, and CuO NPs. (B) Percentage of viable cells according to the concentration of FeO NPs.
Adapted from [190] and [193].

extracellularly, outside the cell [209,210]. In short, the mechanism of intracellular synthesis relies on electrostatic interaction between metal ions that are attracted to the negatively charged membrane. In the case of extracellular synthesis, metal ions are reduced to form NPs by enzymes located on the bacterial cell membrane [211,212].

This reduction is normally mediated by enzymes or other biomolecules produced by bacteria, such as nitrate reductase, hydrogenase, and oxidoreductases, which act as electron donors, facilitating the transformation of metal ions into NPs. These enzymes play a crucial role in controlling nucleation and growth, influencing the size, shape and stability of the synthesized NPs [188]. Similarly, bacteria secrete extracellular polymeric substances, siderophores, and metal-binding proteins, which not only stabilize the synthesized NPs but also influence their physicochemical properties, preventing aggregation and enhancing biocompatibility [209,210]. These biomolecules act as nontoxic stabilizing agents, which exclude extra toxicity through synthetic capping agents to the process [213,214]. This natural stabilization process increases the NPs biocompatibility, which is required for medical and pharmaceutical applications [215,216]. However, some debate exists over NPs synthesis, where some authors point out that extracellular NPs synthesis is more favourable due to easier purification processes when compared to intracellular methods [211]. This method is not only eco-friendly but also offers a route to the synthesis of various NPs with different features [217].

The green synthesis mediated by bacteria is carried out through different steps. The exact methods and conditions for each one (e.g., culture medium composition, incubation times, metal ion concentration) can vary depending on the bacterial species and the targeted NPs' characteristics [218,219], but, in general, they include: (i) Selection of bacterial strain (based on its ability to reduce metal ions); (ii) Cultivation; (iii) Incubation with metal ions; (iv) Reduction and nucleation; (v) Growth and stabilization; (vi) Harvesting (the purification involves several techniques such as centrifugation, filtration, or others); (vii) Characterization; and (viii) Post-processing (optional) (Fig. 8).

3.3.2. *Bacteria-mediated metallic nanoparticle synthesis and applications*

Many bacteria, using different enzymatic and metabolic pathways, have been mediating the synthesis of NPs [211]. Table 4 overviews some bacteria synthesizing metallic NPs with their key associated elements. Some potential applications of bacterially-mediated NPs include medicine, pharmaceuticals, and material sciences [210].

The supernatant from *Bacillus coagulans* was used as a stabilizing and bioreducing agent to synthesize Fe_3O_4 NPs [220]. The process begins with cultivating *Bacillus coagulans* in Brain Heart Infusion (BHI) broth, followed by centrifugation to obtain the cell-free supernatant containing various biomolecules and metabolites. Those revealed an average size of 15 nm, an irregular cubic shape and a monodispersed distribution. Furthermore, they demonstrated antibacterial and antibiofilm activities, particularly against uropathogenic *E. coli* with a minimum inhibitory concentration (MIC) of 150 μg/mL. John *et al.* [221] have biosynthesized CuO NPs with bacteria isolated from an Antarctic consortium, which included *Marinomonas, Rhodococcus, Pseudomonas, Brevundimonas*, and *Bacillus*. First, the bacterial cultures were exposed to Cu sulphate, revealing resistance against concentrations up to 5 mM. The sizes of the NPs ranged from 10 to 70 nm and, thus, depending on the bacterial species, the sizes varied with the different metabolic pathways and secondary compounds produced by bacteria. The MIC for gram-negative bacteria showed between 3.12 and 25 μg/mL, for gram-positive bacteria between 12.5 and 25 μg/mL, and fungi between 12.5 and 25 μg/mL. This may be attributed to differences in sizes and shapes when undertaking antibacterial activities depending on the species of bacteria used in biosynthesis. It has been shown that 30 nm CuO NPs presented better activity against pathogens than the smaller NPs. The same group also used novel bacterial strains, *Rhodococcus, Brevundimonas* and *Bacillus* of the Antarctic consortium for Ag NPs synthesis. Spherical and rod-like NPs were obtained with sizes ranging from 20 to 50 nm [222]. They showed good stability having a negative charge of −32.8 mV, −29.6 mV, and −28.1 mV of *Rhodococcus, Brevundimonas*, and *Bacillus* respectively.

Ag NPs stand out due to their many potential applications, mainly in medicine. One strain of *Paenibacillus sp.* MAHUQ-63 was employed for rapid biosynthesis of Ag NPs and used to control the growth of human pathogens like *Salmonella Enteritidis* and *Candida albicans* [223]. The NPs demonstrated remarkable activity against the microorganisms with morphological and structural damage, proving the use of these bacterially-mediated Ag NPs as an effective antimicrobial agent [223]. *Bacillus pumilus* isolate ROM6 was also used to synthesize Ag NPs with a production efficiency of 90 % at $AgNO_3$ concentrations below 0.9 g/L, showing that 33 mL of supernatant could convert a significant percentage of silver ions into NPs [224]. Even though the synthesis process is not fully understood, the authors point to extracellular mechanisms that use proteins and enzymes (such as nitrate reductase) in the supernatant for the reduction. The Ag NPs revealed a size distribution between 20 and 70 nm and a MIC from 1.4 to 5.6 μg/mL against pathogens such as *S. aureus*, *E. coli*, *P. aeruginosa*, and *A. baumannii*.

Moreover, Ag NPs synthesized by *Aggregatimonas sangjinii* F202Z8T revealed sizes (27–82 nm) and shapes similar to the latter [225]. However, this type of NPs were synthesized intracellularly via nitrate reductase without external stressors or additives such as antibiotics, nutrient stress, or electron donors. The authors identified 17 putative

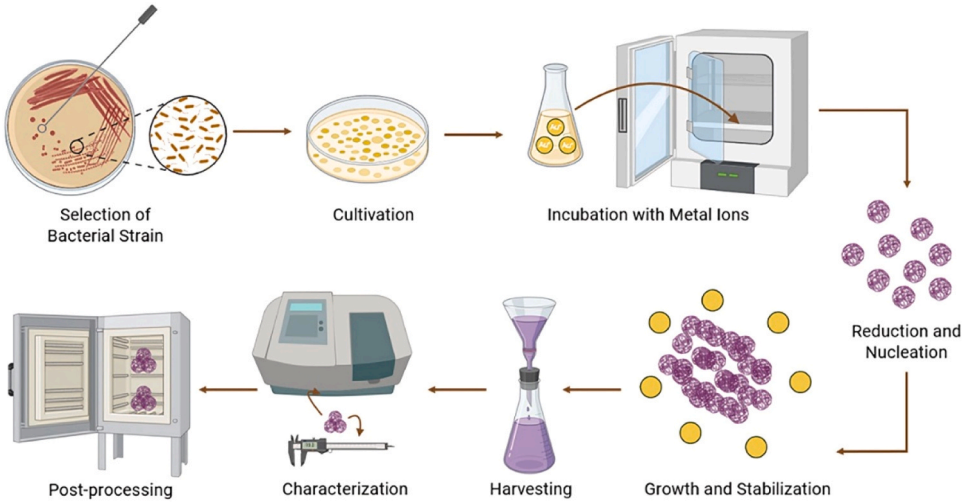

Fig. 8. Schematic representation of bacterially mediated green synthesis of MNPs.

Table 4
Representative list of recent advances in the green synthesis of several types of MNPs using bacteria.

Bacteria	NP	Size (nm)	Shape	Application	Extracellular and/or intracellular	Ref.
Bacillus coagulans	Fe_3O_4	~15	Irregular cubic	Antibacterial Antibiofilm	Extracellular	[220]
Marinomonas, Rhodococcus, Pseudomonas, Brevundimonas, and Bacillus	CuO	10–70	Spherical	Antibacterial	Extracellular	[221]
Rhodococcus, Brevundimonas and Bacillus	Ag	20–30	Spherical and rod-	Antibacterial Antifungal	Extracellular	[222]
Bacillus pumilus	Ag	20–70	Spherical	Antibacterial	Extracellular	[224]
Aggregatimonas sangjinii	Ag	27–87	Spherical	Antibacterial	Intracellular	[225]
Planococcus maritimus	Ag	24.9	Spherical to cubic	Antibacterial Antifungal Anticancer	Extracellular	[227]
Escherichia coli D8 (MF06257)	Ag	6–17	Spherical	Antimicrobial Antifungal	Extracellular	[228]
Pseudomonas alloputida B003 UAM	Ag	9.290–62.750	Quasi-spherical	Antibacterial	Extracellular	[229]
Enterobacter hormaechei	Ag	10–92	Spherical	Antimicrobial	Extracellular	[230]
Bacillus zanthoxyli GBE11	Ag	3–31	Spherical	Antimicrobial	Extracellular	[231]
Cytobacillus firmus	Ag	36–687	Spherical	Antimicrobial	Extracellular	[232]
Lactobacillus plantarum	Ag	~19.2	Spherical	Antimicrobial	Extracellular	[233]
Bacillus thuringiensis	Ag	748	Irregular	Antibacterial	Extracellular	[234]
Bacillus licheniformis	Ag	2–22	Spherical	Antibacterial	Intracellular	[235]
Vibrio alginolyticus	Au	100–150	Irregular	Antioxidant Anticancer	Extracellular	[236]
Rhodococcus Actinobacteria	Au	30–120 40–200	Spherical	Antimicrobial	Intracellular	[237]
Lysinibacillus sp. SH74	Zn	3–5	-	-	-	[238]
Streptomyces sp.	Zn	-	-	Antibacterial	-	[239]
Pseudomonas aeruginosa	Zn	6–21	Spherical	Antimicrobial Larvacidal	Extracellular	[240]
Lactobacillus	CdO	40,48,67	Spherical	Antibacterial	Extracellular	[241]
Pseudoalteromonas shioyasakiensis (PL 2476, AF 2469, and G 2451), and A. macleodii 2328	Se and Te	8–10	Spherical	Antimicrobial Antifouling Anticancer	Intracellular	[242]
Halomonas elongate and Salinicoccus iranensis	Se	30–100	Spherical	-	Intracellular	[48]
Raoultella planticola, Pantoea agglomerans	Ag, AgCl	10–50	Centered cubic crystal	Antimicrobial	-	[243]
Nocardia asteroids	Au	19	Spherical	Antibacterial	-	[244]
Pseudomonas aeruginosa	Se, Ag and Ag_2Se	10–15, 20–30, and 30–40	Spherical and cubic	Antibacterial Antibiofilm Photocatalytic	Extracellular	[245]
Priestia megaterium	Zn	5–14	Semi-spherical	Anticancer	Extracellular	[246]

genes that may play roles in the synthesis, including those involved in stimulating reductive factors, constituting components of the electron transport chain, and regulating enzyme activity [226]. Besides, *Planococcus maritimus,* a gram-positive halotolerant marine bacterium, was used to synthesize this type of NPs [227]. This is characterized by its ability to thrive in saline environments, making it an ideal candidate for biotechnological applications. The synthesis was mediated by extracellular processes, resulting in small, well-defined particles with an average size of 24.9 nm. These NPs exhibited minimal antibacterial activity against most tested strains except for *Pseudomonas aeruginosa*, which showed an inhibition zone of 11 mm. The maximum activity observed was towards the Aspergillus species: 14.33 mm for *Aspergillus niger* and 11.33 mm for *Aspergillus flavus*. Further cytotoxic effects were shown by the Ag NPs to Dalton's Lymphoma Ascites cell lines, with the maximum cell death of 95.4 % in a concentration of 20 μg/mL [227].

Moreover, the bacterial strain *E. Coli* D8 (MF06257) isolated from a sewage water stream in Egypt was used to synthesize Ag NPs with a cost-effective method within 1–2 minutes, and obtained an optimum size and shape for good antimicrobial activity between 6 and 17 nm [228]. The antibacterial potential showed significant inhibition zones, $P < 0.05$, against the test pathogenic microorganisms *S. aureus*, *E. coli*, *P. aeruginosa*, *A. alternata*, *Fr. Keissler*, *F. oxysporum*, and *A. flavus*. The Ag NPs also showed their synergistic effects with fluconazole to elevate the antifungal efficacy. Alternatives to bacterial antibiotic resistance were also explored by Pernas-Pleite *et al.* [229], with the help of Ag NPs synthesized with *Pseudomonas alloputida* B003 UAM culture broths. The size-tuned Ag NPs ranging in size of 9–62 nm were evaluated for their antibacterial activity against *Bacillus subtilis, Escherichia coli, Klebsiella pneumoniae, Pseudomonas aeruginosa, Staphylococcus aureus*, and *Staphylococcus epidermidis*, presenting low MICs values for *Pseudomonas*. Finally, Monowar *et al.* [230] utilized *Enterobacter hormaechei* in the extracellular biosynthesis of spherical, well-dispersed Ag NPs with a zeta potential of -19.73 ± 3.94 mV. The antimicrobial activity against *B. Cereus, S. aureus*, and *C. albicans*, with a biofilm formation ability, showed a bigger zone of inhibition compared to the conventional antibiotics.

Other bacteria used to biosynthesize Ag NPs include *Bacillus zanthoxyli GBE11* [231], *Cytobacillus firmus* [232], *Lactobacillus plantarum* [233] *Bacillus thuringiensis* [234], and *Bacillus licheniformis* [235].

Besides Ag NPs, other bacterial-synthesized NPs have been explored for biological applications. Au NPs, synthesized with the marine microbe *Vibrio alginolyticus,* were explored for cancer treatment [236]. The Au NPs (100–150 nm) showed dose-dependent inhibitory effects against colon carcinoma cells; 15 mg/mL was the IC_{50} value. Test concentration was increased to 25 mg/mL; over 75 % of the cells died, which signified apoptotic-mediated cell death. Au NPs were also synthesized using *Rhodococcus ruber* IEGM 1135, where the particle size was 40–200 nm, with a surface charge of 22 mV, while those from *Rhodococcus*

erythropolis IEGM 766 were smaller, between 30–120 nm, and positively charged at 12 mV [237]. These differences were due to the variety of biomolecules (like proteins, polysaccharides, and organic acids) present in each bacterium which acted as capping agents.

Furthermore, Zn NPs have also been synthesized using, for instance, *Lysinibacillus sp*. [238] and *Streptomyces* species [239]. Furthermore, *Pseudomonas aeruginosa* was used to synthesize this type of NPs following Eq. 4. Their antibacterial and antifungal activity was tested against various bacteria and one unicellular fungus, and the results have demonstrated that the efficacy increases with increasing NP concentration (Fig. 9). The larvicidal activity against *Culex pipiens* reached 56 % after 96 hours at a low concentration of 50 ppm.

$$Zn(CH_3COO)_2 \bullet 2H_2O + CFF \xrightarrow{Stiring} ZnO \bullet H_2O(white\ precipitate) \quad (4)$$

Moreover, CdO NPs were synthesized using Lactobacillus species and their antibacterial activity was studied against fish pathogens *Serratia marcescens*, *Aeromonas hydrophila*, *Vibrio harveyi*, and *Vibrio parahaemolyticus* [241]. 20 mM concentration showed the highest efficacy against all fish pathogens studied, which can be due to the mechanisms of action associated with CdO NPs, including damage to the cell wall of microbes, inhibition of DNA synthesis, and damage to DNA upon entering the cell wall or plasma membrane. In turn, Beleneva et al. [242] isolated four strains of the marine bacteria Pseudoalteromonas shioyasakiensis (PL 2476, AF 2469, and G 2451) and *A. macleodii* 2328. The SEM images showed the formation of Se NPs and Te NPs with sizes between 8 and 10 nm at the surface of the bacteria. The zeta potential of Se NPS was between −20.1 mV and −23.4 mV, while the Te NPs were around −25 mV. The results showed Te NPs are more effective against microbial while Se NPs are more toxic against human dermal fibroblasts and breast cancer cells. Furthermore, Tabibi *et al.* [48] performed the intracellular green synthesis of Se NPs with 1 μL of two different indigenous halophilic bacteria (*Halomonas elongate* and *Alinicoccus iranensis*) varying the Na_2SeO_3 molar concentration (2–8 mM). The maximum Se NPs production was achieved with 8 mM for H. elongate and 6 mM for *S. iranensis*. Spherical NPs with 30 and 100 nm sizes and zeta potentials of −60.6 mV and −51.2 mV were obtained for *S. iranensis* NPs and *H. elongate*, respectively.

3.4. Yeast-mediated synthesis

3.4.1. Overview of yeast biosynthesis mechanisms and advantages

Yeast is a non-pathogenic, unicellular eukaryotic microorganism, a member of the Kingdom Fungi, and classified into two phyla: Ascomycota and Basidiomycota [247]. These microorganisms reproduce either sexually or asexually. The latter is the most common and is grouped as budding yeasts (*Zygosaccharomyces*) and fission yeasts (*Schizosaccharomyces*) [248,249]. Some of the about 1500 reported species are currently used in a wide range of applications. Its most recognized application is in the food industry, and it is used in baking, winemaking, and brewing [250]. Furthermore, they are also used in heterogeneous compounds, biomass production (single-cell proteins), and the biofuels industry [247]. Researchers have recently explored yeast-reducing enzymes as biofactories of metallic NPs, either by extracellular or intracellular routes, including Ag, selenium, titanium, palladium (Pd), cadmium sulfide, and gold NPs [251,252].

Yeast-mediated MNPs biosynthesis is intimately linked with a cellular detoxification mechanism observed in yeast [253]. This mechanism is an adaptive response to metal ion-induced stress, aiming to neutralize excess metal ions and prevent cellular damage. Metal-binding ligands, including phytochelatins, metallothioneins, and glutathione, play crucial roles in metal tolerance and, consequently, MNPs synthesis [253,254]. For example, *Schizosaccharomyces pombe* can scavenge free cadmium ions and synthesize glutathione- and metallothionein-capped cadmium NPs [255]. The interest in this type of microorganism is related to its rapid growth, ease of control in the laboratory using a simple nutrient culture medium, and the synthesis of numerous enzymes [256,257]. As a result, the mass production of metal NPs is facilitated by yeast over bacteria. MNPs are classified as intracellular or extracellular according to the location where they are formed in the yeast. The yeast's intracellular biosynthesis of metal NPs occurs by reducing metal ions inside the yeast cell. In contrast, in extracellular biosynthesis, the metal ions are trapped on the yeast cell wall [258].

In intracellular synthesis, the process begins with the electrostatic interaction between positively charged metal ions and the negatively charged components of the yeast cell wall, facilitating the passive diffusion of metal ions into the cell. Once inside, membrane-bound oxidoreductases and quinones reduce the metal ions, with their enzymatic activity influenced by environmental factors, such as pH [212,257,259]. A pH increase activates pH-sensitive enzymes like nitrate reductase, further driving metal ion reduction through a cascade of redox reactions, leading to MNP formation in the periplasmic space, cytoplasmic membrane, or cell walls [212,257,259].

Extracellular synthesis, on the other hand, involves the secretion of enzymes, such as nitrate reductase, into the surrounding environment or

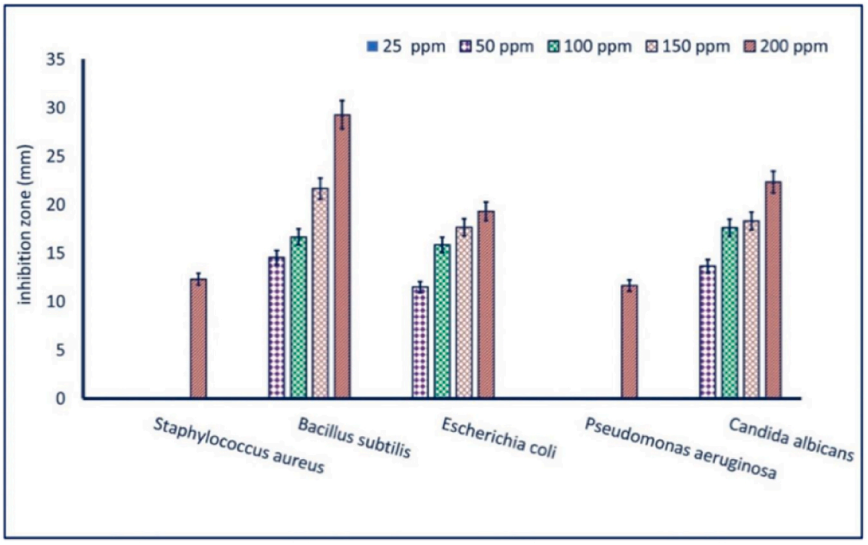

Fig. 9. Inhibition zone of S. aureus, B. subtilis, E. coli, P. aeruginosa, and C. albicans submitted at different concentrations of ZnO NPs. Adapted from [240].

their binding to the cell wall, where they catalyze the reduction of metal ions and facilitate MNPs nucleation [212]. In both pathways, yeast metabolites — including carbonyl groups, terpenoids, phenols, amines, and proteins — contribute as reducing and stabilizing agents, aiding in MNPs formation and stability. Glutathione and phytochelatins, with their redox and nucleophilic properties, bind to metal ions, promoting bioreduction and further supporting MNPs synthesis [253]. These mechanisms reflect yeast's natural stress response and metal detoxification strategy. However, while MNPs formation helps mitigate metal toxicity, there is currently no evidence that yeast utilizes these biosynthesized NPs for metabolic purposes [253,254].

After synthesis, NPs must be recovered and purified. Intracellularly synthesized NPs require physical or chemical cell lysis for release [260, 261], whereas extracellular NPs can be collected more easily through methods like centrifugation or dialysis [261,262]. The choice of intracellular or extracellular synthesis depends on the desired NPs characteristics and ease of downstream processing. Fig. 10 exemplifies yeast biosynthesis through intracellular and extracellular mechanisms.

3.4.2. *Yeast-mediated metallic nanoparticle synthesis and applications*

Yeasts have been shown to synthesize several semiconductor-type NPs. Table 5 provides an overview of several yeasts synthesizing MNPs and some of their major associated elements.

Among the most abundant NPs biosynthesized by yeasts, cadmium sulfide (CdS) NPs are an interesting material for applications in electronics and photonics. Literature reports on the use of various yeast strains for such a purpose, including *Schizosaccharomyces pombe* [263, 264], *Saccharomyces cerevisiae* [265], and *Candida glabrata* [264]. Further, El-Baz *et al.* [266] reported the syntheses of CdS NPs by estimating the growth in yeast strain *Trichosporon jirovecii* with a culture medium enriched in cadmium and cysteine.

Basically, the mechanism of synthesis is based on the intrinsic cadmium detoxification defence mechanism of yeast, which is elicited in the presence of cadmium. Sulfite represents the reducing agent in this mechanism, providing conditions for CdS NPs formation.

Also, Au NPs are particularly interesting to researchers because of their catalytic, electronic, and photophysical properties. Similar to CdS NPs, a number of yeasts have also been reported for the synthesis of Au NPs; For example, *Saccharomyces cerevisiae* [267,268], *Yarrowia lipolytica* [269], *Pichia jadinii* [270], and *Magnusiomyces ingens* [271]. Similar yeast were also presented for the synthesis of Au NPs belonging to different morphologies, as reported for yeast *Pichia jadinii* [270]. Subsequently, *Yarrowia lipolytica* [269] was used to produce different sizes and morphologies of Au NPs by varying the concentrations of chloroauric acid.

Concerning *Saccharomyces cerevisiae*, it has been documented that it can synthesize Au NPs using the free aldehyde group from reducing sugars on the peptidoglycan layer as an electron donor and reduce Au^{3+} to Au^{0} [267]. Lim *et al.* [268] synthesized Ag (5–20 nm) and gold (20–100 nm) NPs with *Saccharomyces cerevisiae* by varying the pH of the medium. It has been reported that the reduction of gold is favoured in an acidic medium whereas Ag reduction was preferred in an alkaline medium.

Zhang *et al.* [271] firstly reported the use of *Magnusiomyces ingens* LH-F1 for synthesizing Au NPs. In this study, several Au NPs shapes and sizes, including sphere, plate, and irregular ones, were synthesized. The length of the plates varied between 16 and 420 nm, and the diameter of the spherical particles varied in the range of 10–80 nm. According to these authors, Au^{3+} ions could be reduced to Au^{0} by biomolecules, unidentified, in the cytoplasm or cell surface. Then, the Au^{0} nanocrystals were capped and stabilized before being released from the cells. Lian *et al.* [272] used *Magnusiomyces ingens* in the synthesis of Se NPs (Se NPs). The work evidenced that the Se NPs were synthesized as spherical shaped, with diameters in the range of 70–90 nm. The results evidenced that Se NPs had antibacterial effects against *Arthrobacter sp.* W1 (Gram-positive). Recently, a novel strain of *Rhodotorula mucilaginosa* R-8441 was documented to synthesize spherical-shaped Se NPs, with a diameter of 83 nm, and rod-shaped particles, with a diameter of 478 nm, intra and extracellular [273].

Furthermore, ZnO spherical NPs were prepared by *Saccharomyces cerevisiae* with diameters ranging between 13 and 20 nm and showing good antibacterial activity against gram-positive *S. aureus* [274]. Besides, they exhibited good photocatalytic activity, reaching 83 % degradation of *Eriochrome Black* T at equilibrium. This type of NPs has

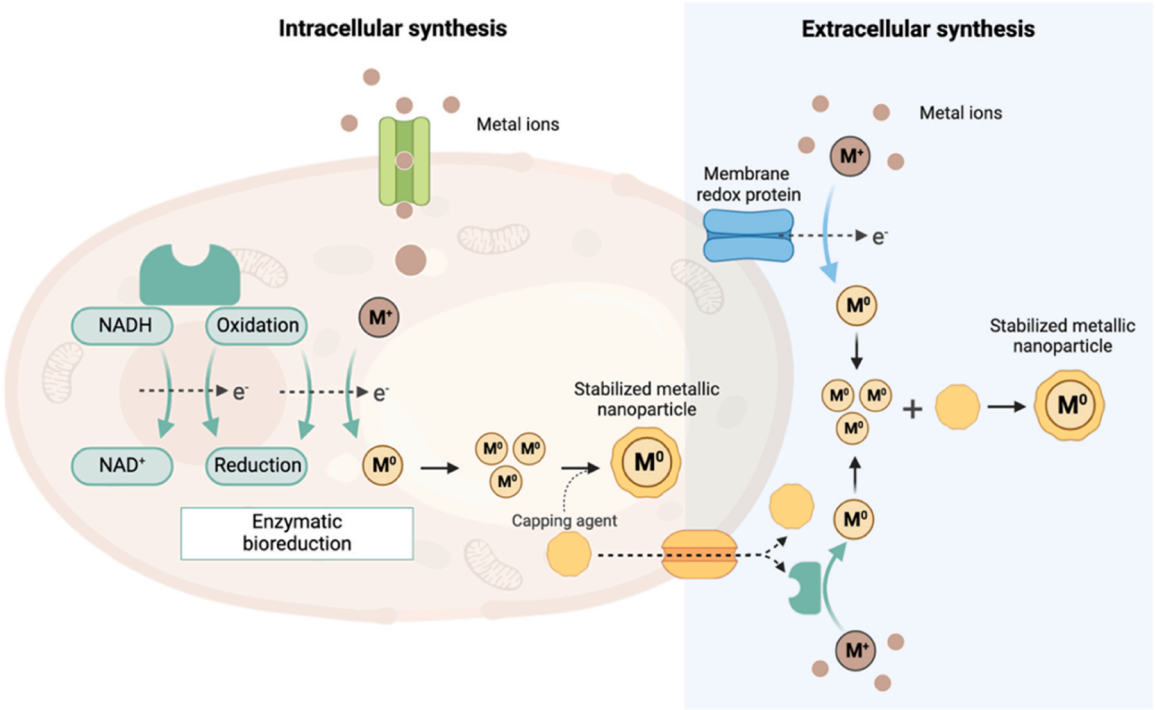

Fig. 10. Schematic representation of yeast biosynthesis intracellular and extracellular mechanisms.

Table 5
Representative list of recent advances in the green synthesis of several types of MNPs using yeast.

Yeast	NP	Size (nm)	Shape	Application	Extracellular and/or intracellular	Ref
Schizosaccharomyces pombe	CdS	1–1.5	Hexagonal	-	Intracellular	[263]
Schizosaccharomyces pombe	CdS	-	-	-	Intracellular	[264]
Saccharomyces cerevisiae	CdS	0.5–4.7	Spherical	Fluorescence and Electrochemical Detection	Intracellular	[265]
Trichosporon jirovecii	CdS	6–15	Spherical	-	Intracellular	[266]
Sachharomyces cerevisiae	Au	-	-	-	Intracellular	[267]
Saccharomyces cerevisiae	Au	20–100	Spherical	-	Extracellular	[268]
Yarrowia lipolytica	Au	Varied	Nanoplates and spherical	-	Intracellular	[269]
Pichia jadinii	Au	< 100	Spherical, triangular, and hexagonal	-	Intracellular	[270]
Magnusiomyces ingens	Au	Plate-shaped: 16–420 Spherical-shaped: 10–80	Spheres, plates (triangle, hexagon, pentagon), and irregularly shaped	Catalytic reduction of nitrophenols	Intracellular	[271]
Magnusiomyces ingens	Se	70–90	Spherical	Antibacterial	Intracellular	[271]
Rhodotorula mucilaginosa	Se	83 and 478	Spherical and rod	-	Intracellular and extracellular	[273]
Sachharomyces cerevisiae	ZnO	13–20	Spherical	Antimicrobial Photocatalytic	-	[274]
Pichia kudriavzevii	ZnO	10–61	Hexagonal	Antimicrobial Antioxidant	Extracellular	[275]
Saccharomyces cerevisiae	Ag	10	Spherical	Photocatalysis	-	[276]
Saccharomyces cerevisiae	Ag	16.07	Spherical	Antibacterial	-	[277]
Saccharomyces cerevisiae	Ag	2–20	Spherical	-	Intracellular	[277]
Saccharomyces cerevisiae	Ag	15	Spherical	Antimicrobial	Extracellular	[278]
MKY3	Ag	3.6	Hexagonal	-	Extracellular	[279]
Candida lusitaniae	Ag/AgCl	2–10	Spherical	Antibacterial	Intracellular and extracellular	[280]
HX-YS	Ag	50–100	Spherical	Antibacterial	-	[281]
LPP−12Y	Ag	50–100	Spherical	Antibacterial	-	[281]
Yarrowia lipolytica	Ag	15	Spherical	Antimicrobial	Intracellular	[282]
Yarrowia lipolytica	Ag	50	Spherical	Biodiesel Synthesis	Intracellular	[283]
Rhodotorula mucilaginosa	Cu_2O	51.6–111.4	Spherical	Anticancer	-	[284]
Saccharomyces cerevisiae	Pd	32	Hexagonal	photocatalytic	-	[285]
Saccharomyces cerevisiae	Se	6 and 153	Spherical	Antifungal	Intracellular	[286]
Saccharomyces cerevisiae	Se	75–709	Spherical	-	Intracellular	[287]
Saccharomyces cerevisiae	Ag	60	Spherical	Antimicrobial	-	[288]
Pichia kudriavzevii	Ag	12	Cubic	Biomedical	-	[289]
Saccharomyces uvarum	Ag	20	Cubic	Biomedical	-	[289]
Pichia fermentans JA2	ZnO	-	Rectangular	Antimicrobial	Extracellular	[290]

also been prepared with a new yeast strain called *Pichia kudriavzevii* [275]. In the synthesis process, a reaction of thermal decomposition was initiated by complexing Zn ions with hydroxyl groups of amino acids. Amino acids were the stabilizers, keeping the NPs stable.

Additionally, the synthesis of Ag NPs is widely described in the literature using yeast, which includes *Saccharomyces cerevisiae* [276–278], Ag-tolerant yeast strain MKY3 [279], and *Candida lusitaniae* [280]. Moreover, Liu *et al.* [277,281] reported the ability of two novel yeast strains (HX-YS and LPP-12Y) to synthesize Ag NPs. According to the yeast strain, the results revealed different optimum pHs for Ag NPs synthesis. The authors concluded that the synthesis of Ag NPs was not only related to the concentration of OH^- and H^+ (which affects the reduction of Ag^+) but also to the reducing substances present in the fermentation broth. Also, *Yarrowia lipolytica* (NCYC 789) facilitates the synthesis of well-defined 15 nm-sized Ag NPs by leveraging the quinonic residues found in its cell-associated melanin [282]. These residues can reduce Ag ions, transitioning between their hydroxyl and quinonic forms. More recently, Katharine *et al.* [283] reported to synthesize Ag NPs (50 nm) *Yarrowia lipolytica* (MTCC 9520) using goat tallow as the carbon source.

For the first time, Hassabo *et al.* [284] studied the synthesis of Cu_2O NPs using marine yeast, isolating twenty yeast isolates from the Red Sea and Giftun island samples. The yeast phenolic compounds (phenols and polyphenols) acted as electron donors, reducing Cu^{+2} to Cu^{+1}, forming Cu_2O. Then, the NPs were further stabilized by the biomolecules present in the marine yeast. Pd NPs were also green synthesized using *Saccharomyces cerevisiae* and have demonstrated photocatalytic activity towards a dye [285].

3.5. Fungi-mediated synthesis

3.5.1. Overview of fungi biosynthesis mechanisms and advantages

The fungal kingdom forms a separate lineage within the eukaryotic domain. Unlike plants, their nutritional mode is heterotrophic; fungi must decompose organic matter to fulfil their nutritional needs. Such decomposition is done through the hyphae, complex networks of filaments that dig into soils and dead organisms. The hyphae drive nutrient cycling and forge important symbiotic relationships with plants through mycorrhizae, whereby the symbionts facilitate root systems and efficiency in nutrient uptake. Apart from decomposers, fungal diversity extends into the flagrant fruiting bodies, such as mushrooms. Another important division within the tree of life of fungi comes with the unicellular yeasts, which are so important in bread baking and fermentation processes [291].

When subjected to stressors such as toxic molecules, temperature, or nutrient deprivation, fungi induce the synthesis of a wide range of biological molecules and enzymes. Such inducible phenomena comprise a strong defence response of fungi to inactivate, or simply tolerate, such extracellular stresses. One such phenomenon is the interaction of fungi with metal ions. Conventionally, these metals are quite detrimental to

fungal survival. However, certain fungal species can convert toxic metals into non-toxic metallic NPs via extracellular enzymes and metabolites [292–295]. This is driven by enzymatic reduction mechanisms that facilitate metal ion transformation and stabilization, mainly through key enzymes such as laccase, reductase and peroxidase. Laccase, a multicopper oxidase, enhances electron transfer, promoting the reduction of metal ions such as Ag^{+} and Au^{3+}. Similarly, fungal reductases catalyse electron transfer reactions, influencing NP nucleation, while peroxidases contribute to oxidative transformations that stabilize metal ions during synthesis [296,297]. It has been demonstrated that in fungi, NPs can be synthesised intracellularly, extracellularly or on the cell surface. Extracellular synthesis of NPs has many advantages compared to intracellular NPs synthesis. For instance, it is more rapid and easily scalable. This is because, during extracellular synthesis, fungi can produce enormous amounts of enzymes and other relevant compounds secreted into the environment, such as extracellular polysaccharides, proteins and siderophores, which function as natural capping agents, enhancing NP stability and preventing aggregation [298]. In intracellular synthesis, these biomolecules accumulate in the fungal cells which could limit production [299–301]. The exact mechanism of extracellular synthesis of Ag NPs in fungi depends on the species. In *Fusarium oxysporum*, the reduction of nicotinamide adenine dinucleotide phosphate (NADPH) to oxidized form ($NADP^{+}$) by enzymes such as nitrate-dependent reductase and the involvement of shuttle quinones are thought to be involved in this process [302,303].

Similarly, the synthesis of Ag NP by *Aspergillus terreus* was catalyzed using the NADH-dependent reductase enzymes to conduct the reduction reaction [304]. On the other hand, Chan and Mashitah [305] have suggested that the diketone compounds might be the responsible agents for reducing Ag ions by the action of many types of macrofungi, which might constitute yet another different mode. Notably, Sastry *et al.* [306] identified intracellular synthesis of Ag NP in *Verticillium sp.*, and now it has turned out to be another different pathway, which differs among the fungal species.

The variety of meta-abilities, the ease of cultivation, and the eco-friendliness of fungi make them very promising candidates for the green synthesis of NPs [307]. Even though the clear synthesis mechanisms are not yet known, it is theorized that biomolecules—mainly fungal enzymes, proteins, and metabolites—are agents responsible for interaction with the metal precursors. For instance, reductase and laccase can act as reducing agents to transform metal ions into elemental nanoparticulate form. Moreover, biomass can provide capping and stabilizing agents, preventing agglomeration of NPs and influencing their size and shape [291]. Furthermore, different species of fungi have different metabolic profiles and enzymatic activities, which result in NPs with different features.

Fungal-mediated green synthesis typically involves five key steps: (i) Fungal selection and preparation (based on the fungi enzymatic profile and desired NPs features); (ii) Metal precursor selection; (iii) Biosynthesis (reduction, capping and stabilization); (iv) Purification and characterization; and (v) Optimization (Fig. 11).

3.5.2. *Fungi-mediated metallic nanoparticle synthesis and applications*

Researchers actively explore various fungi to optimise NP production and tailor their properties. These NPs are attractive for different fields because of their antimicrobial, antioxidant, and catalytic properties. Table 6 provides an overview of several fungi synthesizing MNPs and some of their major associated elements.

The agricultural sector is escalating its demands for better sustainable methods for pest decrease and yield fight pests, fungi and bacteria that affect plants. In turn, mycogenic NPs have been synthesised for pest control. At the same time, these NPs can also help monitor or detect plant diseases, thereby serving as an alternative tool to reduce the dosage of chemical pesticides. Using NPs for pest control decreases the environmental impact and provides an ecologically friendly alternative to conventional chemical pesticides with adverse ecological effects [308,309]

Elgorban *et al.* [310] synthesised spherical shape Ag NPs with a size ranging between 5 and 30 nm using the fungus *Aspergillus versicolor* for disease control in strawberries. The NPs were then evaluated for their antifungal activity against *Sclerotinia sclerotiorum* and *Botrytis cinerea,* two major fungal pathogens affecting strawberry plants, revealing an inhibition of 80.38 % and 74.39 % of the higher tested NPs dose, respectively. Further, current studies indicate that using fungal NPs impacts plant nutrient uptake, positively affecting crop yield [311,312]. Moreover, these NPs can also be designed to deliver nutrients and pesticides to plants and crops. Thus, less waste is produced, and the adverse effects of modern farming on the environment may be effectively reduced [313]. Biosynthesis of ZnO NPs was carried out using *Aspergillus niger* biomass, and the larvicidal efficacy was calculated with white grubs (*Holotrichia sp.*), which is a serious pest in the sugarcane crop [314]. Biosynthesis had been initiated by the grinding of fungal biomass followed by the mixing of the same with an aqueous solution of Zn nitrate hexahydrate. Characterization studies exhibited sizes between 76.2

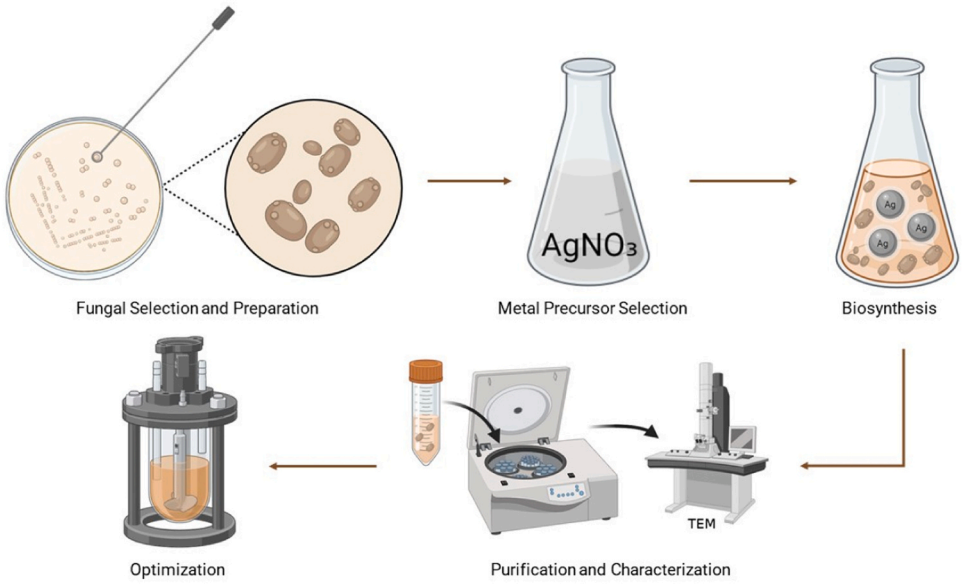

Fig. 11. Main steps in fungi-mediated green synthesis of MNPs.

Table 6
Representative list of recent advances in the green synthesis of several types of MNPs using fungi.

Fungi	NP	Size (nm)	Shape	Application	Extracellular and/or intracellular	Ref.
Aspergillus niger	ZnO	76–183	Spherical	Biopesticide	Extracellular	[314]
Pseudomonas fluorescens, Trichoderma atroviride, and Streptomyces griseus	SiO2	20–100	Irregular spherical	Plant disease management	Extracellular	[315]
Trichoderma harzianum	Ag	5–18	Spherical	Antifungal	Extracellular	[318]
	CuO	38–77 width 135–320 nm length	Elongated fibres			
	ZnO	27–40 width 134–200 nm in length	Fan and bouquet	No action		
Bacillus megaterium	Se	~45	Spherical	Antifungal	Extracellular	[319]
Beauveria bassiana, Metarhizium anisopliae, and Isaria fumosorosea	Ag	varied	Spherical	Insecticidal	Extracellular	[320]
Trichoderma harzianum	ZnO	8–23	Hexagonal, spherical and rod	Fungal antagonist	Extracellular	[321]
Trichoderma harzianum	Ag	6–5	Spherical	Antifungal	Extracellular	[322]
Agaricus bisporus	Ag	67–102	Quasi-spherical	Antimicrobial	-	[323]
Fusarium oxysporum	Ag	5–13	Spherical	Antimicrobial Anticancer	Extracellular	[324]
Guignardia mangiferae (Bios PTK 4)	Ag	5–30	Spherical	Antibacterial Antifungal Anticancer	Extracellular	[325]
Aureobasidium pullulans (ATCC 201253)	Ag	15.1	Spherical	Antibacterial Medical Food packaging	Extracellular	[326]
Trichoderma viride	ZnO	63.3	Hexagonal	Antimicrobial Antibacterial	-	[330]
Xylaria arbuscula	ZnO	-	Hexagonal	Antimicrobial Antioxidant Antinflammatory Antidiabetic Wound healing	Extracellular	[335]
Penicillium oxalicum	Fe	140	Spherical	Decolourisation	-	[337]
Fusarium solani	Au	40–45	Flower	Anticancer	Extracellular	[338]
Trichoderma reesei	Ag	2–25	Spherical	Antibacterial	Extracellular	[339]
Laetiporus versisporus	Au	10	Spherical	Antioxidant	Extracellular	[340]
Rhizopus oryzae	MgO	~20	Spherical	Antimicrobial Mosquitocidal Tanning Effluent Treatment	Extracellular	[341]
Aspergillus terreus	Se	< 100	Spherical	Antimicrobial Decolourisation	Extracellular	[342]

and 183.8 nm. The larvicidal activity of the synthesized ZnO NPs was tested with first-instar larvae of white grubs; larvae started to die within 12 h, and the calculated median lethal dose (LD_{50}) was 12.63 ppm.

Furthermore, SiO_2 NPs biosynthesised using indigenous biocontrol agents like *Pseudomonas fluorescens*, *Trichoderma atroviride*, and *Streptomyces griseus* were also used for plant disease management [315]. The size ranged from 20 to 100 nm with an irregular spherical morphology. The efficacy of NPs was tested on tea pathogens, specifically *Poria hypolateritia* (associated with red root-rot) and *Phomopsis theae* (associated with Phomopsis canker diseases). The highest growth inhibition for *P. theae* was observed with silica NPs synthesised from P. fluorescens at 40 ppm concentration, achieving a rate of 62.16 % on the 15th day of incubation. For *P. hypolateritia*, the silica NPs synthesised from *T. atroviride* showed a notable inhibition rate of 74.76 % at a 3-ppm concentration on the third day of incubation.

Fungus-mediated NPs have been demonstrating significant antimicrobial properties due to their ability to attach the cell walls of microorganisms, penetrate the cell interior, and cause damage to cellular structures, thus proving effective against pathogens [316]. Fátima *et al.* [317] investigated the biological properties of Ag NPs bath-sonicated from the filtrate of *Aspergillus flavus*. These biogenic NPs exhibited a considerable potential bactericidal effect toward many species, comprising *Bacillus cereus*, *Bacillus subtilis*, *Enterobacter aerogenes*, *E. coli*, and *S. aureus*, with *B. subtilis* and *E. coli* being the most susceptible. More importantly, when applied in combination with the tetracycline antibiotics, it complemented the Ag NPs such that it gave a higher inhibition efficacy on the growth of bacteria than when applied alone. Additionally, the NPs also show a dose-dependent antifungal activity against *Aspergillus niger* and *Trichoderma harzianum*.

Also, Consolo *et al.* [318] used a cell-free culture filtrate of *Trichoderma harzianum* for the biosynthesis of Ag, CuO, and ZnO NPs from this fungus, with CuO and ZnO biosynthesis described in the literature for the first time. Ag NPs were chosen because they exhibit antimicrobial activity against bacteria, fungi and viruses; Crop diseases caused by fungi and bacteria have been reduced by CuO NPs due to multisite mode of action, offering less chance for pathogen resistance; and antibacterial activity of ZnO was attributed to photo-oxidising, photocatalytic effects and was considered biosafe. The NPs showed different morphology as well as size although the synthesis parameters were identical. The Ag NPs were spherical with sizes of 76.2–183.8 nm; CuO NPs appeared to be elongated fibres with 38–77 nm in width and 135–320 nm in length; Finally, the ZnO NPs appeared to have fan and bouquet shapes with sizes ranging between 27–40 nm in width and 134–200 nm in length. Both Ag and CuO NPs exhibit similar dose-dependent inhibition of mycelial growth against the phytopathogens *Alternaria alternata, Pyricularia oryzae* and *Sclerotinia sclerotiorum*. In contrast, for the ZnO NPs, no antifungal behaviour against these studied phytopathogens was detected.

Other recent works on describing fungi biosynthesis MNPs for agriculture applications include *Bacillus megaterium* [319], *Beauveria bassiana, Metarhizium anisopliae,* and *Isaria fumosorosea* [320], *Trichoderma*

harzianum [321,322], *Agaricus bisporus* [323].

Husseiny *et al.* [324] explored the potential of Ag NPs synthesised by *Fusarium oxysporum* for anticancer applications. It was noted that these NPs effectively inhibited the growth of *E. coli* and *S. aureus* bacteria, which have a cytotoxic impact on tumour cells. When exposed to the NPs, the MCF-7 cells, human breast adenocarcinoma cell lines, attained a low IC_{50} value of 121.23 μg/cm^3. The low value obtained shows high cytotoxicity and, therefore, can be highly used to control tumours. The authors believe that the NPs disrupt mitochondrial respiration in the tumour cells, generating toxic reactive oxygen species that interfere with the synthesis of Adenosine triphosphate, the molecule responsible for energy production. This ultimately damages the tumour cell's nucleic acids, potentially leading to its death.

Likewise, in their investigation of the anti-tumour potential of fungal-derived Ag NPs, *Balakumaran et al.* [325] evaluated their cytotoxic effects on HeLa (human cervical carcinoma) and MCF-7 tumour cells, along with normal Vero cells derived from African monkey kidney. The study revealed a higher degree of cytotoxicity towards the tumour cell lines when compared to the normal Vero cells. Microscopic examination further indicated that the tumour cells underwent apoptosis, a programmed cell death characterised by condensed nuclei, membrane damage, and apoptotic bodies [325]. These findings suggest the potential of these green-synthesised NPs for targeted cancer therapy.

Moreover, scientists are investigating the numerous opportunities associated with using fungi to develop new innovative materials that can find application in, for instance, food preservation and medicine. Wypij *et al.* [326] studied a new film material derived from natural sugar, pullulan, synthesised by the fungus *Aureobasidium pullulans*. Spherical Ag NPs with sizes in the range of 4–46 nm were incorporated into the pullulan using a green synthesis approach mediated by another fungus, *Fusarium culmorum* (JTW1 strain) (Fig. 12) [326]. The resulting films were evaluated for various properties, including water resistance, light-blocking ability, and antibacterial activity against foodborne pathogens and other bacteria. Including Ag NPs in prepared films slightly decreased water absorption and transmission of light, and at the same time, it kept smoothness. Strong antibacterial properties were determined in samples containing Ag NPs and in the films with incorporated NPs: the highest activity was registered against *Listeria monocytogenes*, a bacterium often responsible for food spoilage. Thus, it can be concluded that films made from pullulan extracted from fungi and biogenetic Ag NPs could be useful for developing more effective protective food packaging and medical products because of their natural antibacterial effect.

The highly variable morphology of fungal NPs received tremendous attention from researchers based on various factors, such as biocompatibility, non-toxicity, high functionality, and eco-friendly nature, which have multifaceted industrial applications. Their high surface area and tunable surface chemistry in catalysis make them valuable catalysts for these chemical reactions.

Au NPs, synthesised using the fungus *Aspergillus terreus*, have been proven to detect high-sensitivity mercury ions, making them useful for environmental monitoring and water quality assessment [327]. In cosmetics, fungal NPs act as an efficient vector of biomimetic topical delivery of active principles in achieving better penetration into skin layers, bioavailability, and controlled release; hence, they are conducive to skincare and anti-ageing [328]. For instance, chitosan NPs, synthesised using the fungus *Mucor rouxii*, have been revealed to deliver hyaluronic acid, a common ingredient in skincare, to deeper skin layers, hence improving its moisturising and anti-ageing effects [329]. In addition, they are used to introduce features such as biocidal properties, sun protection features, and stain-release mechanisms, and they are found in textiles to facilitate better dyeing and, thus, better and longer-lasting colour. ZnO NPs synthesised using the fungus *Trichoderma viride* have been shown to effectively impart antimicrobial activity to cotton fabrics, rendering them resistant to bacterial growth and odour [330]. In the environmental field, due to their compatibility with biotic and abiotic systems and notorious pollutant-degradation ability, fungal NPs can improve environmental conditions and sustain their existence [331].

Moreover, fungal NPs have been targeted for several applications in mould environments, including water and soil treatment, air treatment, renewable energy, and industrial use. Titanium dioxide (TiO_2) NPs prepared using the fungus *Aspergillus flavus* can degrade soil organic pollutants [332,333]. Further insights into the synthesis, properties, and diverse applications of bio-fabricated TiO_2 NPs can be found in the comprehensive review by Saisruthi *et al.* [334]. Another application involves air cleaning by capturing-degradation of airborne pollutants. The fungus *Trichoderma viride* synthesised by ZnO NPs that could remove volatile organic compounds from indoor air while CuO NPs synthesised using the fungus *Penicillium citrinum* were capable of removing microbial contaminants [318,330].

Moreover, ZnO NPs synthesised using the endophytic fungus *Xylaria arbusculae* for photocatalytic degradation of photodegradable plastic were also identified as suitable renewable energy materials [335]. The emerging interdisciplinary branch of science is fungal nanobionics, derived from the relationship between mycology and nanotechnology. This will consequently open the door for further expansion in the industrial production of NPs on a large scale for use in fields such as energy [336].

Other recent works describing fungi biosynthesis MNPs include *Penicillium oxalicum* [337], *Fusarium solani* [338], *Trichoderma reesei* [339], *Laetiporus versisporus* [340] and *Rhizopus oryzae* [341].

4. Physicochemical reaction properties influence on metallic nanoparticles' synthesis and stability

The physicochemical properties of the synthesis environment significantly affect the production of NPs since they are determinants for

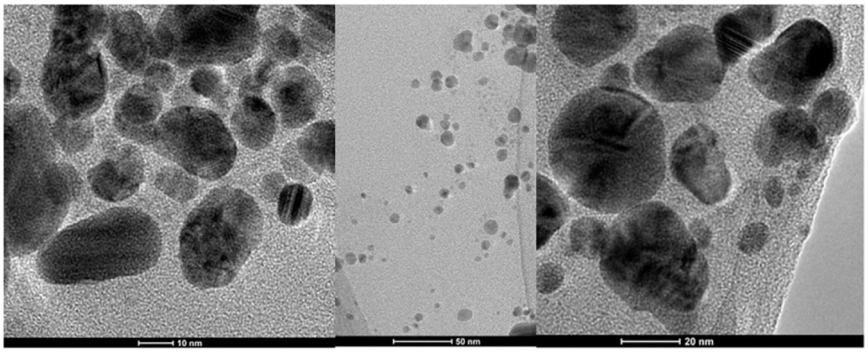

Fig. 12. Ag NPs from the Fusarium culmorum strain JTW1 observation by TEM micrographs.
Adapted from [326].

nucleation, growth, morphology, and aggregation. As a result, the size, shape, stability, and functionality of NPs are highly dependent on the conditions used during their synthesis. Therefore, the interplaying factors must be understood to optimize NPs involved in different applications, from biomedicine to electronics. The present section reviews the synthesis and stability of the NPs considering the following critical physicochemical parameters: extraction and reaction solvent, extract concentration, molarity of metallic salt, temperature, pH, and reaction time.

4.1. Extraction and reaction solvent

The solvent used to extract organic reducing agents and used in the synthesis reaction highly influences the NPs' physicochemical properties, purity, yield, and biological and chemical properties.

Solvents with a higher alcohol content have been shown to facilitate the extraction of organic reducing agents (including phenolic compounds) from *Eucalyptus globulus*, thus influencing the nucleation and growth processes [343]. Compared to those synthesized using pure ethanol, 96 % alcohol as a solvent produced FeO NPs with better magnetic properties, monodispersed, smaller in size, and improved colloidal stability [343]. The latter NPs also demonstrated higher removal efficacy for heavy metals (such as chromium and cadmium). However, the type of NPs to be synthesized also determines the solvent's effect. For instance, ethanolic extracts from hawthorn berries were more efficient in synthesizing Ag NPs, whereas water-based extract was superior in synthesizing Cu NPs [344]. The variation can be attributed to ethanol's stabilizing qualities being diminished with increasing temperature. Since Cu NPs are highly dependent on robust stabilizing agents, aqueous extracts facilitate their formation, as water can dissolve higher flavonoids and carbohydrate concentrations. Moreover, the synthesis process is improved, and the particle size is significantly decreased in an alkaline environment, effectively maintained in water-based solutions [344].

Other works directly compared the effect of the solvent on the synthesis of NPs. Water, methanol, and acetone were used to extract plant compounds from *Costus igneus* leaves, which has been shown to affect the ZnO NPs produced [345]. Hot water has been found to produce ZnO NPs with the highest purity (99.89 %) and the smallest particle size (94 nm), when compared to the other solvents. Furthermore, the water-extracted ZnO NPs revealed more significant growth inhibition against gram-positive and gram-negative bacteria and better antioxidant properties. In turn, Rufai et al. [346] demonstrated the effects of a solvent's polarity on phytochemical extraction from plants and their ability to alter NPs properties. The authors gained the phytochemicals from *Deinbollia pinnata* leaves by three different polarity solvents: n-hexane, ethyl acetate, and ethanol for the synthesis of NPs. The filtered ethyl acetate leaves behind TiO_2 NPs, which are rather crystalline, uniform in shape, although semi-spherical when in nature, and these TiO_2 NPs portray the highest photocatalytic activity because more of the hydroxyl compound extracts are present to serve as stabilizing agents. Also, this solvent enhanced the photocatalytic performance in deleting methyl orange dye under UV light irradiation, achieving 98.7 % conversion of methyl orange within 150 minutes.

Although the works reported so far describe using single solvents, mixed solvents with different polarities have been reported. Tesfaye *et al.* [347] demonstrated that using a binary solvent of methanol and distilled water favoured the synthesis of Ag NPs compared to methanol, ethanol, distilled water, or ethanol/distilled water alone. Furthermore, Chowdhury *et al.* [348] explored the presence of ethanol as a co-solvent with water in the Pd NPs synthesized using polyvinyl alcohol (PVA) as a stabilizer. The water/ethanol ratio influenced the reduction kinetics of Pd^{2+} ions to Pd^0 and primarily affected the PVA encapsulation around the NPs. Adding ethanol to the aqueous medium led to a gradual decrease in the encapsulation of synthesized Pd NPs, negatively impacting their electrocatalytic activity.

4.2. Extract concentration

The functional moieties extracted from the selected biological entity play a fundamental role in the synthesis of NPs. These reduce metal ions to zero-valent oxidation states from mono- or divalent oxidation states to zero-valent oxidation states. Generally, a higher extract concentration contains a larger supply of reducing agents, which are directly involved in reducing metal ions and, as a result, forming a larger number of nucleation sites [349]. Therefore, the extract's concentration plays a determining role in the biosynthesis of NPs and their features and functional properties. Fe_2O_3 NPs were synthesized with *Cola nitida* leaf extract, and the Taguchi method was used for the optimization of different parameters of their synthesis in a systematic manner— namely the optimal volume of the extract [350]. The extract concentration was ranked as the second most influential parameter in the synthesis of these NPs, according to the statistical analysis. The optimal volume of *Cola nitida* extract was determined to be 10 mL and Fe_2O_3 NPs with a surface area of 125.31 m^2/g [350].

Ag NPs were synthesized using *Ilex paraguariensis* extract and the enlargement of the extract concentration from 2.5 % v/v to 7.5 % v/v increased the average Ag NPs diameter from 70 nm to 144 nm, respectively [351]. However, their PDI was not significantly affected. The increase in size, according to the authors, is due to an increased availability of the reducing biomolecules that favour Ag ions' reduction and an enhancement of the Ostwald ripening process. Moreover, the lower extract concentration led to a high NPs colloidal stability over the 10-month-long storage period, indicating that there is a need for an optimal balance between the concentration of the extract and the efficiency of the phytochemicals capping [351]. Additionally, increasing the concentration of Ephedra extract from 1 to 4 mL led to smaller and uniformly distributed Au NPs [352]. These effects result from higher phytochemical concentrations that induce an increase in nucleation rate. Conversely, lower extract concentrations lead to slower nucleation rates and the growth of larger NPs due to prolonged growth phases. The same behaviour was found by Sharma *et al.* [349] during the synthesis of Ag NPs through an aqueous lichen extract, varying the Ag nitrate and lichen extract volume ratios from 1:1–1:9. The 1:1 extract-to-$AgNO_3$ volume ratio yields a well-defined and intense band corresponding to a narrower particle size distribution. The synthesis of smaller NPs results from the limited availability of metal ions per nucleation site. The rate constant of bioreduction of Ag^+ to Ag^0 was determined to be 5.3×10^{-3} min^{-1}. Al-Radadi [353] found that increasing the volume of licorice root extract (1 mL, 2 mL, 3 mL, 4 mL, and 6 mL) increased the synthesis of Au NPs—the optimized condition of 4 mL produced NPs with an average diameter of 43.17 nm.

Using *Moringa oleifera* leaf extract, an optimal volume of 20 mL was quantified to synthesize Ag NPs with a narrow, sharp, and symmetrical absorption peak [354]. Increasing the extract volume to 25 mL demonstrated that excess bioactive compounds favoured existing NPs' growth over new ones' nucleation. This trend was also observed in synthesizing ZnO NPs with pomegranate peel extract [355]. Using extract volumes of 20 mL, 30 mL, and 40 mL, average diameters of 18.53 nm, 29.88 nm, and 30.34 nm, respectively, were observed (Fig. 13). However, the optical bandgap decreases with increasing extract, decreasing from 2.87 eV to 1.92 eV when doubling the extract volume from 20 to 40 mL. ZnO NPs obtained with a greater extract volume revealed greater antibacterial efficacy [355].

However, Ag NPs were also synthesized with less than 1 mL extract volumes using *Andrographis paniculata* extract [356]. When studying 0.6, 0.7, 0.8, 0.9-, and 1-mL extract volumes, an increase from 0.6 to 0.8 mL gradually increased the concentration of Ag NPs. However, further increase to 0.9 and 1 mL reduced the intensity and a redshift of the absorption bands. Larger extract volumes resulted in increased self-agglomeration NPs that formed clusters due to excessive $AgNO_3$ precipitation [356].

The amount of biomass also plays a vital role in affecting the

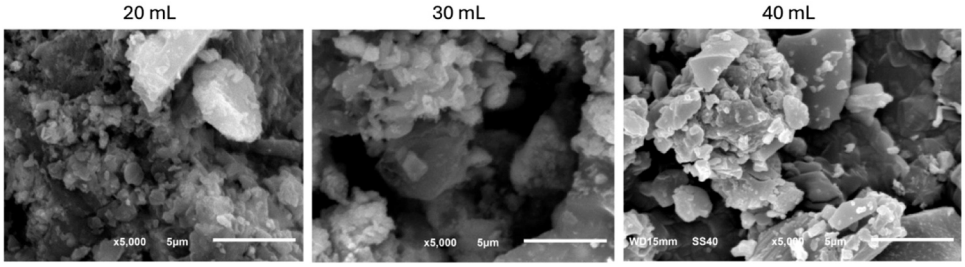

Fig. 13. SEM images of ZnO NPs green-synthesized with 20, 30, and 40 mL of *Moringa oleifera* leaf extract. Adapted from [355].

properties and quantity of microbial-mediated synthesis of NPs. For example, Seshadri *et al.* [357] successfully synthesized spherical PbS NPs using the active biomass of *Rhodosporidium diobovatum*. These PbS NPs were in the size range from 2–5 nm, thus establishing the possibility of size control during fungal-mediated MNPs synthesis.

4.3. Molarity of metallic salt

Increasing the molarity of the metallic salts leads to an increase in atoms to be reduced in a directly proportional manner, generally enhancing the synthesis of NPs. Increasing the concentration of metallic salts has a significant effect on the nucleation process. Lower molarity could potentially limit the number of nucleation centres, which will result in large NPs due to slower nucleation rates. Higher molarity will enable a higher rate of nucleation, hence resulting in more NPs with smaller sizes. There is, however, the need to find the optimum molarity since beyond this point, it is not efficient in the enhancement of the synthesis and may affect the preferred characteristics of the NPs. The effects brought about by molarity must be considered concerning other factors affecting the reaction. As demonstrated by Kumari and Padma [358], the optimum synthesis of Ag NPs is seen with 10 mM of the precursor metal $AgNO_3$. However, the authors reemphasize the interdependence of different reaction parameters, such as temperature, time, and extract concentration, which really direct the efficacy of the MNPs synthesis. The same optimum concentration was determined during the synthesizing of Ag-NPs using extracts of *Salvia verticillata* and *Filipendula ulmaria* extracts [359].

Besides its effect on synthesis efficiency, the molarity affects the MNPs size, phase, and crystallinity. Studies on the synthesis of TiO_2 NPs using *Tinospora cordifolia* revealed that an increase in molarity from 0.1 M to 0.5 M corresponded to an increase in the size of crystallites, indicating a rise in crystallinity with the increase in molarity [360]. At the same time, however, one has to note that this is not a linear relationship but is interlinked with the synthesis conditions. Molarity alone cannot be said to be the single deciding factor for the NPs phase and size variations. For example, in the presence of highly acidic pH and higher calcination temperatures, high molarity results in the formation of smaller-sized NPs, as stated by the authors [360]. In the case of ZnO NPs synthesized using the plant leaf extract *Artemisia haussknechtii*, high crystallinity was observed in NPs synthesized at a Zn nitrate hexahydrate concentration of 0.1 M [361]. The authors also identified the fact that smaller NPs were formed at higher molarities compared to those formed at lower molarities.

The optimisations of Ag NPs synthesis with *Cannabis sativa* aqueous leaf extract were found to have the ideal 3 mM $AgNO_3$ for striking a balance between the availability of Ag ions for reduction and the phytochemicals acting as reducing agents [362]. Further increasing up to 4 mM led to a broadened surface plasmon resonance (SPR) peak, reduced in intensity, and redshifted, portraying the formation of larger or agglomerated NPs. It has been shown that in the synthesis of Ag NPs from *Prosopis juliflora* leaf extract, 1 mM $AgNO_3$ provided optimum conditions for the synthesis of NPs [363]. Further, this fact bares relevance not only to the kinetics of the synthesis but also to the stability of NPs with time, rendering the importance of the molarity, regarding the long-term stability of NPs [363]. Optimal concentrations of $AgNO_3$ with *Laggera tomentosa* were 2 mM, which resulted in the highest peak intensity of absorbance [364]. The increase of metallic salt concentration—8 mM and 9 mM—had been characterized by the absence of UV-Vis peaks, which showed total aggregation of Ag NPs due to excess salt concentration.

Metal concentration can also impact the size and features of fungi-mediated synthesized NPs. The effect of cadmium chloride ($CdCl_2$) concentration on the production of cadmium sulphide NPs using the bacterium *Lactobacillus sp*. and the yeast *Saccharomyces cerevisiae* [365] was studied. A high concentration of $CdCl_2$ solution, 0.25 M at 60 °C with reaction times of 10–20 min was used. The synthesized CdS NPs showed a smaller size in yeast, 3.57 ± 0.1 nm, compared to *Lactobacillus sp*., which was 4.93 ± 0.23 nm. This may be owing to more effective detoxification mechanisms within the cells of yeast at the cellular level compared to the simpler bacterial cells of *Lactobacillus sp*. Extracellular enzymes produced by microorganisms are well documented and play a vital role as reducing agents in the synthesis of NPs. There is an increasing body of evidence that suggests that cofactors, like NADH and reduced form of NADPH dependent enzymes, act as reducing agents and transfer the electrons from NADH by NADH-reliant enzymes, which act as electron carriers [366,367]. Extracellular Au NPs synthesis by *R. capsulata* was done by reduction of gold by NADH-reliant reductase enzymes [262]. Similar enzyme machinery was used in *Stenotrophomonas maltophilia* [368].

4.4. Temperature

Another determinant factor in green synthesis is temperature; it affects the size distribution, morphology, phase stability, and reaction kinetics of the NPs. Normally, with higher temperatures, reactions increase in rate and provide energy available for nucleation and growth, hence in the morphology and size of the NPs.

Jain and Mehata [369], when synthesizing Ag NPs from the leaf extracts of *Ocimum Sanctum*, correlated the increased temperature with a decrease in the particle size. This is explained in the context that the kinetic energy of the molecules increased, which in turn increases the rate of consumption of Ag ions and leaves little opportunity for the particle to grow, resulting in smaller-sized particles of nearly uniform size distribution. Recently, similar results were obtained for Ag NPs synthesized using *Arecanut* Seed extract [370]. The temperature-dependent behaviour was attributed to the accelerated reduction of Ag ions and homogeneous nucleation at higher temperatures. Similar results were obtained using *Houttuynia cordata* (Thunb) rhizome extracts [371]. Moreover, the synthesis of Ag NPs using *Ginkgo biloba* leaves revealed that temperatures above 60°C resulted in a blue shift characteristic of not homogeneously dispersed NPs despite a trend toward reduced particle size [372]. Moreover, the temperature of 60°C has been identified as optimal for the synthesis of Ag NPs, balancing the nucleation rate and the MNPs desirable physical characteristics [372].

The behaviour is also dependent on the type of synthesized NPs. For example, the synthesis of ZnO NPs using cherry extract revealed that increasing reaction temperature resulted in larger NPs, ranging from 87.5 to 116 nm [373]. At 25°C, small NPs with more controlled growth and crystallization processes were formed due to a slow reduction of metal ions. With increased temperatures (60 °C and 90 °C), a swift reaction kinetics led to larger NPs due to a higher reduction rate of metal ions (Fig. 14). Furthermore, the authors associate high temperatures with increased instability of the extract's reducing agent, namely ascorbic acid, which leads to a less effective reduction process and uncontrolled aggregation [373].

Similar to what was found for the influence of pH, reaction temperature also strongly influences the biosynthesis of Au NPs from *Ephedra* [352]. The minimum temperature to form Au NPs by changing the reaction temperature from 15 °C to 35 °C was 20 °C. The temperatures higher than 25 °C, that is, at 30 °C and 35 °C, were too high and destabilized the NPs or degraded the phytochemicals responsible for reduction and capping.

Synthesis of MgO NPs using *Dalbergia sissoo* leaf extract has also been revealed to be very sensitive to reaction temperature as it affects the thermal stability of the phytochemicals involved during the synthesis [374]. Due to this aggregation phenomenon, temperatures of 30, 40, and 50 °C were the only lower temperatures that favoured NP synthesis, while higher temperatures such as 60 and 70 °C inhibited the synthesis process. Moreover, the E_g values of 4.13 eV, 4.97 eV and 5.24 eV were obtained for 30, 40, and 50 °C, respectively, indicating that lower synthesis temperatures yielded NPswith lower E_g values. The optimum temperature for a better synthesis yield and the most appropriate E_g was found to be 30 °C [374].

Concerning fungi-mediated synthesis, Phanjom and Ahmed [375] tested the effect of temperature variation on the synthesis of Ag NPs using *Aspergillus oryzae* MTCC 1846. Their study used a range of temperatures from 10, 30, 50, 70, and 90 °C and found a significant effect on the particle size and reaction rate. Increasing the temperature from 10 °C to 90 °C led to forming smaller Ag NPs (4–9 nm diameter) within a shorter time frame (20 minutes). Conversely, the decrease in temperature led to an increase in NP size up to 24 nm and a reaction time of up to 6 hours. Such observations suggest that the temperature may play a role in regulating the reduction kinetics and nucleation processes during the Ag NP synthesis by *A. oryzae* MTCC 1846. Shahzad *et al.* [376] noted that with *Aspergillus fumigatus* BTCB10, at a relatively low temperature of 25 °C, the fungus produced Ag NPs of about 322.8 nm. However, as the temperature increased to 55 °C, it was shown that the size of the Ag NPs increased up to about 1073.45 nm.

4.5. pH

The pH value of the reaction is one of the most fundamental parameters in the biosynthesis of NPs, and it has a large effect on the size, shape, and rates of synthesis, as well as their respective properties. The pH value influences the number of H^+ or OH^- ions, which are required to polymerize the metal-oxygen bond in the growth process [377]. Generally, an increase in pH enhances the nucleation centers, hence improving the reduction rate of metal ions to metal NPs [378]. This fact is partially due to the protonation-deprotonation equilibrium of the biomolecules in the biological extract. Protonation-deprotonation equilibrium affects the electron donation ability of the biomolecules, which consequently influences the reduction rate of metal salts [378]. A few studies have shown, in a quantitative way, the effect of pH on the synthesis of different kinds of NPs through biosynthesis from various biological sources.

Platinum NPs were biosynthesized using orange peel extract and tended to have an irregular distribution at lower pH values, with sizes of ~2.2 nm [379]. In contrast, a more homogeneous distribution was noted with decreased particle sizes at pH 9 and 11, both being ~2 nm and 1.8 nm, respectively. But this trend is reversed at a very high pH, that is, pH 13, large clusters develop with increased particle sizes, averaging 2.8 nm. According to the authors, this tendency towards aggregate is linked to reducing the availability of protons in alkaline conditions, needed for the stabilization of the NPs in the process of synthesis. In addition, high pH can cause the deprotonation of functional groups associated with the bio-reducing agents. It influences the dynamics of stabilization and capping of the bio-reducing agents, which are not able to control the nucleation and growth of the NPs [379].

A similar behaviour was found in MgO NPs synthesizing [380]. The alteration of reaction pH from 7 to 3 increased MgO NPs size from ~ 20–44 nm. Moreover, this shift in pH induced a shape alteration, transitioning from spherical to hexagonal morphology. The results are consistent with the ones from other research studies in which spherical NPs were formed due to higher pH levels. Lima *et al.* [351] employed an aqueous extract of *Ilex paraguariensis* to produce Ag NPs at different pH values. It was observed that higher pH values yielded more spherical NPs compared to ellipsoidal shapes observed at lower pH levels.

However, this tendency appears to be multifactorial and dependent, for instance, on the type of NPs to be synthesized. Also, using orange peel extract, Thi *et al.* [381] obtained an opposite correlation between pH and particle size. The authors found that lower pH values produced spherical-like ZnO NPs with distinct grain boundaries and less coagulation, while at higher pH values, the particles coagulate into larger clusters or blocks. Specifically, at pH 6, the average size varied between 10 and 20 nm, and at pH 8 and 10, larger clusters with average sizes of 400 nm and 370 nm were formed, respectively (Fig. 15A). Furthermore, the pH value of synthesis also actively influences the antibacterial activity of ZnO NPs. Higher pH values are associated with greater ROS production. The bactericidal rate against *S. aureus* was lowest at a pH of 4 and highest at a pH of 10.

It should be noted that the biosynthesis of NPs generally has an optimal pH, which must be determined on a case-by-case basis. For instance, the biosynthesis of Au NPs from *Ephedra* revealed the optimal pH to be 4 while below 3 no reaction occurred [352]. The authors

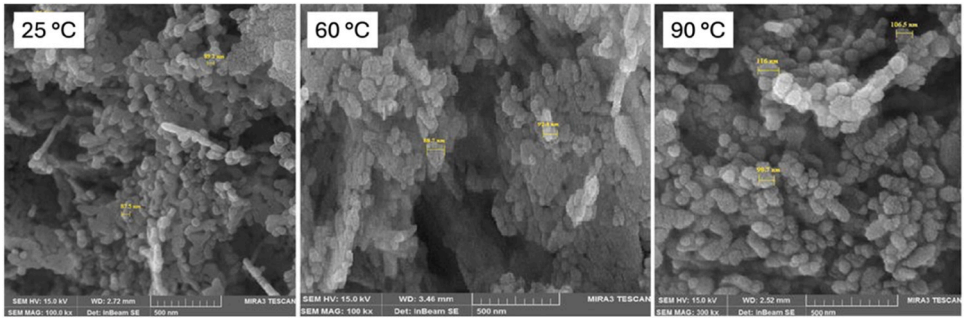

Fig. 14. SEM images of ZnO NPs synthesized using cherry extract at 25 °C, 60 °C, and 90 °C.
Adapted from [373].

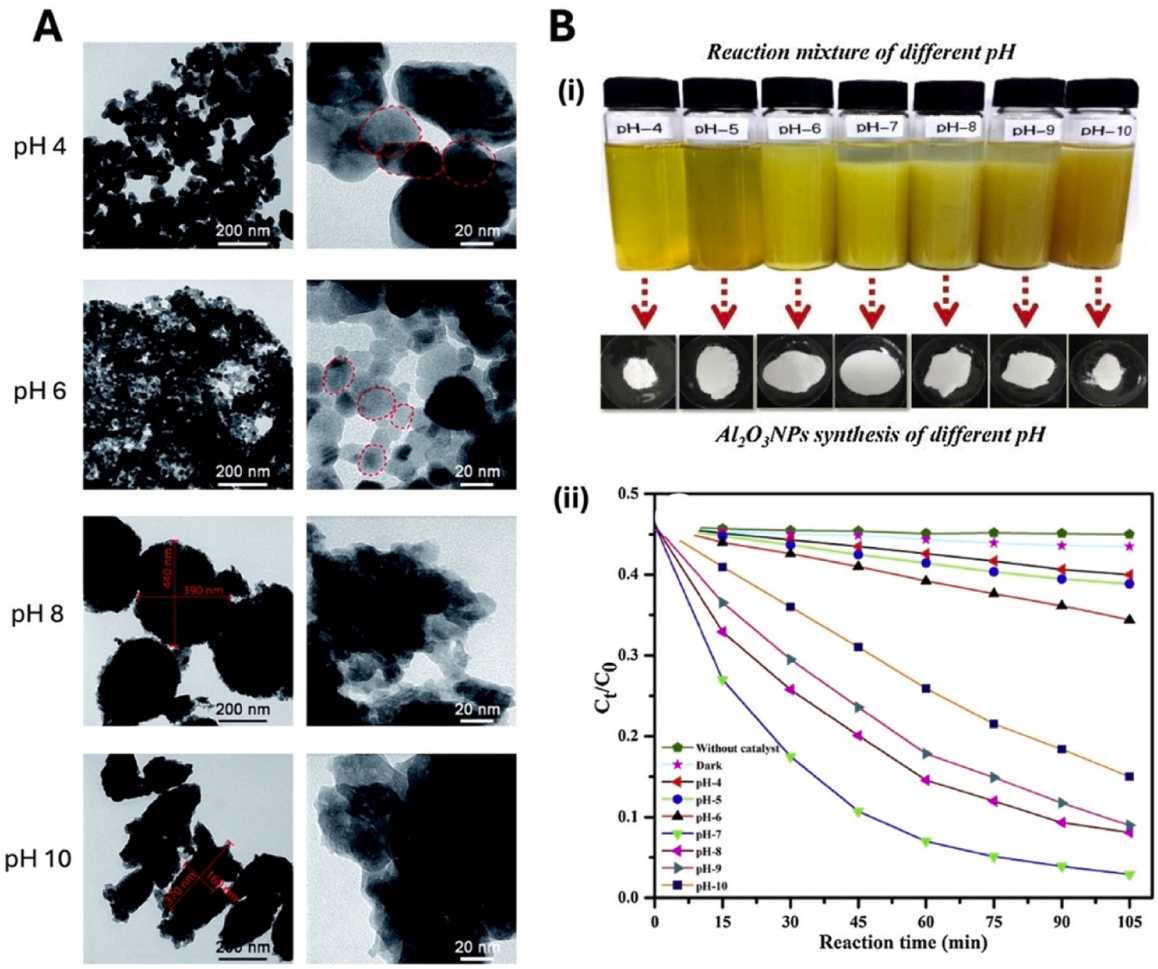

Fig. 15. TEM images of ZnO NPs synthesized using orange fruit peel extract at different pH values (pH 4, 6, 8, and 10); (B) i. Representation of Al_2O_3 NPs synthesized using Prunus yedoensis leaf extract at different pH values (from 4 to 10); and ii- the effect of nitrate molecules removal without catalyst, dark, and Al_2O_3 NPs synthesized from pH 4–10.
Adapted from [381] and [383].

associate pH-dependent behaviour with the interaction of hydrogen ions with the functional groups in the *Ephedra* extract.

The pH also affects the NPs' point of zero charge, which determines NPs interaction and adsorption behaviour to other molecules. Recently, Gherbi *et al.* [382] demonstrated the impact of the reaction pH in the photocatalytic activity of green synthesized ZnO NPs using *Portulaca oleracea* leaves extract.

A significant difference was found in the NPs bandgap value according to the reaction pH. Lower pH values resulted in smaller bandgap energies (e.g., at pH 4 =2.97 eV while pH 11 =3.97 eV), associated with greater photocatalytic efficiency. pH has also been shown to influence the morphology of NPs, which affects the generation and reactivity of the photocatalytic species. Considering that the latter (such as hydroxyl radicals and superoxide ions) are involved in the degradation of pollutants, it is concluded that the reactivity of NPs is also primarily affected by the pH of synthesis. *Prunus yedoensis* leaf extract was used to synthesize Al_2O_3 NPs at a pH range from 4–10 [383]. The synthesis of these particles was accompanied by yellow colour precipitation, which was more pronounced at pH 7 (Fig. 15B.i). It was also demonstrated that the rate constant (k) for nitrate removal varies with the pH at which the NPs were synthesized. The Al_2O_3 NPs exhibited the highest photocatalytic activity under natural sunlight irradiation at pH 7, achieving up to 94 % removal from aqueous solutions (Fig. 15B.i).

Gericke and Pinches [384] found that a shift in pH can control the form and size of NPs in *Verticillium luteoalbum*. Under acidic conditions at pH 3, spherical NPs with a diameter of less than 10 nm were produced. When the pH was increased to 5, the NP size also increased, and well-defined shapes like hexagons, triangles, rods, and spheres were produced. Remarkably, at pH 7 and 9, the synthesis gave a mixture of small, spherical particles and larger ones with irregular and undefined shapes. Another study showed the effect of the initial pH on the morphology of gold NPs synthesized by *Aspergillus terreus* IF0 [385]. The authors showed that a change in the initial pH of the fungal extract from 5, 8, and 10 resulted in the formation of elongated, triangular, and rod-shaped Au NPs, respectively. Moreover, the study achieved a size range of 10–19 nm for Au NPs synthesized at pH 10.

The pH value during the NPs' green synthesis reaction significantly impacts their morphological, structural, optical, and reactivity properties. Recent investigations on the pH influence on nanoparticle biosynthesis are available in [349,370,386,387].

4.6. Reaction time

The reaction time also determines their physicochemical properties, more especially on particle size distribution and morphology. Darroudi *et al.* [388] noticed that longer reaction times (48 h) lead to the formation of Ag NPs with more homogeneous and narrower size distributions and smaller diameters, down to about 5 nm. The authors relate the longer reaction times with the complete reduction of Ag ions to metallic Ag, which allows for more homogeneous processes of nucleation and

growth. Similarly, Manosalva *et al.* [389] determined the synthesis of Ag NPs from the leaf extract synthesis reaction was still underway even 20 h after initiating the reaction. Younas *et al.* [354] also determined the development of sharper SPR bands as the reaction time progresses, indicating the progressive reduction of Ag ions to Ag NPs and the formation of more homogeneous NPs with better distributions over the reaction time. At the same time, though, the authors established 24 h as the optimal reaction time for the generation of the desired characteristics of the NPs, including size, distribution, and stability, all of which play a critical role in its efficiency as an antibacterial agent. However, since this is a multifactor phenomenon, the relation of size to reaction time is not linear. For example, in the synthesis of Fe_3O_4 NPs using green tea extract, there was an increase in crystallite size from 7.5 nm to 12 nm, while sizes increased from 20 to 25 nm by increasing the reaction time from 2 h to 10 h, respectively [390] (Fig. 16 A and B). This increased, in turn, the changes in the associated magnetic properties. Increasing the reaction time from 2 h to 10 h increased saturation magnetization from 23 emu/g to 49 emu/g at room temperature (Fig. 16 C i and ii).

Ren *et al.* [391] proved the influence of the reaction time on the synthesis of composites like graphene oxide/chitosan/gold NPs (rGO/CHS/AuNPs). The reaction time has been shown to reduce graphene oxide (GO) and the size/distribution of Au NPs on the rGO surface. Longer reaction times have led to a redshift of UV–vis absorption peaks, which indicates a higher deoxygenation degree and restoration of graphene, meaning a fuller reduction of the GO. In addition, it results in larger sizes of Au NPs, indicating the nucleation and growth processes of Au NPs to be time dependent. Optimizing reaction times is imperative when fine-tuning the NPs' physicochemical parameters and the performance inherent to them, as depicted by the composites, which exhibited enhanced catalytic activity when reaction times are optimized.

Although most reported works involve reaction times in the order of hours, rapid syntheses requiring only a few minutes to synthesize the NPs are also reported. Philip *et al.* [392] reported the synthesis of well-dispersed Ag and Au NPs from *Murraya koenigii* leaf in just 1 minute of reaction. Spherical Au NPs using *Mangifera indica* leaf extract were synthesized within 2 min and demonstrated high stability over 5 months [393]. Furthermore, Ag nanorods using *Piper nigrum* extract were synthesized within 3 min [394] while Ag NPs were synthesized from *Nyctanthes arbor-tristis* within 20 min of reaction time [395].

Table 7 summarizes key findings, main conclusions and impact of physicochemical conditions on MNPs synthesis properties.

5. Green vs chemically synthesized nanoparticle: Comparative studies

Green synthesis of NPs is environmentally friendly since it avoids harmful chemicals such as sodium borohydride, hydrazine, or sodium dodecyl sulphate, which are necessary for chemical synthesis [396,397]. As a result, the environmental toxicity of chemical processes and their associated costs can be addressed using green synthesis methods. However, these are not the only factors that distinguish both approaches. These methods yield NPs with distinct shapes, sizes, stability, and properties. This section explores recent comparative studies elucidating the physicochemical and functional disparities between NPs produced through chemical versus green methodologies. Table 7 provides a summary of the key findings.

Green-synthesized Ag NPs using *Mussaenda frondosa* leaf extract were compared to chemically synthesized employing sodium citrate [398]. Ag NPs with a broader size range of 30–60 nm and a range of shapes (rod, spherical, triangle, and quasi-spherical) were produced using the plant extract. Compared to the latter, the chemically

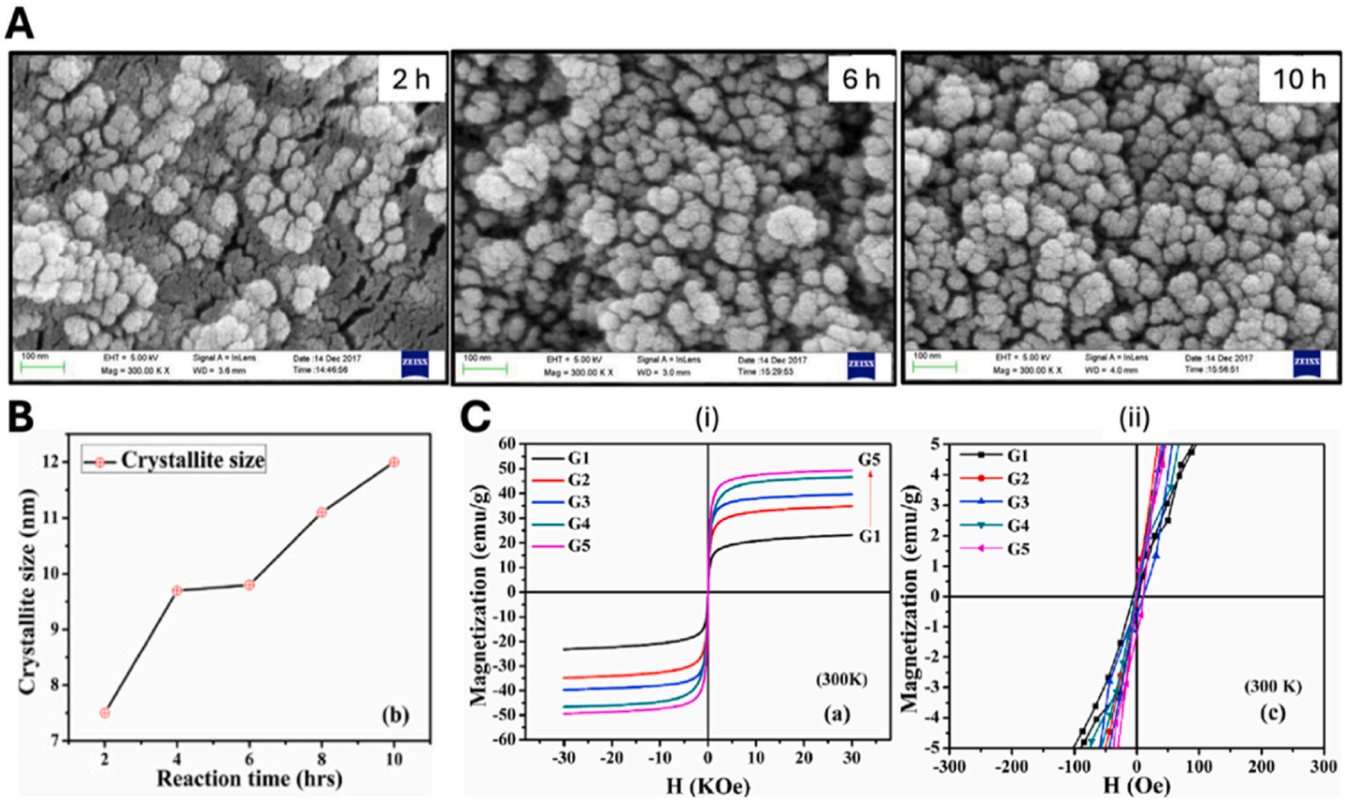

Fig. 16. (A) Field emission scanning electron microscope images of Fe_3O_4 NPs at the reaction times of 2 h, 6 h, and 10 h; (B) Fe_3O_4 NPs crystallite size as a function of reaction time; (C) Room-temperature magnetization curves (i) and its enlarged view (ii) for the samples at the reaction times of 2, 4, 6, 8 and 10 h (G1, G2, G3, G4 and G5, respectively).
Adapted from [390].

Table 7
Summary of optimal physicochemical conditions for green MNPs synthesis. The table outlines key findings and main conclusions from various works, highlighting the impact of solvent choice, extract concentration, metal salt molarity, temperature, pH, and reaction time on MNPs properties.

Parameter	Key works	Main Findings	Ref
Solvent	96 % ethanol extract of *Eucalyptus globulus* enhanced the magnetic properties and colloidal stability of FeO NPs.	Solvent choice affects NP size, stability, and biological properties	[343]
	Purer ZnO NPs with enhanced antibacterial and antioxidant properties were obtained with *Costus igneus* water extract	Water extracts produce smaller MNPs and influence MNPs properties	[345]
	Methanol/water mixture favored the synthesis of Ag NPs using *Vernonia amygdalina*, while an ethanol/water mixture promoted Pd NPs formation with polyvinyl alcohol (PVA).	Mixed solvents can optimize MNP synthesis	[347]
Extract concentration	Using 20 mL of *Moringa oleifera* extract produced smaller, more stable Ag NPs than using 25 mL.	Higher extract concentrations increase nucleation sites, reducing MNP size but risking agglomeration	[354]
	10 mL of *Cola nitida* extract was ideal for Fe_2O_3 NPs synthesis	Optimal extract volume balances MNP size and colloidal stability	[350]
	Increasing extract volume from 20 do 40 mL progressively increased ZnO NPs using pomegranate peel extract	Excess extract can promote particle growth over new nucleation	[355]
Metal salt molarity	Optimal synthesis was achieved with 3 mM $AgNO_3$ and *Cannabis sativa* aqueous extract, outperforming 4 mM concentrations	Higher molarity increases nucleation, producing smaller particles, but too high molarity can cause aggregation	[362]
	Artemisia haussknechtii extract yielded highly crystalline ZnO NPs at 0.1 M	Molarity affects NP crystallinity and phase	[361]
	Lactobacillus sp. bacteria produced smaller CdS NPs than *Saccharomyces cerevisiae* yeast at 0.25 M	Yeast synthesizes smaller CdS NPs at higher molarity due to efficient detox mechanisms	[365]
Temperature	*Ocimum sanctum* extract produced smaller Ag NPs as temperature increased	Higher temperatures generally reduce NP size by accelerating nucleation	[369]
	Prunus avium (cherry) extract yielded larger ZnO NPs as the temperature increased from 60 to 90 °C	Extremely high temperatures degrade reducing agents or destabilize NPs	[373]
	Aspergillus oryzae extract formed smaller Ag NPs (4–9 nm) as the temperature rose from 10 °C to 90 °C	Fungi produce smaller NPs at higher temperatures	[375]
pH	ZnO NPs with orange peel extract measured 10–20 nm at pH 6, increasing to 400–370 nm at pH 8 and 10	Alkaline pH increases nucleation and reduces NP size, but extreme pH can cause aggregation	[381]
	MgO NPs shifted from spherical to hexagonal shapes, and Ag NPs changed from spherical to ellipsoidal at lower pH levels	pH influences MNP morphology and activity	[380] [351]
	Ephedra extract produced optimal Au NPs at pH 4, with no reaction occurring below pH 3	Optimal pH varies by NP type and biological system	[352]
Reaction time	The optimal synthesis time for Ag NPs using glucose was 24 hours (maximizing size control, distribution, stability, and functionality), while *Moringa oleifera* required 48 hours	Longer reaction enhances MNP uniformity and stability, by allowing for more homogeneous processes of nucleation and growth	[388] [354]
	Ultra-fast Ag NP synthesis was achieved in just 1 min using *Murraya koenigii* extract	Fast synthesis possible	[392]
	Fe_3O_4 NPs synthesized with green tea extract grew larger and showed increased magnetization over longer reaction times	Reaction time affects NP properties	[390]

synthesized showed less crystallinity but smaller, more homogeneous sizes ranging from 9 to 14 nm and spherical shapes. Additionally, green synthesized Ag NPs demonstrated greater stability and enhanced antioxidant activity, showing a scavenging activity of DPPH of 91 % at a concentration of 5 mg/mL, in contrast to 79 % for the same concentration of the chemically synthesized (Fig. 17A). This difference is explained by the presence of biomolecules (such as flavonoids and phenolic compounds) on the surface of the NPs that demonstrate antioxidant properties. Similar results were also verified for green-synthesized Ag NPs using Cucumis sativus and Oryza sativa L. compared to commercial chemical counterparts (from Pantian nano Material Co., Ltd.) [399]. They exhibited long-term antibacterial effects and boosted plant photosynthesis by increasing chlorophyll content. Unlike chemical synthesis, which produces excessive reactive oxygen species (ROS), the green Ag NPs were less toxic to plants. Barabadi *et al.* [68] uncovered that Zataria multiflora-derived Ag NPs exhibit a spherical shape and an average diameter of 25.5 nm. Notably, these NPs demonstrate superior antibacterial efficacy to commercial chemical Ag NPs (CAS number 7440–22–4 with a <100 nm particle size) when tested against Staphylococcus aureus, with MIC values of 4 and 8 μg/mL, respectively.

Further, the MgO NPs synthesized with the leaf extract of Lawsonia inermis showed higher antibacterial activity against gram-positive bacteria such as Bacillus subtilis and Staphylococcus aureus and gram-negative bacteria such as Escherichia coli and Proteus vulgaris than the chemically prepared one (Fig. 17B) [372]. This may be due to organic biomolecules attached on the surface of green-synthesized NPs and the smaller size. On the other hand, the green-synthesized ZnO NPs (using the peel extract of Musa acuminata) showed sizes between 20 and 90 nm (Fig. 17C.i) and triangular and spherical shapes, while the chemically synthesized ones showed sizes between 20 and 200 nm, an irregular morphology, with a higher degree of aggregation (Fig. 17C.ii) [373]. The authors have emphasized the higher stability of the green NPs due to the presence of capping by positively charged organic molecules derived from the extract. The green NPs, moreover, showed higher efficiency of photocatalytic degradation; they were able to remove 100 % of certain dyes, whereas the chemically synthesized ZnO NPs removed 87.71 % of the dyes. They further showed better reusability for multiple runs [400]. The same trend was observed in the ZnO NPs synthesized using *Phoenix roebelenii* palm leaves, where it managed to remove 98 % of methylene blue dye under UV illumination for 105 minutes [401]. This could be attributed to the bioactive compounds increasing the pollutants' interaction through adsorption and availability of reactive sites. The increased surface area and hydroxyl groups on the surface increase the generation of ROS and boosts the photodegradation efficiency. In addition, surface oxygen vacancies on the green-produced ZnO enhance electron-hole pair separation and produce a higher amount of superoxide active radicals. The absence of bioactive compounds on the chemically synthesized NPs impairs their photodegradation efficiency [401].

Karimi *et al.* [402] used jasmine flower extract to synthesize TiO_2 NPs, as opposed to the chemical synthesis method involving ethanol-induced chemical reduction of the ions. This was due to the presence of alkaloids, coumarins, and flavonoids within the extract, which served as catalysts during the process of synthesis and imparted special biological properties to the NPs. The green-synthesized TiO_2 NPs showed a diameter of the inhibition zone to be 14 mm for *Escherichia coli* and 12 mm for Klebsiella pneumoniae, whereas the chemically

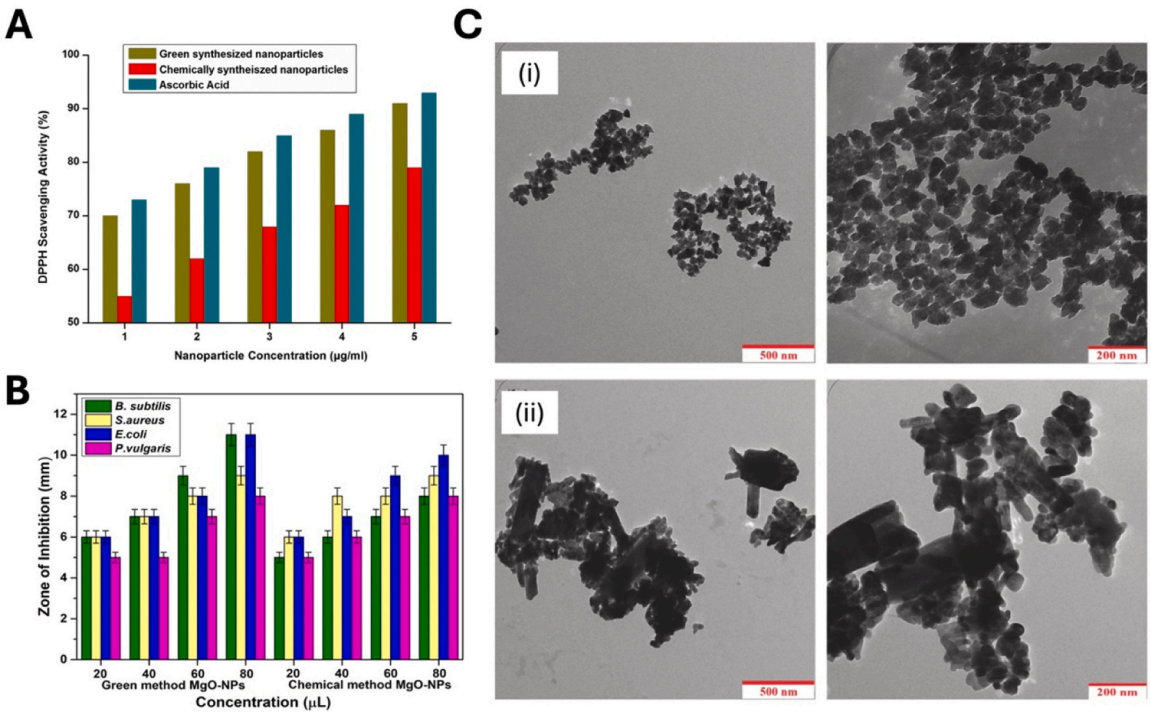

Fig. 17. (A) DPPH scavenging activity of Ag NPs at concentrations from 1 to 5 µg/mL for both green and chemically synthesized NPs; (B) Antibacterial activity of green and chemically-synthesized MgO NPs against *Bacillus subtilis*, *Staphylococcus aureus* gram-positive and *Escherichia coli*, Proteus vulgaris gram-negative bacteria; and (C) TEM images of (i) green and (ii) chemical ZnO NPs.
Adapted from [398,49] and [400].

synthesized NPs yielded a lesser value, that is, 12 mm and 11 mm, respectively. The inhibition zone was 8 mm for all gram-positive bacteria such as Staphylococcus aureus.

Alongside physicochemical variations in Table 7, real application demonstrates that MNPs, prepared by green routes, surpass chemically prepared counterparts in many applications and many cases. Environmental sustainability, for instance, demonstrates green ZnO and TiO_2 NPs exhibiting significantly improved photocatalytic activity in water cleaning with greater degradation of organic pollutants, better recyclability, and lower toxicity than their chemically prepared counterparts [269,400,401]. This enhanced performance is due to plant extracts' bioactive molecules, which increase surface functionalization, improve electron-hole pair separation, and boost ROS production, improving photodegradation efficiency [402].

Similarly, green-synthesized Ag and MgO NPs in biomedical applications exhibit higher antibacterial activity, demonstrating high efficiency against multidrug-resistant pathogens, superior to commercial chemically synthesized Ag NPs [89,397]. Such attributes make them candidates for antimicrobial coatings, dressings of wounds, and biomedical devices where chemical synthesis conventionally employs harmful stabilizing agents which can compromise biocompatibility [49]. Furthermore, biosynthesized TiO_2 NPs exhibit enhanced antibacterial and photocatalytic efficiency, making them a double-edge material for applications in biomedicine and purification of the environment [402]. The native biomolecules of plant-derived natural biomolecules of NPs including flavonoids, polyphenols, and alkaloids render them bioavailable and biocompatible to provide a safer drug delivery, cancer therapy, and tissue engineering where the NPs prepared chemically suffer from limitations based on toxicity [398].

In agriculture, green-synthesized Ag NPs have been reported to promote growth and resistance against bacterial and fungal infections and minimize phytotoxicity risks of chemically synthesized NPs [399]. Unlike the chemical counterparts that are known to cause oxidative stress and uncontrolled ROS production, green NPs exhibit controlled release and prolonged antimicrobial activity, which is beneficial for eco-friendly crop protection [399]. In addition, ZnO NPs prepared from *Phoenix roebelenii* palm leaves effectively degraded 98 % of methylene blue dye under UV light for 105 minutes with higher efficiency compared to chemically synthesized ZnO NPs due to their higher surface reactivity and bioactive functional groups [401].

Moreover, green synthesis protocols are critical in reducing toxic waste as well as promoting environmentally friendly nanotechnology solutions. Traditional chemical synthesis is predicated on toxic precursors such as sodium borohydride, hydrazine, and sodium dodecyl sulfate, all of which are toxic to human health and the environment [396,397](371, 372). Green processes eliminate the need for these toxic reagents and ensure high-yielding, inexpensive, and scalable manufacture, rendering them a more sustainable and feasible option for industrial applications. With these advantages, green-synthesized MNPs have the potential to revolutionize industries like health, environmental cleaning, and green agriculture with a vision of ecological nanotechnology with enhanced functional performance.

6. Biocompatibility, toxicity, biodistribution and degradation pathways

Conducting compatibility and cytotoxicity assays for NPs is essential, irrespective of their intended application, given human manipulation from the synthesis process to its final application. NPs' toxicity and genotoxicity should first be established through *in vitro* and then *in vivo* assessment. NPs toxicity is associated with inflammation responses, the generation of reactive oxygen and nitrogen species in excessive amounts, and elevated production of inflammatory cytokines, which in turn may contribute, through potential pathways, to the elicitation of cytotoxicity [403,404]. Many tests allow assessing the cytotoxicity of NPs, but they are mainly based on three assays: (i) proliferation and metabolic activity assays, (ii) Apoptosis, and (iii) Membrane integrity damage [404].

Other methods for evaluating nanotoxicity include hemocompatibility, immuno-toxicity and oxidative stress assays. *In vivo* toxicity methods include histopathology, clearance, haematology and biodistribution assays [405].

Therefore, this section will detail studies that explore the biocompatibility and toxicity of green-synthesized NPs, both *in vitro* and *in vitro*.

6.1. In vitro assays

To better understand the possible toxicity of MNPs, assessing the biocompatibility of the extract employed in their synthesis is essential, whenever feasible. Gharbavi *et al.* [406] conducted a comprehensive hemocompatibility evaluation, evaluating not just the selenium (Se) NPs derived from *Vaccinium arctostaphylos L.* fruit extract but also the impact of the extract itself and the metallic precursor (sodium selenite). In these assays, blood compatibility was inferred from the extent of haemolysis observed in red blood cells, characterized by membrane disruption and the subsequent release of haemoglobin into the blood plasma. Remarkably, all samples exhibited comparable haemolytic activity, showing a concentration-dependent trend. Moreover, even at high concentrations like 800 μg/mL, the haemolysis rates remained below 13.29 ± 1.6 %, which indicates appropriate biocompatibility of both MNPs and the extract used (Fig. 18. A). A similar hemocompatibility profile was found for Se NPs synthesized using *Orthosiphon stamineus* leaf extract, revealing maximum haemolysis of 6.4 % at the highest concentration of 200 μg/mL [407]. When treating peripheral blood mononuclear cells (PBMCs) with 100 μg of biogenic Se NPs, maximum cell viability of 74.28 % was obtained, with a small fraction of cells in early apoptotic (18.03 %), late apoptotic (2.82 %), and necrotic (4.87 %) stages. These viability values are close to those obtained in the untreated control (80.96 % viable cells), confirming the MNPs' biocompatibility.

Anjum *et al.* [408] evaluated the biocompatibility of core-shell Au–Ag and hybrid bimetallic NPs (BNPs) of Au–ZnO and Ag–ZnO synthesized from *Manilkara zapota* leaf extract. They assessed the lethal concentration of brine shrimp to increasing concentrations from 25 to 200 mg/mL. The LC_{50} values of the MNPs allowed for the classification of toxicity: LC_{50} > 100 mg/mL represents non-toxicity; LC_{50} 30–100 mg/mL shows mild toxicity; LC_{50} 10–30 mg/mL indicates moderate toxicity; and LC_{50} 1–10 mg/mL is toxic. All samples showed moderate toxicity behavior. Ag–ZnO, Au–Ag, and Au–ZnO showed an LC_{50} of 21.63 ± 0.61, 25.73 ± 2.5, and 20.96 ± 1.89 mg/mL, respectively. Haemolysis assays showed haemolytic activity to be less than 5 %, hence safe for use on humans. Ag–ZnO NPs revealed the lowest percentage of haemolysis as 3.16 ± 0.18 % compared to Au–Ag and Au–ZnO as 4.22 ± 0.34 % and 3.76 ± 0.53 %, respectively. On the other hand, Ag NPs prepared through radish seed extract showed significant compatibility with human blood despite the time-dependent haemolysis exhibited by the Ag NPs, synthesized at pH 8 [409]. At a dosage concentration of 1000 μg/mL, the haemolysis percentage remained within the minimum values up to 3 hours before gradually increasing. However, the haemolytic activity remained relatively low at the end of the 12-hour incubation period with the Ag NPs (Fig. 18. B). Muhmud *et al.* [410] evaluated the hemocompatibility of Ag MNPs synthesized using *Syzygium cymosum* leaf extract at various pHs; 5, 7, 8, and 10. Ag NPs synthesized at pH 8 recorded the highest haemolysis values against rat and human red blood cells, reaching 4.59 and 4 %, respectively, within acceptable hemocompatibility thresholds (Fig. 18. C). Although the difference may not be significant, it indicates the impact of pH on hemocompatibility profiles, increasing the need to consider pH levels in NPs synthesis.

Similar tests were used in the comparative biocompatibility study between chemically and green-synthesized FeO NPs [411]. A 24 h lethality assay for brine shrimp showed that chemically synthesized ones showed significant mortality at a lower 2 mg/mL concentration. On the

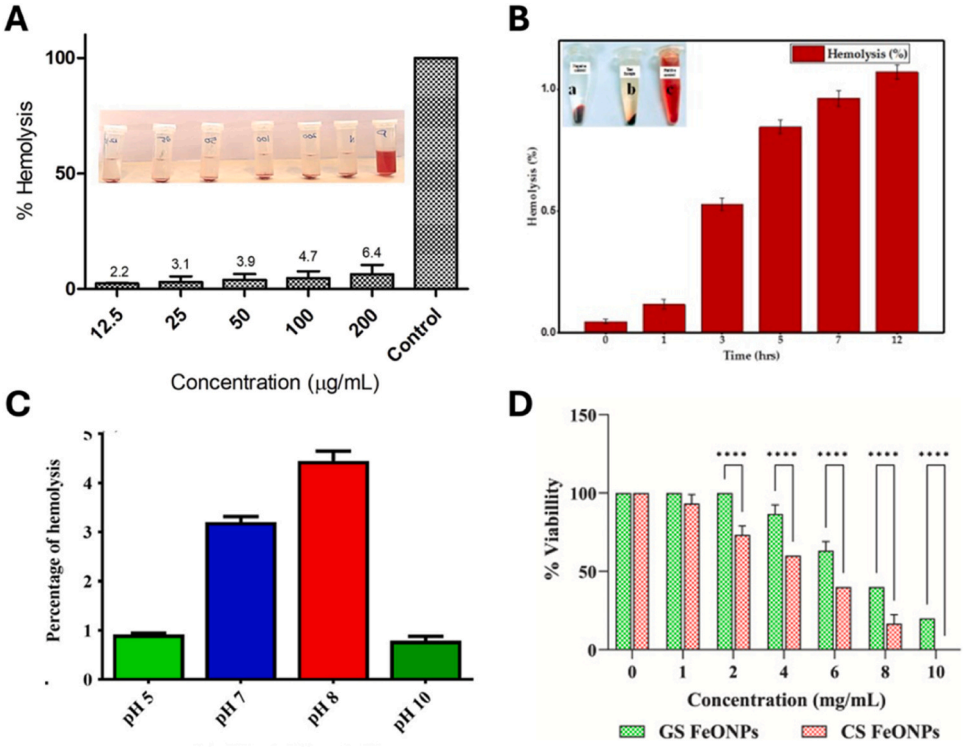

Fig. 18. (A) Haemolysis (%) effect of increasing concentrations of Se NPs derived from *Vaccinium arctostaphylos* L. fruit extract; (B) Time-dependent haemolysis (%) effect of 1000 μg/mL Ag NPs derived from radish seed extract. Inset: (a) negative control, (b) sample, and (c) positive control; (C) Haemolysis (%) effect of Ag NPs derived *Syzigyum cymosum* extract and synthesized at different pH levels (5, 7, 8, and 10); and (D) Effect of increasing concentrations of green (G.S.) and chemically synthesized (C.S.) FeO NPs on brine shrimp viability (%), * ** *$p < 0.0001$ significance.
Adapted from [406,409–411].

other hand, their green-synthesized counterparts showed this effect at a higher 6 mg/mL concentration. In addition, the cytotoxicity studies on peripheral blood mononuclear cells (PBMCs) were performed using the MTT assay, and a less cytotoxic effect of green synthesized FeO NPs was seen. At a 100 μg/mL concentration, green NPs showed a cell viability of 84.04 ± 0.94 %, and the chemical variant showed only 53.68 ± 1.50 % viability (Fig. 18. D). Based on ISO 10993–5:2009, which stipulates a non-toxic treatment as that with cell viability over 70 %, the green synthesized NPs fall in the non-toxic range [412]. It can thus be clearly noticed that synthesis methods make a difference in the environmental impact of NPs.

Abdelmigid *et al.* [413] showed a comparison between the chemical and green-synthesized ZnO for biocompatibility, and the use of two kinds of extracts in green synthesis: *Punica granatum peel* and coffee ground extracts. Here, assessment of the cytotoxic effects against the monkey kidney cell line (Vero E6) revealed extract, time, and dose-dependent manners. ZnO NPs produced from coffee ground extracts demonstrated a significant reduction of cell viability from 100 μg/mL. On the other hand, the ZnO NPs prepared from *Punica granatum* peel exhibited similar behaviour at a lower 60 μg/mL concentration. This toxic effect is more marked in chemically synthesized products, which considerably reduce cell viability from 40 μg/mL onwards. Table 8 provides a summary of *in vitro* toxicity's main findings.

6.2. In vivo assays

Although *in vitro* assays allow for an initial screening of MNPs, in vivo assays are essential for establishing more accurate biological and toxicological profiles. This type of assay allows to evaluate the systemic and cumulative effects of MNPs, which include their metabolism, toxicity in different tissues and organs, biodistribution and bioaccumulation. Furthermore, it is necessary to emphasize that in vitro tests do not allow to mimic the complex interactions of living biological organisms (such as blood circulation, immune response, and interaction with proteins, among others) and, therefore, do not allow to predict their holistic behaviour in living organisms. Several studies have demonstrated that the toxicity and hepatocellular damage of NPs is influenced by size, dose, shape and conjugated ligands [414,415], so there may be significant differences between chemical and green synthesized NPs. Veeragoni *et al.* [416] investigated the toxicity and biodistribution of green synthesized Ag NPs from *Padina tetrachromatic* (Ag PTs) compared to chemically synthesized NPs (Ag NPs) using Swiss albino mice. Initially, *in vitro* screening revealed that green Ag PTs induced fewer chromosomal aberrations and micronuclei than chemical Ag NPs. These findings were corroborated in Swiss albino mice, where Ag-PTs did not significantly increase the number of aberrant metaphases. In contrast, Ag-NPs showed a considerably higher number of aberrant metaphases and total aberrations in both single ($P < 0.05$) and multiple-dose treatments ($P < 0.001$). Moreover, Ag-PTs generated fewer micronuclei in bone marrow polychromatic erythrocytes (PCEs) compared to Ag-NPs, both in single (5.71 ± 0.76 % vs. 12.64 ± 0.87 %) and multiple dose treatments (8.51 ± 0.81 % vs. 14.15 ± 1.16 %). Similarly, Ag-PTs reduced micronucleus generation in peripheral blood PCEs compared to Ag-NPs, with single dose treatments yielding 5.12 ± 0.57 % vs. 7.02 ± 0.35 % and multiple dose treatments producing 7.4 ± 0.59 % vs. 10.11 ± 0.91 % (Fig. 19). Biodistribution studies showed that both types of MNPs were distributed throughout the body, with higher accumulation in the liver, spleen, and kidney. However, green Ag-PTs exhibited preferential accumulation in tumours, likely due to phytochemicals on the MNPs surface that enhance circulation and retention in tumours. Histopathological tests supported the latter results; green NPs caused mild vacuolar degeneration in the liver and slight hypertrophy in the spleen, while chemical MNPs induced severe effects, including multifocal necrosis in the liver and moderate follicular atrophy in the spleen [416].

Ultra-small Au NPs synthesized using egyptian propolis extract were administered to male albino rats to assess biodistribution and acute toxicity at 10 mg/kg doses and 100 mg/kg [417]. Higher doses of Au NPs accumulated in liver, kidney, and brain tissues were 4.41, 2.96, and 0.3 times higher than the doses with the lower doses. Notably, the blood-brain barrier was not crossed by Au NPs as their accumulation in brain tissue was confined to only glial cells. Further, there was no damage or inflammation observed in the cerebral cortex. However, higher doses showed signs of congestion with cellular changes in liver

Table 8
Summary comparison of physicochemical properties and functional activity of several metallic NPs synthesized by chemical and green approaches.

NP	Synthesis approach	Size (nm)	Morphology	Stability	Functionalization	Activity	Ref
Ag	Chemical (Commercial)	< 100	Spherical	Not reported	Citrate-reduced AgNs	< antibacterial efficacy (MIC=8 μg/mL)	[98]
	Green (*Zataria multiflora*)	25.5	Spherical	Not reported	Flavonoids, polyphenols, proteins	> antibacterial efficacy (MIC=4 μg/mL)	
Ag	Chemical	9–14	Spherical	Lower	Sodium citrate	< antioxidant activity	[398]
	Green (*Mussaenda frondose*)	30–60	Several	Higher	Tannins, terpenoids, phenolic compounds	> antioxidant activity	
Ag	Chemical (Commercial)	5–25	Not reported	Lower	No coating reported	< Photosynthetic pigment content + Toxicity	[399]
	Green (*Cucumis sativus* and *Oryza sativa L.*)	20–40	Not reported	Higher	Amino acids, reducing sugars, organic acids, fatty acids	Long-term antibacterial properties Promote photosynthesis - toxicity	
ZnO	Chemical	20–200	Irregular, rod, and spherical	Lower	No coating reported	< Photocatalytic degradation efficiency (87.71 %)	[400]
	Green (*Musa acuminata*)	20–90	Triangular and spherical	Higher	Polyphenols, catechoalamines, proteins, fatty acids, fiber, amines, potassium	> Photocatalytic degradation efficiency (100 %) > Reusability	
MgO	Chemical	24	Spherical	Not reported	No coating reported	< Antibacterial activity	[49]
	Green (*Lawsonia inermis*)	20	Spherical	Not reported	Linalol, α-terpineol, eugenol, 2-hydroxy−1,4-naphtoquinone, hexadecanoic acid	> Antibacterial activity	
TiO2	Chemical	31–42	Spherical	Not reported	No coating reported	< Antibacterial activity	[402]
	Green (Jasmine flower)	32–48	Spherical	Not reported	Alkaloids, coumarins, flavonoids, terpenoids, essential oils	> Antibacterial activity > Photocatalytic activity	

Table 9
Overview of in vitro assays findings of green synthesized metallic nanoparticles highlighting hemocompatibility, cell viability, and toxicity main findings.

NP	Biological route	Toxicity values	Toxicity findings	Ref
Se	Plant (*Vaccinium arctostaphylos L.*)	Haemolysis < 13.29 % at 800 μg/mL; Normal HEK−293 cells (IC_{50} = 384.44 ± 47.16 μg/mL);	Low haemolysis even at high concentrations	[406]
Se	Plant (*Orthosiphon stamineus*)	Haemolysis 6.4 % at 200 μg/mL; PBMC viability 74.28 %; untreated viability 80.96 %	Low haemolysis (at high concentrations; PBMC viability like untreated conditions	[407]
Ag–ZnO, Au–Ag, and Au–ZnO	Plant (*Manilkara zapota*)	LC_{50}: 20–25 mg/mL; Haemolysis < 5 %	Moderate toxicity in brine shrimp; Low haemolysis	[408]
Ag	Plant (Radish seed)	Haemolysis < 3 % up to 3 h at 1000 μg/mL	Time-dependent haemolysis but low overall haemolytic activity	[409]
Ag	Plant (*Syzygium cymosum*)	Haemolysis 4 % (human RBCs), 4.59 % (rat RBCs)	pH affects hemocompatibility; Haemolysis within safe thresholds	[410]
FeO	Plant (*Cardiospermum L.*) vs. Chemical	24 h lethality: green at 6 mg/mL, chemical at 2 mg/mL. PBMC viability: green 84 %, chemical 53 % at 100 μg/mL	Green MNPs are non-toxic while chemical MNPs are toxic	[411]
ZnO	Plant (*Punica granatum*, coffee grounds)	Toxicity in monkey kidney cell line from 60 μg/mL (coffee grounds) and 100 μg/mL (*Punica granatum*)	Dose-dependent toxicity; Coffee-ground are less toxic than *Punica granatum* MNPs	[413]

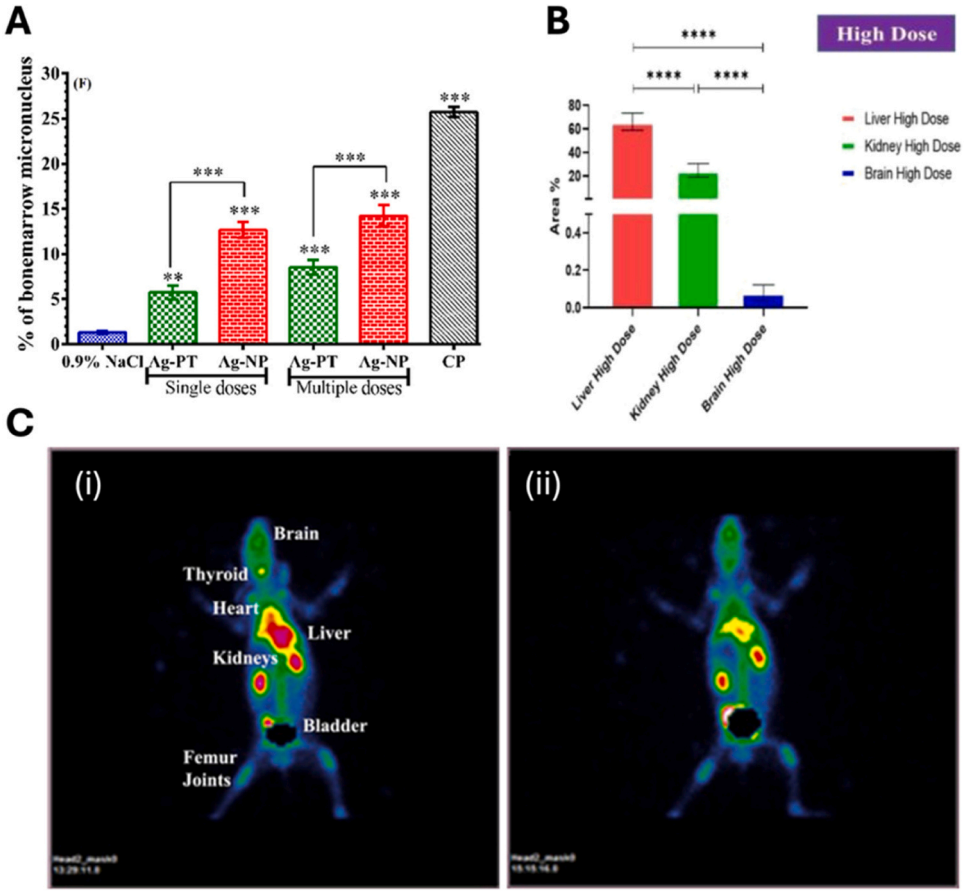

Fig. 19. Percentage of bonemarrow micronucleus in Swiss albino mice treated with Ag PTs and Ag NPs 5 mg/kg bw post-treatment of single and multiple doses (0.9 % NaCl-negative control; CP 40 mg/kg bw-positive control); (B) Mean area percentage of high drug (100 mg/kg) distribution on the studied tissues. *p ≤ 0.05, * *p ≤ 0.01, * **p ≤ 0.001, * ** *p ≤ 0.001; (C) Static SPECT of radiolabeled green synthesized FeONPs with doxorubicin and gamma-emitting radionuclide (99mTc) distribution on rabbit models after (i) 30 min and (ii) 120 min upon administration.
Adapted from [416].

and kidney tissues. Thus, a low dose of 10 mg/kg is suggested for living organisms [417].

Raoof *et al.* [418] radiolabelled green synthesised FeO NPs, using green tea extract, with doxorubicin and gamma-emitting radionuclide technetium-99m (99mTc) to investigate their biodistribution in a rabbit model. Single photon emission computed tomography (SPECT) shows higher detection sensitivity compared to MRI and was the imaging modality used in this study. In this case, after 30 minutes of injection, the radiolabeled NPs significantly accumulated in the liver, bladder, heart, and kidneys, whereby maximum accumulation was seen within the liver due to the role that this organ has in the reticuloendothelial system. In addition, FeO NPs facilitated extended residence of the radionuclide, which is advantageous for diagnostic imaging and targeted drug therapy. This extended residence did not lead to adverse

reactions or acute toxicity in the rabbits during the observation time. Biodegradation products of NPs should be incorporated into the normal iron pool in the blood and afterwards metabolized and excreted without damage to the biological system [418]. Similar conclusions have been drawn with Ag NPs synthesized using *Syzygium cymosum* following intravenous injection to male Wister rats at doses of 5, 10, and 50 mg/kg body weight (B.W.) at three-time points: 1, 7, and 28 days. Biochemical studies show there were no significant differences statistically ($P > 0.05$) in liver function biomarkers (alanine aminotransferase (ALT), aspartate aminotransferase (AST), alkaline phosphatase (ALP), gamma-glutamyl transferase (γ-GT), and albumin) and kidney function biomarkers (creatinine and uric acid) from the bAgNP-treated and control groups until 28 days [410]. Histopathological examination of vital organs, including the liver, kidneys, lungs, spleen, heart, and brain, did not identify any tissue lesions or significant abnormalities in the bAgNP-treated groups compared to the control group.

Nonetheless, Vasappa *et al.* [419] reported that Au NPs synthesized by *Lactobacillus plantarum* significantly elevated the level of key liver enzymes such as alanine aminotransferase, aspartate aminotransferase, and alkaline phosphatase, indicating acute liver damage and dysfunction. Besides, significant changes in bilirubin levels further demonstrated the hepatotoxicity of these green-synthesized Au NPs. A similar toxicity profile was observed when Au NPs were functionalized with the antibiotic's ciprofloxacin, cefotaxime, and ceftriaxone. Functionalization of NPs with the antibiotic levofloxacin reversed the hepatotoxicity; the levofloxacin-NP complex did not induce hepatotoxicity with minimal changes in enzyme levels as against animal controls. Biodistribution assays showed that free and antibiotic-conjugated NPs preferred accumulating in the spleen and liver. High concentrations of NPs in these organs after 24 hours of administration were decreased over 168 hours, pointing toward their clearance [419]. Levofloxacin-NP complex indicated a higher clearance rate, thus underlining the role of NPs functionalization for changing toxicity and innate clearance. The main routes for body elimination of free GNPs and those functionalized with antibiotics are hepatobiliary and renal pathways [419]. Most NPs, being around 12 nm in size, are taken up by the liver's Kupffer cells and secreted by bile, hence eliminated via the hepatobiliary route and excreted in the faeces. The minority, for NPs smaller than 6 nm, are cleared by the renal system and excreted in urine. This route enables faster elimination compared to the hepatobiliary route [419]. Table 10 provides a summary of *in vivo* toxicity biodistribution, histopathology and clearance pathways main findings.

6.3. Long-term biocompatibility and degradation pathways

Green-synthesized MNPs are generally considered more biocompatible due to the absence of harmful reducing agents and the presence of biocompatible capping agents derived from biological sources. Nonetheless, the number of *in vivo* and *in vitro* studies assessing the long-term behavior of green synthesized MNPs in biological systems is quite limited. The biocompatibility of these is significantly reliant on their intrinsic characteristics (such as particle size, shape, surface charge) as well as the nature of the biomolecules used for their synthesis which, in turn, determines cellular uptake, biodistribution, and possible cytotoxic actions over extended durations [420–422]. For example, small NPs have a higher viability to cross the membrane of a cell and be deposited in organelles, which may modify intracellular pathways and generate oxidative stress [423].

While there are still a few studies specifically focused on the biodegradation of green-synthesized MNPs, it is anticipated that the mechanisms involved will resemble those seen in MNPs synthesized through traditional methods. In the human body, enzymes such as oxidoreductases and hydrolases play a crucial role in breaking down MNPs. Additionally, immune cells like macrophages can engulf MNPs through phagocytosis, exposing them to ROS and acidic environments that induce dissolution [424–426]. However, the complex nature of MNPs, which can act as both pro- and anti-oxidants, adds layers of complexity to their biological effects, highlighting the need for more research to ensure their safe and effective application in biomedical fields [427]. Furthermore, MNPs quickly attach to proteins in biological fluids, creating a dynamic "protein corona" that affects how they are recognized by cells, their potential uptake by phagocytic cells, and the initiation of degradation or clearance processes [428]. The formation of the protein corona gives a new biological identity to MNPs, affecting how they interact with living systems and determining their fate *in vivo* [429]. In turn, the composition of this protein corona is shaped by the type of MNP material, as different materials exhibit unique binding patterns with various proteins [428]. Once these MNPs are taken up by cells, their degradation can be sped up by interactions with specific proteins like apoferritin, which may change the structure and properties of the protein [430]. After degradation, the metal ions or smaller complexes released from the MNPs can either be metabolized or excreted, depending on the organism's metabolic capabilities and the chemical characteristics of the metal [430].

In the environment, MNPs are subjected to natural degradation processes through microbial activity, photocatalysis, and chemical oxidation [431]. Microorganisms in soil and aquatic systems can interact with MNPs, producing extracellular enzymes that act as

Table 10
Overview of in vivo assays findings of green synthesized metallic nanoparticles highlighting cell viability, toxicity main findings, biodistribution, histopathology and clearance pathways findings.

NP	Biological route	Toxicity values	Toxicity findings	Biodistribution	Histopathology	Clearance	Ref
Ag	Plant (*Padina tetrachromatic*)	Single dose: 5.71 ± 0.76 %; Multiple dose: 8.51 ± 0.81 % MN; $P < 0.05$–0.001	Fewer chromosomal aberrations and micronuclei than chemical MNPs	Liver, spleen, kidney, tumour (higher retention)	Mild vacuolar degeneration (liver), slight spleen hypertrophy	Hepatobiliary, renal	[416]
Au	Plant (Egyptian propolis)	10 mg/kg: minimal toxicity; 100 mg/kg: liver/kidney congestion	Dose-dependent toxicity; No brain damage even at high doses	Liver, kidney, brain	Cellular changes in liver and kidney	Hepatobiliary, renal	[417]
FeO	Plant (green tea)	No acute toxicity observed during observation	Extended residence time for imaging and drug delivery without adverse reactions	Liver, bladder, heart, kidneys	No tissue damage	Metabolized, excreted via blood iron pool	[418]
Ag	Plant (*Syzygium cymosum*)	No statistical differences ($P > 0.05$) in ALT, AST, ALP, γ-GT, creatinine, uric acid	No significant changes in liver/kidney biomarkers or histopathology until 28 days	Liver, kidney, lungs, spleen, heart, brain	No lesions or abnormalities	Hepatobiliary, renal	[410]
Au	Bacteria (*Lactobacillus plantarum*)	Increased ALT, AST, ALP, bilirubin	Elevated liver enzymes and bilirubin, indicating hepatotoxicity; Functionalization with levofloxacin reduced toxicity	Liver, spleen	Severe hepatocellular damage in unmodified MNPs	Hepatobiliary (major), renal (minor, <6 nm)	[419]

reducing agent, that facilitate their reduction or dissolution and break down into less harmful components [432,433]. Sunlight can also accelerate MNPs degradation via photocatalytic reactions altering their structure and reactivity. High-energy photons excite the metal's surface electrons, generating ROS that break down both the organic capping agents and the metallic core, releasing metal ions. The significant changes in the physical and chemical structure of MNPs can influence their reactivity, potentially reducing their environmental persistence and toxicity [434]. Although this process helps to reduce the persistence of MNPs in the environment, the ions released can still affect ecosystems based on their concentration and local conditions.

While green synthesis offers clear benefits, there is still a significant gap in the understanding of the long-term biocompatibility and degradation pathways. Most existing research has concentrated on acute toxicity and short-term effects, with few studies exploring chronic exposure or the cumulative impact of MNPs that persist in biological and ecological systems. The complexity of biological environments and the variability in green synthesis methods require detailed evaluations on a case-by-case basis to fully understand the long-term outcomes. Future research should aim to establish standardized protocols for assessing chronic biocompatibility, long-term biodistribution, and complete degradation pathways to ensure the safe and sustainable application of green-synthesized MNPs in several industries [435].

7. Challenges and limitations

The potential of green synthesis, independent of the biosynthesis mediator used, is reflected by the amount of work reported and the knowledge it reflects. While green synthesis using plants and algae is environmentally friendly, the widespread application of this technology is hampered by significant material-related constraints due to the seasonality and geographic restrictions of many plants and algae [436]. In addition, the composition of the extracts varies significantly with geographic and seasonal differences, which hinders consistent production of MNPs, the establishment of standardized protocols, and scalability [437]. Moreover, most extract preparation and synthesis processes lack references describing the decision regarding extraction or synthesis process selection. Critical parameters like temperature, concentration, time, and the medium in which the extract is prepared, along with factors like centrifugation, are inconsistently applied, with some researchers incorporating them while others do not.

Such inconsistencies and the lack of integrated characterization result in an incomplete understanding of the mechanisms by which phytocompounds influence MNP synthesis. Despite the advantages of green synthesis, several challenges hinder its widespread adoption and industrial scalability. These include batch-to-batch variability, inconsistencies in biological extracts, and challenges in maintaining consistent MNPs properties. Additionally, the impact of environmental factors such as hydrostatic pressure and microbial activity must be further explored [438]. Understanding how these conditions affect biosynthesis mechanisms could lead to improved reproducibility and efficiency in NP production. Addressing these inconsistencies requires real-time monitoring and bioprocess engineering strategies, alongside appropriate analytical characterization techniques, to improve reproducibility and quality control.

In the comprehensive review conducted by Kumar et al. [29], it was also noted that one of the major production challenges is the need for robust NPs stabilization to prevent agglomeration, which directly impacts NPs functionality. Furthermore, it was emphasized that NPs demonstrating better performance in aqueous environments tend to show enhanced biocompatibility, an essential aspect when targeting biomedical and environmental applications. These findings align with our observation that the solution stability and formulation environment play a key role in the success of green-synthesized MNPs.

Since the main aim of green approaches is to enhance nanoparticle synthesis's sustainability, environmental impact studies of when this synthesis is scaled up for the industry are essential without losing the advantages of green synthesis [439]. Although many MNPs have shown promising results against bacteria, fungi, free radicals, cancer cells, and parasites and favourable toxicity and neurotoxicity assessments, the long-term effects of MNPs are mostly unknown [197]. Thus, prophylactic studies of the potential nanoparticle toxicity to human health and the environment are needed, and the cost-benefit ratio of green synthesis needs to be assessed.

Concerning bacterial-mediated synthesis, one major challenge is controlling the size and morphology of MNPs. Different sizes and shapes of MNPs result in different physical, chemical, and biological properties due to the complex interplay of the enzymatic reaction and cellular processes within metal ion bioreduction. The coordination of factors within the bioreduction of metal ions may depend on growth condition variations, such as pH, temperature, and nutrient availability, which may affect the synthetic process and size and shape [214,440]. A fundamental understanding is required nested within biological and engineering principles. Explorations in this area involve genetic and metabolic engineering of bacterial strains for MNPs synthesis [211]. One approach suggests controlling the reduction and nucleation processes by manipulating enzyme expression and metabolic pathways. This would help to control the size, shape, and composition of the yielded MNPs. The manipulation of MNPs' properties can also be undertaken by fine-tuning growth conditions such as pH, temperature, and nutrient levels [441]. Inclusion of MNP templates or seeding material entrapped into the bacterial culture is an innovative approach that will allow the nucleation and growth of MNPs and guide size and morphology through processes that result from biological processes in the bacterial environment while concurrently providing external signalling factors that shape the formed NPs [442,443].

The current restrictions in manipulating the MNPs' properties also prevent large-scale fungal and yeast-mediated biosynthesis [444]. The complex processes depend on species, reaction conditions, and metabolites, resulting in variable features [445]. However, the specific mechanisms are not generally acknowledged or completely understood. Examples are the role of anthraquinone pigments NADH-dependent nitrate reductase in reducing metal ions. Optimization strategies that can be applied include improving purification methods by a 3.5-fold increase and a threefold reduction in cost [446]. In this regard, the statistical design of experiments and high-throughput microbioreactor systems have also optimized other biosynthetic pathways, for example, Taxol, for which significant yield improvements could be obtained in 5 L bioreactors [447]. The introduction of CtvA into other species of fungi also has the potential to diversify and scale up other fungal natural products for drug development [448]. Further improvement in the recovery and purification of MNPs is being undertaken to streamline the recovery and purification processes, while in situ purification methods are further coming up for directly separating particles during the preparatory processes, thus reducing the cost and time. Nonetheless, purifying and isolating MNPs from the mixtures with microorganisms' biomass and biomolecules is still challenging, hence the need for effective techniques concerning the downstream processing of MNPs in the mixture [448]. Table 11 summarizes the main challenges and limitations of green synthesis using plants, algae, bacteria, yeast, and fungi and the proposed overcoming strategies.

8. Conclusion

Green synthesis is a valuable approach to producing MNPs, which enclose environmentally friendly and sustainable methods that involve using either natural products or biological systems - such as plants, algae, yeast, bacteria, and fungi- in reducing metal ions for creating nanostructured materials. Generally, green synthesis methods have fewer chemicals and are usually economically affordable, simple, and clean compared with other physical and chemical methodologies.

Plants are mainly used for green synthesis due to their availability,

Table 11
Challenges and limitations of green synthesis (using plants, algae, bacteria, yeast, and fungi) and the proposed overcoming strategies.

	Challenges and Limitations	Overcoming Strategies
Plants and algae	Seasonality and geographic restrictions	-
	High variability	Optimize the synthesis parameters and develop standardized protocols
	Unclear role of phytocompounds and biosynthesis mechanisms	Experimental evidence and comprehensive integration of multiple characterization techniques
	Environmental and scale-up limitations	Advance green synthesis processes and conduct environmental impact studies
	Low conversion rates and yields	Select different biological alternatives and optimize reaction parameters
	Biocompatibility	Understand the underlying chemical processes and environmental impacts
Bacteria	Size and morphology control of the MNPs	Genetic and metabolic engineering Tuning growth conditions MNPs templating and seeding
	Consistent and reproducible synthesis of MNPs across different batches	Real-time monitoring of critical parameters, coupled with feedback control systems
	Scalability	Bioprocessing techniques (bioreactor systems and downstream processing methodologies)
	Batch-to-batch variability in MNPs' properties	Knowledge of the underlying physiological and genetic factors that influence the NPs' synthesis within bacterial cells
	Regulatory considerations in biomedical and environmental applications	MNPs' properties, comprehensive characterization, and biological impact assessments ensure quality control standards
	Biocompatibility	Understand the underlying chemical processes and environmental impacts
	Scalability and consistency	Strain selection and genetic engineering
	Yield optimization	Strict control of parameters
	Mechanism elucidation	Advanced research
Fungi and yeast	Downstream processing	Development of *in-situ* techniques
	Biocompatibility	Understand the underlying chemical processes and environmental impacts

ease of access, and richness in phytochemicals (involving both primary and secondary metabolites). The metabolites help to reduce metal ions into stable NPs through bioreduction. As a result, this further advocates for better handling and eco-friendliness of plant-mediated biosynthesis than the microorganism-mediated process because of the high-water solubility of phytochemicals from plants. Similarly, algae are a renewable biomass highly reported and validated for producing MNPs. The high phytochemical diversity extracted from algae can reduce and act as a capping agent, avoiding high temperatures, pressures, or toxic chemicals. These molecules may themselves have biological properties—for example, antibacterial, anti-inflammatory, antifungal, anticancer, and antioxidant activities—that enhance the functionality of MNPs, hence broadening their applicability.

During bacterial biosynthesis, metal ions are reduced via enzymes and biomolecules produced outside the cells. These bacteria synthesize extracellular polymeric substances, which cap MNPs, thus achieving their stabilization and dispersibility. This natural self-stabilization provides greater biocompatibility with a simpler purification step route of extracellular synthesis, making this method quite preferred. The versatile nature of bacteria enables them to metabolize a wide range of substances and occupy diverse ecological niches, underlining their role in environmental processes and biotechnological applications, including nutrient cycling, degradation of organic matter, and nitrogen fixation. Since it is a unicellular eukaryote non-pathogen, yeast could be suitable for green biosynthesis in nanotechnology. Yeast enzymes can catalyse through both routes, and the cells are unable to command their metabolic machinery to work or produce MNPs. Practicality during recovery and purification steps makes the extracellular route more convenient and more accessible to scale up, when compared to the intracellular route, which is more frequently associated with implementing labour-intensive protocols. Fungal metabolic pathways enable metal NP synthesis through different mechanisms: intracellular, extracellular, or cell surface synthesis pathways. Metabolic diversity among the species of fungi was demonstrated to affect the size, morphology, and surface charge of NPs and, therefore, properties tailoring for specific applications.

Although green synthesis has been focused on improved biocompatibility, green-synthesized NPs must undergo thorough testing for their compatibility, toxicity, and biodistribution. Assays related to proliferation and metabolic activity, apoptosis, or membrane integrity assessments may provide corresponding information about the cytotoxicity of the NPs. In this respect, mechanisms of toxicity and interaction with biological systems must be clarified so that the development of biocompatible nanomaterials can be sustainable. Comparability studies between the MNPs synthesized in green and chemical processes regarding their structural attributes, stability, and activities establish a very clear case of the benefits of green synthesis in producing MNPs.

The application of MNPs synthesized by green methods demonstrates great potential, especially in the biomedical field. In this area, the enhancement of biocompatibility, combined with the antimicrobial properties of biomolecules used in synthesis, stabilization, and capping, enables safer and more effective applications. These have already been tested in fish hatcheries, dressings for small mammals, and in both human and animal cells, including those of monkeys. Beyond biomedicine, other promising applications exist, including their use in thermal nanofluids. For example, zeta potential results have shown these fluids to be more stable and less toxic for handlers, suggesting possible uses in lubricating fluids as well. Additionally, their ability to remove water pollutants like dyes further expands their range of applications. However, this potential is contrasted by the limited understanding of the long-term effects of nanoparticles on humans and the environment.

In conclusion, the present review outlines the principles of green synthesis using plants and microorganisms, representing the several phases from the mixture of biological systems with metal ions to the formation of MNPs with different shapes, sizes, and functionalities. It also elaborates on recent advances in the biosynthesis processes of various kinds of MNPs for multiple applications, together with the impacts of physicochemical factors on the reaction synthesis and their optimization. Further, it clarifies challenges and limitations in this field while proposing strategies to overcome them and further diffuse green synthesis methods within nanotechnology.

CRediT authorship contribution statement

Lima Rui: Writing – review & editing, Supervision, Funding acquisition. **Ribeiro João:** Supervision, Funding acquisition. **Afonso Inês:** Writing – original draft, Conceptualization. **Nobrega Glauco:** Writing – review & editing, Writing – original draft, Conceptualization. **Cardoso Beatriz:** Writing – review & editing, Writing – original draft, Validation, Conceptualization.

Declaration of Competing Interest

The authors declare that they have no known competing financial interests or personal relationships that could have appeared to influence

the work reported in this paper.

Acknowledgements

The authors acknowledge the partial financial support of the projects, PTDC/EEI-EEE/2846/2021 (https://doi.org/10.54499/PTDC/EEI-EEE/2846/2021) and 2022.06207.PTDC (https://doi.org/10.54499/2022.06207.PTDC) through national funds (OE), within the scope of the Scientific Research and Technological Development Projects (IC&DT) program in all scientific domains (PTDC), through the Foundation for Science and Technology, I.P. (FCT, I.P). The authors also acknowledge the partial financial support within the Research and Development Units Project Scope: UIDB/04077/2020 (Mechanical Engineering and Resource Sustainability Center (MEtRICs)), UIDB/00532/2020 and LA/P/0045/2020 (ALiCE) and the partial financial support of the projects provided by Portugal's national funding FCT/MCTES (PIDDAC) to Centro de Investigação de Montanha (CIMO) (UIDB/00690/2020 and UIDP/00690/2020) and SusTEC (LA/P/0007/2020). Glauco Nobrega was supported by the doctoral grant PRT/BD/153088/2021, financed by the Portuguese Foundation for Science and Technology (FCT), and with funds from MCTES/República Portuguesa, under the MIT Portugal Program. Inês S. Afonso acknowledges the financial support of MEtRICs through 2022.03151.PTDC. Inês S. Afonso was supported by the doctoral grant 2024.05919.BDANA, financed by FCT.

Data Availability

Data will be made available on request.

References

[1] V.V. Mody, R. Siwale, A. Singh, H.R. Mody, Introduction to metallic nanoparticles, J. Pharm. Bioallied Sci. 2 (4) (2010) 282, https://doi.org/10.4103/0975-7406.72127.

[2] P.G. Jamkhande, N.W. Ghule, A.H. Bamer, M.G. Kalaskar, Metal nanoparticles synthesis: an overview on methods of preparation, advantages and disadvantages, and applications, J. Drug Deliv. Sci. Technol. 53 (2019) 101174, https://doi.org/10.1016/j.jddst.2019.101174.

[3] O. Maťátková, J. Michailidu, A. Miškovská, I. Kolouchová, J. Masák, A. Čejková, Antimicrobial properties and applications of metal nanoparticles biosynthesized by green methods, Biotechnol. Adv. 58 (2022) 107905, https://doi.org/10.1016/j.biotechadv.2022.107905.

[4] R.J. Fernandes, B.D. Cardoso, A.R.O. Rodrigues, A. Pires, A.M. Pereira, J. P. Araújo, L. Pereira, P.J. Coutinho, Zinc/magnesium ferrite nanoparticles functionalized with silver for optimized photocatalytic removal of malachite green, Materials 17 (13) (2024) 3158, https://doi.org/10.3390/ma17133158.

[5] Z. Zhang, S. Yao, Y. Hu, X. Zhao, R.J. Lee, Application of lipid-based nanoparticles in cancer immunotherapy, Front. Immunol. 13 (2022) 967505, https://doi.org/10.3389/fimmu.2022.967505.

[6] J.E.N. Dolatabadi, Y. Omidi, Solid lipid-based nanocarriers as efficient targeted drug and gene delivery systems, TrAC Trends Anal. Chem. 77 (2016) 100–108, https://doi.org/10.1016/j.trac.2015.12.016.

[7] B.D. Cardoso, V.F. Cardoso, S. Lanceros-Méndez, E.M. Castanheira, Solid magnetoliposomes as multi-stimuli-responsive systems for controlled release of doxorubicin: assessment of lipid formulations, Biomedicines 10 (5) (2022) 1207, https://doi.org/10.3390/biomedicines10051207.

[8] B.D. Cardoso, A.R.O. Rodrigues, M. Bañobre-López, B.G. Almeida, C.O. Amorim, V.S. Amaral, P.J. Coutinho, E.M. Castanheira, Magnetoliposomes based on shape anisotropic calcium/magnesium ferrite nanoparticles as nanocarriers for doxorubicin, Pharmaceutics 13 (8) (2021) 1248, https://doi.org/10.3390/pharmaceutics13081248.

[9] A. Khajavinia, A. El-Aneed, Carbon-based nanoparticles and their surface-modified counterparts as MALDI matrices, Anal. Chem. 95 (1) (2023) 100–114, https://doi.org/10.1021/acs.analchem.2c04537.

[10] G. Singh, M. Esmaeilpour, A. Ratner, Effect of carbon-based nanoparticles on the ignition, combustion and flame characteristics of crude oil droplets, Energy 197 (2020) 117227, https://doi.org/10.1016/j.energy.2020.117227.

[11] S.M. Dizaj, A. Mennati, S. Jafari, K. Khezri, K. Adibkia, Antimicrobial activity of carbon-based nanoparticles, Adv. Pharm. Bull. 5 (1) (2015) 19, https://doi.org/10.5681/apb.2015.003.

[12] B. Wang, C. Wang, X. Yu, Y. Cao, L. Gao, C. Wu, Y. Yao, Z. Lin, Z. Zou, General synthesis of high-entropy alloy and ceramic nanoparticles in nanoseconds, Nat. Synth. 1 (2) (2022) 138–146, https://doi.org/10.1038/s44160-021-00004-1.

[13] Y. Jiang, X. Zhang, Z. Shen, X. Li, J. Yan, B.W. Li, C.W. Nan, Ultrahigh breakdown strength and improved energy density of polymer nanocomposites with gradient distribution of ceramic nanoparticles, Adv. Funct. Mater. 30 (4) (2020) 1906112, https://doi.org/10.1002/adfm.201906112.

[14] S. Wu, J. Ning, F. Jiang, J. Shi, F. Huang, Ceramic nanoparticle-decorated melt-electrospun PVDF nanofiber membrane with enhanced performance as a Lithium-Ion Battery Separator, ACS Omega 4 (15) (2019) 16309–16317, https://doi.org/10.1021/acsomega.9b01541.

[15] J.M. Chan, P.M. Valencia, L. Zhang, R. Langer, O.C. Farokhzad, Polymeric nanoparticles for drug delivery, Cancer Nanotechnol.: Methods Protoc. (2010) 163–175, https://doi.org/10.1007/978-1-60761-609-2_11.

[16] F. Carreiró, A.M. Oliveira, A. Neves, B. Pires, D.Nagasamy Venkatesh, A. Durazzo, M. Lucarini, P. Eder, A.M. Silva, A. Santini, Polymeric nanoparticles: production, characterization, toxicology and ecotoxicology, Molecules 25 (2020) 3731, https://doi.org/10.3390/molecules25163731.

[17] J.W. Hickey, J.L. Santos, J.-M. Williford, H.-Q. Mao, Control of polymeric nanoparticle size to improve therapeutic delivery, J. Control. Release 219 (2015) 536–547, https://doi.org/10.1016/j.jconrel.2015.10.006.

[18] A. Nyabadza, É. McCarthy, M. Makhesana, S. Heidarinassab, A. Plouze, M. Vazquez, D. Brabazon, A review of physical, chemical and biological synthesis methods of bimetallic nanoparticles and applications in sensing, water treatment, biomedicine, catalysis and hydrogen storage, Adv. Colloid Interface Sci. 321 (2023) 103010, https://doi.org/10.1016/j.cis.2023.103010.

[19] Z.-C. Shi, S.-X. Wei, T.-L. Xie, Q. Liu, C.-T. Au, S.-F. Yin, High-throughput synthesis of high-purity and ultra-small iron phosphate nanoparticles by controlled mixing in a chaotic microreactor, Chem. Eng. Sci. 280 (2023) 119084, https://doi.org/10.1016/j.ces.2023.119084.

[20] L. Marinescu, D. Ficai, O. Oprea, A. Marin, A. Ficai, E. Andronescu, A.-M. Holban, Optimized synthesis approaches of metal nanoparticles with antimicrobial applications, J. Nanomater. 2020 (1) (2020) 6651207, https://doi.org/10.1155/2020/6651207.

[21] A. Reverberi, N. Kuznetsov, V. Meshalkin, M. Salerno, B. Fabiano, Systematical analysis of chemical methods in metal nanoparticles synthesis, Theor. Found. Chem. Eng. 50 (2016) 59–66, https://doi.org/10.1134/S0040579516010127.

[22] J. Ai, E. Biazar, M. Jafarpour, M. Montazeri, A. Majdi, S. Aminifard, M. Zafari, H. R. Akbari, H.G. Rad, Nanotoxicology and nanoparticle safety in biomedical designs, Int. J. Nanomed. (2011) 1117–1127, https://doi.org/10.2147/IJN.S16603.

[23] S. Hua, M.B. De Matos, J.M. Metselaar, G. Storm, Current trends and challenges in the clinical translation of nanoparticulate nanomedicines: pathways for translational development and commercialization, Front. Pharmacol. 9 (2018) 790, https://doi.org/10.3389/fphar.2018.00790.

[24] E. Mancini, A. Raggi, A review of circularity and sustainability in anaerobic digestion processes, J. Environ. Manag. 291 (2021) 112695, https://doi.org/10.1016/j.jenvman.2021.112695.

[25] P.T. Anastas, J.C. Warner, Green Chemistry: Theory and Practice, Oxford University Press, 2000, https://doi.org/10.1093/oso/9780198506980.001.0001.

[26] G. Pal, P. Rai, A. Pandey, Green synthesis of nanoparticles: A greener approach for a cleaner future. Green synthesis, characterization and applications of nanoparticles, Elsevier, 2019, pp. 1–26, https://doi.org/10.1016/B978-0-08-102579-6.00001-0.

[27] Z. Yang, Z. Li, X. Lu, F. He, X. Zhu, Y. Ma, R. He, F. Gao, W. Ni, Y. Yi, Controllable biosynthesis and properties of gold nanoplates using yeast extract, Nano-Micro Lett. 9 (2017) 1–13, https://doi.org/10.1007/s40820-016-0102-8.

[28] A. Abbasifar, F. Shahrabadi, B. ValizadehKaji, Effects of green synthesized zinc and copper nano-fertilizers on the morphological and biochemical attributes of basil plant, J. Plant Nutr. 43 (8) (2020) 1104–1118, https://doi.org/10.1080/01904167.2020.1724305.

[29] J.A. Kumar, T. Krithiga, S. Manigandan, S. Sathish, A.A. Renita, P. Prakash, B. N. Prasad, T.P. Kumar, M. Rajasimman, A. Hosseini-Bandegharaei, A focus to green synthesis of metal/metal based oxide nanoparticles: various mechanisms and applications towards ecological approach, J. Clean. Prod. 324 (2021) 129198, https://doi.org/10.1016/j.jclepro.2021.129198.

[30] D. Gupta, A. Boora, A. Thakur, T.K. Gupta, Green and sustainable synthesis of nanomaterials: recent advancements and limitations, Environ. Res. 231 (2023) 116316, https://doi.org/10.1016/j.envres.2023.116316.

[31] W.-K. Shin, J. Cho, A.G. Kannan, Y.-S. Lee, D.-W. Kim, Cross-linked composite gel polymer electrolyte using mesoporous methacrylate-functionalized SiO2 nanoparticles for lithium-ion polymer batteries, Sci. Rep. 6 (1) (2016) 26332, https://doi.org/10.1038/srep26332.

[32] A.V. Nomoev, S.P. Bardakhanov, M. Schreiber, D.G. Bazarova, N.A. Romanov, B. B. Baldanov, B.R. Radnaev, V.V. Syzrantsev, Structure and mechanism of the formation of core–shell nanoparticles obtained through a one-step gas-phase synthesis by electron beam evaporation, Beilstein J. Nanotechnol. 6 (1) (2015) 874–880, https://doi.org/10.3762/bjnano.6.89.

[33] C.-Z. Zhong, S. Xu, Z.-H. Liu, J.-J. Lu, Y.-M. Yang, J.-S. Li, N.-L. Wang, K. Wu, C.-J. Ding, H.-Y. Zeng, Fabrication of hierarchical core–shell carbon microspheres@ layered double hydroxide@ polyphosphazene architecture in flame-retarding polypropylene, Eur. Polym. J. 177 (2022) 111405, https://doi.org/10.1016/j.eurpolymj.2022.111405.

[34] M.T. Yassin, A.A.-F. Mostafa, A.A. Al-Askar, F.O. Al-Otibi, Facile green synthesis of silver nanoparticles using aqueous leaf extract of Origanum majorana with potential bioactivity against multidrug resistant bacterial strains, Crystals 12 (5) (2022) 603, https://doi.org/10.3390/cryst12050603.

[35] F.A. Alahdal, M.T. Qashqoosh, Y.K. Manea, R.K. Mohammed, S. Naqvi, Green synthesis and characterization of copper nanoparticles using Phragmanthera austroarabica extract and their biological/environmental applications, Sustain. Mater. Technol. 35 (2023) e00540, https://doi.org/10.1016/j.susmat.2022.e00540.

[36] P. Dadhwal, H.K. Dhingra, V. Dwivedi, S. Alarifi, H. Kalasariya, V.K. Yadav, A. Patel, Hippophae rhamnoides L.(sea buckthorn) mediated green synthesis of copper nanoparticles and their application in anticancer activity, Front. Mol. Biosci. 10 (2023), https://doi.org/10.3389/fmolb.2023.1246728.
[37] V.B. Raghavendra, S. Shankar, M. Govindappa, A. Pugazhendhi, M. Sharma, S. C. Nayaka, Green synthesis of zinc oxide nanoparticles (ZnO NPs) for effective degradation of dye, polyethylene and antibacterial performance in waste water treatment, J. Inorg. Organomet. Polym. Mater. (2022) 1–17, https://doi.org/10.1007/s10904-021-02142-7.
[38] R. Álvarez-Chimal, V.I. García-Pérez, M.A. Álvarez-Pérez, R. Tavera-Hernández, L. Reyes-Carmona, M. Martinez-Hernandez, J.Á. Arenas-Alatorre, Influence of the particle size on the antibacterial activity of green synthesized zinc oxide nanoparticles using Dysphania ambrosioides extract, supported by molecular docking analysis, Arab. J. Chem. 15 (6) (2022) 103804, https://doi.org/10.1016/j.arabjc.2022.103804.
[39] A.M. Hamada, A.A. Radi, F.A. Al-Kahtany, F.A. Farghaly, A review: zinc oxide nanoparticles: advantages and disadvantages, J. Plant Nutr. 47 (4) (2024) 656–679, https://doi.org/10.1080/01904167.2023.2280127.
[40] L. Xiansong, G. Huamin, Q. Shixing, C. Luguo, D. Yuxing, Z. Dan, X. Xiaobing, Research on nickel morphology of dependence on the microwave-assisted polyol method, Phys. Status Solidi (a) 207 (2) (2010) 360–363, https://doi.org/10.1002/pssa.200925175.
[41] Y. Wu, L. Kong, Advance on toxicity of metal nickel nanoparticles, Environ. Geochem. Health 42 (2020) 2277–2286, https://doi.org/10.1007/s10653-019-00491-4.
[42] D. Tsuchida, Y. Matsuki, J. Tsuchida, M. Iijima, M. Tanaka, Allergenicity and bioavailability of nickel nanoparticles compared to nickel microparticles in mice, Materials 16 (5) (2023) 1834, https://doi.org/10.3390/ma16051834.
[43] Y. Lin, H. Feng, R. Chen, B. Zhang, L. An, One-dimensional TiO 2 nanotube array photoanode for a microfluidic all-vanadium photoelectrochemical cell for solar energy storage, Catal. Sci. Technol. 10 (13) (2020) 4352–4361, https://doi.org/10.1039/D0CY00342E.
[44] Y. Zhu, Z. Zhang, N. Lu, R. Hua, B. Dong, Prolonging charge-separation states by doping lanthanide-ions into {001}/{101} facets-coexposed TiO2 nanosheets for enhancing photocatalytic H2 evolution, Chin. J. Catal. 40 (3) (2019) 413–423, https://doi.org/10.1016/S1872-2067(18)63182-1.
[45] S.-N. Sun, C. Wei, Z.-Z. Zhu, Y.-L. Hou, S.S. Venkatraman, Z.-C. Xu, Magnetic iron oxide nanoparticles: synthesis and surface coating techniques for biomedical applications, Chin. Phys. B 23 (3) (2014) 037503, https://doi.org/10.1088/1674-1056/23/3/037503.
[46] A.G. Roca, L. Gutiérrez, H. Gavilán, M.E.F. Brollo, S. Veintemillas-Verdaguer, M. del Puerto Morales, Design strategies for shape-controlled magnetic iron oxide nanoparticles, Adv. Drug Deliv. Rev. 138 (2019) 68–104, https://doi.org/10.1016/j.addr.2018.12.008.
[47] M. Gui, J.K. Papp, A.S. Colburn, N.D. Meeks, B. Weaver, I. Wilf, D. Bhattacharyya, Engineered iron/iron oxide functionalized membranes for selenium and other toxic metal removal from power plant scrubber water, J. Membr. Sci. 488 (2015) 79–91, https://doi.org/10.1016/j.memsci.2015.03.089.
[48] M. Tabibi, S. Aghaei, M.A. Amoozegar, R. Nazari, M.R. Zolfaghari, Characterization of green synthesized selenium nanoparticles (SeNPs) in two different indigenous halophilic bacteria, BMC Chem. 17 (1) (2023) 115, https://doi.org/10.1186/s13065-023-01034-w.
[49] A. Akshaykranth, N. Jayarambabu, V.R. Tumu, R.K. Rajaboina, Comparative study on antibacterial activity of MgO nanoparticles synthesized from Lawsonia inermis leaves extract and chemical methods, J. Inorg. Organomet. Polym. Mater. 31 (2021) 2393–2400, https://doi.org/10.1007/s10904-021-01915-4.
[50] N.Y.S. Kozhevnikova, A.S. Vorokh, A.A. Uritskaya, Cadmium sulfide nanoparticles prepared by chemical bath deposition, Russ. Chem. Rev. 84 (3) (2015) 225, https://doi.org/10.1070/RCR4452.
[51] N. Badry, A. Ebnawaled, M. Wahman, Cadmium sulfide nanoparticles: preparation, characterization, and biomedical applications, SVU-Int. J. Med. Sci. 7 (1) (2024) 842–864, https://doi.org/10.3390/molecules28093857.
[52] R. Ding, Y. Li, Y. Yu, Z. Sun, J. Duan, Prospects and hazards of silica nanoparticles: biological impacts and implicated mechanisms, Biotechnol. Adv. 69 (2023) 108277, https://doi.org/10.1016/j.biotechadv.2023.108277.
[53] M. Alaqarbeh, S.F. Adil, T. Ghrear, M. Khan, M. Bouachrine, A. Al-Warthan, Recent progress in the application of palladium nanoparticles: a review, Catalysts 13 (10) (2023) 1343, https://doi.org/10.3390/catal13101343.
[54] C. Burda, X. Chen, R. Narayanan, M.A. El-Sayed, Chemistry and properties of nanocrystals of different shapes, Chem. Rev. 105 (4) (2005) 1025–1102, https://doi.org/10.1021/cr030063a.
[55] P. Buffat, J.P. Borel, Size effect on the melting temperature of gold particles, Phys. Rev. A 13 (6) (1976) 2287.
[56] Y.L. Hewakuruppu, L.A. Dombrovsky, C. Chen, V. Timchenko, X. Jiang, S. Baek, R.A. Taylor, Plasmonic "pump–probe" method to study semi-transparent nanofluids, Appl. Opt. 52 (24) (2013) 6041–6050, https://doi.org/10.1364/AO.52.006041.
[57] M. Fleischmann, P.J. Hendra, A.J. McQuillan, Raman spectra of pyridine adsorbed at a silver electrode, Chem. Phys. Lett. 26 (2) (1974) 163–166, https://doi.org/10.1016/0009-2614(74)85388-1.
[58] J. Langer, D. Jimenez de Aberasturi, J. Aizpurua, R.A. Alvarez-Puebla, B. Auguié, J.J. Baumberg, G.C. Bazan, S.E. Bell, A. Boisen, A.G. Brolo, Present and future of surface-enhanced Raman scattering, ACS Nano 14 (1) (2019) 28–117, https://doi.org/10.1021/acsnano.9b04224.
[59] C. Molardi, S. Korganbayev, W. Blanc, D. Tosi, Characterization of a nanoparticles-doped optical fiber by the use of optical backscatter reflectometry. Advanced Sensor Systems and Applications VIII, SPIE, 2018, pp. 380–385.
[60] A. Beisenova, A. Issatayeva, I. Iordachita, W. Blanc, C. Molardi, D. Tosi, Distributed fiber optics 3D shape sensing by means of high scattering NP-doped fibers simultaneous spatial multiplexing, Opt. Express 27 (16) (2019) 22074–22087.
[61] Deepika, Nanotechnology implications for high performance lubricants, SN Appl. Sci. 2 (2020) 1–12, https://doi.org/10.1007/s42452-020-2916-8.
[62] S.K. Das, E. Marsili, Bioinspired Metal Nanoparticle: Synthesis, Properties and Application. Croacia, InTech, 2011.
[63] C.J. Murphy, Nanocubes and nanoboxes, Science 298 (5601) (2002) 2139–2141.
[64] I. Khan, K. Saeed, I. Khan, Nanoparticles: Properties, applications and toxicities, Arab. J. Chem. 12 (7) (2019) 908–931, https://doi.org/10.1016/j.arabjc.2017.05.011.
[65] S.L. Brock, Nanostructures and Nanomaterials: Synthesis, Properties and Applications By Guozhang Cao (University of Washington), Imperial College Press (distributed by World Scientific), London, 2004 xiv+ 434 pp. $78.00. ISBN 1-86094-415-9, ACS Publications, 2004.
[66] T.K. Sau, A.L. Rogach, Complex-shaped metal nanoparticles: bottom-up syntheses and applications, John Wiley & Sons, 2012, https://doi.org/10.1595/147106713X664617.
[67] I. Ghiuta, D. Cristea, D. Munteanu, Synthesis methods of metallic nanoparticles-an overview, Bull. Transilv. Univ. Brasov. Ser. I: Eng. Sci. (2017) 133–140.
[68] S. Sun, H. Zeng, Size-controlled synthesis of magnetite nanoparticles, J. Am. Chem. Soc. 124 (28) (2002) 8204–8205, https://doi.org/10.1021/ja026501x.
[69] M. Lei, M. Gao, X. Yang, Y. Zou, A. Alghamdi, Y. Ren, Y. Deng, Size-controlled Au nanoparticles incorporating mesoporous ZnO for sensitive ethanol sensing, ACS Appl. Mater. Interfaces 13 (44) (2021) 51933–51944, https://doi.org/10.1021/acsami.1c07322.
[70] J. Quinson, L. Kacenauskaite, J. Bucher, S.B. Simonsen, L. Theil Kuhn, M. Oezaslan, S. Kunz, M. Arenz, Controlled synthesis of surfactant-free water-dispersible colloidal platinum nanoparticles by the Co4Cat process, ChemSusChem 12 (6) (2019) 1229–1239, https://doi.org/10.1002/cssc.201802897.
[71] T.S. Rodrigues, A.G. da Silva, P.H. Camargo, Nanocatalysis by noble metal nanoparticles: controlled synthesis for the optimization and understanding of activities, J. Mater. Chem. A 7 (11) (2019) 5857–5874, https://doi.org/10.1039/C9TA00074G.
[72] M. Grzelczak, J. Pérez-Juste, P. Mulvaney, L.M. Liz-Marzán, Shape control in gold nanoparticle synthesis, Colloïd. Synth. Plasmon.Nanomet. (2020) 197–220.
[73] J. Singh, T. Dutta, K.-H. Kim, M. Rawat, P. Samddar, P. Kumar, Green'synthesis of metals and their oxide nanoparticles: applications for environmental remediation, J. Nanobiotechnol. 16 (1) (2018) 1–24, https://doi.org/10.1186/s12951-018-0408-4.
[74] S. Ramanathan, S.C. Gopinath, M.M. Arshad, P. Poopalan, V. Perumal, Nanoparticle synthetic methods: Strength and limitations. Nanoparticles in Analytical and Medical Devices, Elsevier, 2021, pp. 31–43, https://doi.org/10.1016/B978-0-12-821163-2.00002-9.
[75] C.L. DeCastro, B.S. Mitchell, Nanopart. Mech. attrition, Synth., Funct., Surf. Treat. Nanopart. 5 (2002).
[76] M. Duan, J.G. Shapter, W. Qi, S. Yang, G. Gao, Recent progress in magnetic nanoparticles: synthesis, properties, and applications, Nanotechnology 29 (45) (2018) 452001, https://doi.org/10.1088/1361-6528/aadcec.
[77] Y.-P. Sun, X.-Q. Li, W.-X. Zhang, H.P. Wang, A method for the preparation of stable dispersion of zero-valent iron nanoparticles, Colloids Surf. A Physicochem. Eng. Asp. 308 (1-3) (2007) 60–66, https://doi.org/10.1016/j.colsurfa.2007.05.029.
[78] J. Vidal-Vidal, J. Rivas, M. López-Quintela, Synthesis of monodisperse maghemite nanoparticles by the microemulsion method, Colloids Surf. A Physicochem. Eng. Asp. 288 (1-3) (2006) 44–51, https://doi.org/10.1016/j.colsurfa.2006.04.027.
[79] B. Yuliarto, N.L.W. Septiani, Y.V. Kaneti, M. Iqbal, G. Gumilar, M. Kim, J. Na, K. C.-W. Wu, Y. Yamauchi, Green synthesis of metal oxide nanostructures using naturally occurring compounds for energy, environmental, and bio-related applications, N. J. Chem. 43 (40) (2019) 15846–15856, https://doi.org/10.1039/C9NJ03311D.
[80] A.A. Silva, A.M.F. Sousa, C.R. Furtado, N.M. Carvalho, Green magnesium oxide prepared by plant extracts: synthesis, properties and applications, Mater. Today Sustain. (2022) 100203, https://doi.org/10.1016/j.mtsust.2022.100203.
[81] J. Jeevanandam, Y.S. Chan, M.K. Danquah, Biosynthesis of metal and metal oxide nanoparticles, ChemBioEng Rev. 3 (2) (2016) 55–67, https://doi.org/10.1002/cben.201500018.
[82] F.K. Alsammarraie, W. Wang, P. Zhou, A. Mustapha, M. Lin, Green synthesis of silver nanoparticles using turmeric extracts and investigation of their antibacterial activities, Colloids Surf. B: Biointerfaces 171 (2018) 398–405, https://doi.org/10.1016/j.colsurfb.2018.07.059.
[83] R. Álvarez-Chimal, J.Á. Arenas-Alatorre, Green synthesis of nanoparticles. A biological approach, 2023. ⟨https://doi.org/10.5772/intechopen.1002203⟩.
[84] V. Makarov, A. Love, O. Sinitsyna, S. Makarova, I. Yaminsky, M. Taliansky, N. Kalinina, "Green" nanotechnologies: synthesis of metal nanoparticles using plants, Acta Nat. (англоязычная версия) 6 (1 (20)) (2014) 35–44.
[85] O. Nikhitha Surendran, M. Haridas, G. Szakacs, A. Sabu, Modified plant metabolites as nutraceuticals, Plant Metab.: Methods, Appl. Prospects (2020) 167–180.
[86] K.B. Narayanan, N. Sakthivel, Green synthesis of biogenic metal nanoparticles by terrestrial and aquatic phototrophic and heterotrophic eukaryotes and

biocompatible agents, Adv. Colloid Interface Sci. 169 (2) (2011) 59–79, https://doi.org/10.1016/j.cis.2011.08.004.
[87] X. Huang, H. Wu, S. Pu, W. Zhang, X. Liao, B. Shi, One-step room-temperature synthesis of Au@ Pd core–shell nanoparticles with tunable structure using plant tannin as reductant and stabilizer, Green. Chem. 13 (4) (2011) 950–957.
[88] M. Yehia, S. Labib, S. Ismail, Structural and magnetic properties of nano-NiFe2O4 prepared using green nanotechnology, Phys. B: Condens. Matter. 446 (2014) 49–54, https://doi.org/10.1016/j.physb.2014.04.032.
[89] Y.N. Tan, J.Y. Lee, D.I. Wang, Uncovering the design rules for peptide synthesis of metal nanoparticles, J. Am. Chem. Soc. 132 (16) (2010) 5677–5686, https://doi.org/10.1021/ja907454f.
[90] A.M.E. Shafey, Green synthesis of metal and metal oxide nanoparticles from plant leaf extracts and their applications: a review, Green. Process. Synth. 9 (1) (2020) 304–339, https://doi.org/10.1515/gps-2020-0031.
[91] A.K. Jha, K. Prasad, V. Kumar, K. Prasad, Biosynthesis of silver nanoparticles using Eclipta leaf, Biotechnol. Prog. 25 (5) (2009) 1476–1479, https://doi.org/10.1002/btpr.233.
[92] X. Wang, L. Yuan, H. Deng, Z. Zhang, Structural characterization and stability study of green synthesized starch stabilized silver nanoparticles loaded with isoorientin, Food Chem. 338 (2021) 127807, https://doi.org/10.1016/j.foodchem.2020.127807.
[93] S. Pirtarighat, M. Ghannadnia, S. Baghshahi, Green synthesis of silver nanoparticles using the plant extract of Salvia spinosa grown in vitro and their antibacterial activity assessment, J. Nanostruct. Chem. 9 (2019) 1–9, https://doi.org/10.1007/s40097-018-0291-4.
[94] S. Yousefzadeh-Valendeh, M. Fattahi, B. Asghari, Z. Alizadeh, Dandelion flower-fabricated Ag nanoparticles versus synthetic ones with characterization and determination of photocatalytic, antioxidant, antibacterial, and α-glucosidase inhibitory activities, Sci. Rep. 13 (1) (2023) 15444, https://doi.org/10.1038/s41598-023-42756-0.
[95] J.L. Gardea-Torresdey, E. Gomez, J.R. Peralta-Videa, J.G. Parsons, H. Troiani, M. Jose-Yacaman, Alfalfa sprouts: a natural source for the synthesis of silver nanoparticles, Langmuir 19 (4) (2003) 1357–1361, https://doi.org/10.1021/la020835i.
[96] D. Rehana, D. Mahendiran, R.S. Kumar, A.K. Rahiman, Evaluation of antioxidant and anticancer activity of copper oxide nanoparticles synthesized using medicinally important plant extracts, Biomed. Pharmacother. 89 (2017) 1067–1077, https://doi.org/10.1016/j.biopha.2017.02.101.
[97] K. Vijayaraghavan, T. Ashokkumar, Plant-mediated biosynthesis of metallic nanoparticles: a review of literature, factors affecting synthesis, characterization techniques and applications, J. Environ. Chem. Eng. 5 (5) (2017) 4866–4883, https://doi.org/10.1016/j.jece.2017.09.026.
[98] H. Barabadi, F. Mojab, H. Vahidi, B. Marashi, N. Talank, O. Hosseini, M. Saravanan, Green synthesis, characterization, antibacterial and biofilm inhibitory activity of silver nanoparticles compared to commercial silver nanoparticles, Inorg. Chem. Commun. 129 (2021) 108647, https://doi.org/10.1016/j.inoche.2021.108647.
[99] E.N. Gecer, R. Erenler, C. Temiz, N. Genc, I. Yildiz, Green synthesis of silver nanoparticles from Echinacea purpurea (L.) Moench with antioxidant profile, Part. Sci. Technol. 40 (1) (2022) 50–57, https://doi.org/10.1080/02726351.2021.1904309.
[100] K. Muthu, S. Rini, S.M. Nagasundari, B. Akilandaeaswari, Photocatalytic reduction and antioxidant potential of green synthesized silver nanoparticles from Catharanthus roseus flower extract, Inorg. Nano-Met. Chem. 51 (4) (2021) 579–589, https://doi.org/10.1080/24701556.2020.1799404.
[101] K.S. Allemailem, H. Khadri, M. Azam, M.A. Khan, A.H. Rahmani, F. Alrumaihi, R. Khateef, M.A. Ansari, E.A. Alatawi, M.H. Alsugoor, Ajwa-dates (Phoenix dactylifera)-mediated synthesis of silver nanoparticles and their anti-bacterial, anti-biofilm, and cytotoxic potential, Appl. Sci. 12 (9) (2022) 4537, https://doi.org/10.3390/app12094537.
[102] M. Yoro, A. Garba, J.W.K. Jonah, Characterization and Pathogenic Study of Plant Mediated Silver Nanoparticles Utilizing Psidium guajava Stem Bark Extract, 2023.
[103] S.A. Dhar, R.A. Chowdhury, S. Das, M.K. Nahian, D. Islam, M.A. Gafur, Plant-mediated green synthesis and characterization of silver nanoparticles using Phyllanthus emblica fruit extract, Mater. Today.: Proc. 42 (2021) 1867–1871, https://doi.org/10.1016/j.matpr.2020.12.222.
[104] S. Ikram, Synthesis of gold nanoparticles using plant extract: an overview, Nano Res. 1 (5) (2015).
[105] K. Kaur, B. Ahmed, J. Singh, M. Rawat, G. Kaur, M. AlKahtani, E.A. Alhomaidi, J. Lee, Bryonia laciniosa Linn mediated green synthesized Au NPs for catalytic and antimicrobial applications, J. King Saud. Univ. -Sci. 34 (4) (2022) 102022, https://doi.org/10.1016/j.jksus.2022.102022.
[106] B. Gami, K. Bloch, S.M. Mohammed, S. Karmakar, S. Shukla, A. Asok, S. Thongmee, S. Ghosh, Leucophyllum frutescens mediated synthesis of silver and gold nanoparticles for catalytic dye degradation, Front. Chem. 10 (2022) 932416, https://doi.org/10.3389/fchem.2022.932416.
[107] V. Sekar, M.M. Al-Ansari, J. Narenkumar, L. Al-Humaid, P. Arunkumar, A. Santhanam, Synthesis of gold nanoparticles (AuNPs) with improved anti-diabetic, antioxidant and anti-microbial activity from Physalis minima, J. King Saud. Univ. -Sci. 34 (6) (2022) 102197, https://doi.org/10.1016/j.jksus.2022.102197.
[108] N.A. Patil, S. Udgire, D. Shinde, P.D. Patil, Green synthesis of gold nanoparticles using extract of Vitis vinifera, Buchananialanzan, Juglandaceae, Phoenix dactylifera plants, and evaluation of antimicrobial activity, Chem. Methodol. 7 (2023) 15–27, https://doi.org/10.22034/CHEMM.2022.355289.1597.
[109] S. Shah, S.A. Shah, S. Faisal, A. Khan, R. Ullah, N. Ali, M. Bilal, Engineering novel gold nanoparticles using Sageretia thea leaf extract and evaluation of their biological activities, J. Nanostruct. Chem. 12 (1) (2022) 129–140, https://doi.org/10.1007/s40097-021-00407-8.
[110] K. Shakerimanesh, F. Bayat, A. Shahrokhi, A. Baradaran, E. Yousefi, M. Mashreghi, A. Es-Haghi, M.E.T. Yazdi, Biomimetic synthesis and characterisation of homogenouse gold nanoparticles and estimation of its cytotoxity against breast cancer cell line, Mater. Technol. 37 (13) (2022) 2853–2860, https://doi.org/10.1080/10667857.2022.2081287.
[111] S.M. Mousavi-Kouhi, A. Beyk-Khormizi, V. Mohammadzadeh, M. Ashna, A. Es-haghi, M. Mashreghi, V. Hashemzadeh, H. Mozafarri, M. Nadaf, M. E. Taghavizadeh Yazdi, Biological synthesis and characterization of gold nanoparticles using Verbascum speciosum Schrad. and cytotoxicity properties toward HepG2 cancer cell line, Res. Chem. Intermed. (2022) 1–12, https://doi.org/10.1007/s11164-021-04600-w.
[112] T.U. Rahman, H. Khan, W. Liaqat, M.A. Zeb, Phytochemical screening, green synthesis of gold nanoparticles, and antibacterial activity using seeds extract of Ricinus communis L, Microsc. Res. Tech. 85 (1) (2022) 202–208, https://doi.org/10.1002/jemt.23896.
[113] R. Rey-Méndez, M.C. Rodríguez-Argüelles, N. González-Ballesteros, Flower, stem, and leaf extracts from Hypericum perforatum L. to synthesize gold nanoparticles: effectiveness and antioxidant activity, Surf. Interfaces 32 (2022) 102181, https://doi.org/10.1016/j.surfin.2022.102181.
[114] S.S. Asl, F. Tafvizi, H. Noorbazargan, Biogenic synthesis of gold nanoparticles using Satureja rechingeri Jamzad: a potential anticancer agent against cisplatin-resistant A2780CP ovarian cancer cells, Environ. Sci. Pollut. Res. 30 (8) (2023) 20168–20184, https://doi.org/10.1007/s11356-022-23507-6.
[115] N. Sher, M. Ahmed, N. Mushtaq, Biogenic synthesis of gold nanoparticles using Heliotropium eichwaldi L and neuroprotective potential via anticholinesterase inhibition in rat brain, Appl. Organomet. Chem. 37 (4) (2023) e7000, https://doi.org/10.1002/aoc.7000.
[116] A.A. Ezhilarasi, J.J. Vijaya, K. Kaviyarasu, L.J. Kennedy, R.J. Ramalingam, H. A. Al-Lohedan, Green synthesis of NiO nanoparticles using Aegle marmelos leaf extract for the evaluation of in-vitro cytotoxicity, antibacterial and photocatalytic properties, J. Photochem. Photobiol. B: Biol. 180 (2018) 39–50, https://doi.org/10.1016/j.jphotobiol.2018.01.023.
[117] N.C.Z. Moghadam, S.A. Jasim, F. Ameen, D.H. Alotaibi, M.A. Nobre, H. Sellami, M. Khatami, Nickel oxide nanoparticles synthesis using plant extract and evaluation of their antibacterial effects on Streptococcus mutans, Bioprocess Biosyst. Eng. 45 (7) (2022) 1201–1210, https://doi.org/10.1007/s00449-022-02736-6.
[118] H. Balto, M. Amina, R.S. Bhat, H.M. Al-Yousef, S.H. Auda, A. Elansary, Green synthesis of nickel nanoparticles using salvadora persica and their application in antimicrobial activity against oral microbes, Microbiol. Res. 14 (4) (2023) 1879–1893, https://doi.org/10.3390/microbiolres14040128.
[119] C. Yuan, B. Jiang, X. Xu, Y. Wan, L. Wang, J. Chen, Anti-human ovarian cancer and cytotoxicity effects of nickel nanoparticles green-synthesized by Alhagi maurorum leaf aqueous extract, J. Exp. Nanosci. 17 (1) (2022) 113–125, https://doi.org/10.1080/17458080.2021.2011860.
[120] S. Uddin, L.B. Safdar, S. Anwar, J. Iqbal, S. Laila, B.A. Abbasi, M.S. Saif, M. Ali, A. Rehman, A. Basit, Green synthesis of nickel oxide nanoparticles from Berberis balochistanica stem for investigating bioactivities, Molecules 26 (6) (2021) 1548, https://doi.org/10.3390/molecules26061548.
[121] A.H. Hashem, M.A. Al Abboud, M.M. Alawlaqi, T.M. Abdelghany, M. Hasanin, Synthesis of nanocapsules based on biosynthesized nickel nanoparticles and potato starch: Antimicrobial, antioxidant, and anticancer activity, Starch-Stärke 74 (1-2) (2022) 2100165, https://doi.org/10.1002/star.202100165.
[122] H. Gebretinsae, M. Tsegay, Z. Nuru, Biosynthesis of nickel oxide (NiO) nanoparticles from cactus plant extract, Mater. Today Proc. 36 (2021) 566–570, https://doi.org/10.1016/j.matpr.2020.05.331.
[123] P. Karpagavinayagam, A.E.P. Prasanna, C. Vedhi, Eco-friendly synthesis of nickel oxide nanoparticles using Avicennia marina leaf extract: morphological characterization and electrochemical application, Mater. Today Proc. 48 (2022) 136–142, https://doi.org/10.1016/j.matpr.2020.04.183.
[124] E. Gobinath, M. Dhatchinamoorthy, P. Saran, D. Vishnu, R. Indumathy, G. Kalaiarasi, Synthesis and characterization of NiO nanoparticles using Sesbania grandiflora flower to evaluate cytotoxicity, Results Chem. 6 (2023) 101043, https://doi.org/10.1016/j.rechem.2023.101043.
[125] R. Thrilokraj, R.V. Hegde, A. Ghosh, A.S. Limaye, H.B. Rode, B. Sridhar, R. B. Dateer, A sustainable approach for nickel nanoparticles synthesis: expeditious access to N-heterocycles under heterogeneous condition and photophysical studies, N. J. Chem. 47 (17) (2023) 8268–8276.
[126] S. Hussain, M. Ali Muazzam, M. Ahmed, M. Ahmad, Z. Mustafa, S. Murtaza, J. Ali, M. Ibrar, M. Shahid, M. Imran, Green synthesis of nickel oxide nanoparticles using Acacia nilotica leaf extracts and investigation of their electrochemical and biological properties, J. Taibah Univ. Sci. 17 (1) (2023) 2170162, https://doi.org/10.1080/16583655.2023.2170162.
[127] N. Sundaresan, S. Ravichandran, Biosynthesis of nickel oxide nanoparticles using Evolvulus alsinoides extract and their potential photocatalytic and invitro anticancer activity, Inorg. Chem. Commun. 150 (2023) 110489, https://doi.org/10.1016/j.inoche.2023.110489.
[128] Q. Zhang, J. Cao, P. Zhao, Y. Zhang, Y. Li, S. Xu, J. Ye, C. Qian, Green synthesis of nickel ferrite nanoparticles for efficient enhancement of lignocellulosic hydrolysate-based biohydrogen production, Biochem. Eng. J. 194 (2023) 108885, https://doi.org/10.1016/j.bej.2023.108885.

[129] J.M. Badr, Chemical constituents of Phragmanthera austroarabica AG Mill and JA Nyberg with potent antioxidant activity, Pharmacogn. Res. 7 (4) (2015) 335, https://doi.org/10.4103/0974-8490.158436.
[130] A.M. Awwad, N.M. Salem, A.O. Abdeen, Biosynthesis of silver nanoparticles using Loquat leaf extract and its antibacterial activity, Adv. Mater. Lett. 4 (5) (2013) 338–342, https://doi.org/10.5185/amlett.2012.11453.
[131] S. Mukherjee, V. Sushma, S. Patra, A.K. Barui, M.P. Bhadra, B. Sreedhar, C. R. Patra, Green chemistry approach for the synthesis and stabilization of biocompatible gold nanoparticles and their potential applications in cancer therapy, Nanotechnology 23 (45) (2012) 455103, https://doi.org/10.1088/0957-4484/23/45/455103.
[132] K.E. Alsamhary, Moringa oleifera seed based green synthesis of copper nanoparticles: characterization, environmental remediation and antimicrobial activity, Saudi J. Biol. Sci. 30 (11) (2023) 103820, https://doi.org/10.1016/j.sjbs.2023.103820.
[133] P. Senthilkumar, M. Aravind, K. Janakiraman, M. Kamalesh, M. Saruhasan, A. K. Jagadeesan, B.P. Naveen Prasad, B. Torsykbayeva, Green synthesis of MgO nano particle loaded onto carbon for effective rhodamine B dye removal, Environ. Qual. Manag. 34 (1) (2024) e22298, https://doi.org/10.1002/tqem.22298.
[134] J.A. Kumar, S. Sathish, D. Prabu, J. Giri, E. Makki, J. Jayaprabakar, G. K. Ziyayeva, O. Baigenzhenov, T. Sathish, T. Praveenkumar, Waste shrimp shell mediated Chitosan-Magnesium Oxide nanocomposite: synthesis, characterization and exploitation towards acenaphthene removal from aqueous solution, Alex. Eng. J. 104 (2024) 124–135, https://doi.org/10.1016/j.aej.2024.06.014.
[135] K. Shubhashree, R. Reddy, A.K. Gangula, G. Nagananda, P.K. Badiya, S. S. Ramamurthy, P. Aramwit, N. Reddy, Green synthesis of copper nanoparticles using aqueous extracts from Hyptis suaveolens (L.), Mater. Chem. Phys. 280 (2022) 125795, https://doi.org/10.1016/j.matchemphys.2022.125795.
[136] L. Chompunut, T. Wanaporn, W. Anupong, M. Narayanan, M. Alshiekheid, A. Sabour, I. Karuppusamy, N.T.L. Chi, R. Shanmuganathan, Synthesis of copper nanoparticles from the aqueous extract of Cynodon dactylon and evaluation of its antimicrobial and photocatalytic properties, Food Chem. Toxicol. 166 (2022) 113245, https://doi.org/10.1016/j.fct.2022.113245.
[137] J. Gu, F. Chen, Z. Zheng, L. Bi, H. Morovvati, S. Goorani, Novel green formulation of copper nanoparticles by Foeniculum vulgare: chemical characterization and determination of cytotoxicity, anti-human lung cancer and antioxidant effects, Inorg. Chem. Commun. 150 (2023) 110442, https://doi.org/10.1016/j.inoche.2023.110442.
[138] A. Oraibi, A.A. Rashad, M.H. Ahmed, Carum carvi mediated green synthesis of copper nanoparticles and its effect on Solanum lycopersicum seedlings, J. Arid. Agric. 9 (2023) 9–15, https://doi.org/10.25081/jaa.2023.v9.8191.
[139] P. Zambare, A. Survase, S. Kanase, Green synthesis of copper nanoparticles using leaf extract of ocimum sanctum and its antimicrobial activity, Int. J. Pharm. Investig. 13 (1) (2023), https://doi.org/10.5530/223097131692.
[140] K. Parvathalu, K. Rajitha, B. Chandrashekar, K. Sathvik, K. Pranay Bhasker, B. Sreenivas, M. Pritam, P. Pushpalatha, K. Moses, P. Bala Bhaskar, Biomimetic synthesis of copper nanoparticles using tinospora cordifolia plant leaf extract for photocatalytic activity applications, Plasmonics (2023) 1–10, https://doi.org/10.1007/s11468-023-02037-y.
[141] S. Hameed, J. Iqbal, M. Ali, A.T. Khalil, B.A. Abbasi, M. Numan, Z.K. Shinwari, Green synthesis of zinc nanoparticles through plant extracts: establishing a novel era in cancer theranostics, Mater. Res. Express 6 (10) (2019) 102005, https://doi.org/10.1088/2053-1591/ab40df.
[142] S. Ahmed, S.A. Chaudhry, S. Ikram, A review on biogenic synthesis of ZnO nanoparticles using plant extracts and microbes: a prospect towards green chemistry, J. Photochem. Photobiol. B: Biol. 166 (2017) 272–284, https://doi.org/10.1016/j.jphotobiol.2016.12.011.
[143] T. Iqbal, A. Raza, M. Zafar, S. Afsheen, I. Kebaili, H. Alrobei, Plant-mediated green synthesis of zinc oxide nanoparticles for novel application to enhance the shelf life of tomatoes, Appl. Nanosci. (2022) 1–13, https://doi.org/10.1007/s13204-021-02238-z.
[144] M. Rafique, R. Tahir, S.S.A. Gillani, M.B. Tahir, M. Shakil, T. Iqbal, M. O. Abdellahi, Plant-mediated green synthesis of zinc oxide nanoparticles from Syzygium cumini for seed germination and wastewater purification, Int. J. Environ. Anal. Chem. 102 (1) (2022) 23–38, https://doi.org/10.1080/03067319.2020.1715379.
[145] T. Gur, I. Meydan, H. Seckin, M. Bekmezci, F. Sen, Green synthesis, characterization and bioactivity of biogenic zinc oxide nanoparticles, Environ. Res. 204 (2022) 111897, https://doi.org/10.1016/j.envres.2021.111897.
[146] K. Dulta, G. Koşarsoy Ağçeli, P. Chauhan, R. Jasrotia, P. Chauhan, A novel approach of synthesis zinc oxide nanoparticles by bergenia ciliata rhizome extract: antibacterial and anticancer potential, J. Inorg. Organomet. Polym. Mater. 31 (2021) 180–190, https://doi.org/10.1007/s10904-020-01684-6.
[147] S. Thomas, G. Gunasangkaran, V.A. Arumugam, S. Muthukrishnan, Synthesis and characterization of zinc oxide nanoparticles of Solanum nigrum and its anticancer activity via the induction of apoptosis in cervical cancer, Biol. Trace Elem. Res. 200 (6) (2022) 2684–2697, https://doi.org/10.1007/s12011-021-02898-6.
[148] T.M. Abdelghany, A.M. Al-Rajhi, R. Yahya, M.M. Bakri, M.A. Al Abboud, R. Yahya, H. Qanash, A.S. Bazaid, S.S. Salem, Phytofabrication of zinc oxide nanoparticles with advanced characterization and its antioxidant, anticancer, and antimicrobial activity against pathogenic microorganisms, Biomass Convers. Biorefin. 13 (1) (2023) 417–430, https://doi.org/10.1007/s13399-022-03412-1.
[149] S. Donga, S. Chanda, Caesalpinia crista seeds mediated green synthesis of zinc oxide nanoparticles for antibacterial, antioxidant, and anticancer activities, BioNanoScience 12 (2) (2022) 451–462, https://doi.org/10.1007/s12668-022-00952-8.
[150] N. Konappa, S.M. Joshi, N. Dhamodaran, S. Krishnamurthy, S. Basavaraju, S. Chowdappa, S. Jogaiah, Green synthesis of Callicarpa tomentosa routed zinc oxide nanoparticles and their bactericidal action against diverse phytopathogens, Biomass-.-. Convers. Biorefin. (2022) 1–12, https://doi.org/10.1007/s13399-022-03438-5.
[151] M. Kumar, D. Kaushik, A. Kumar, P. Gupta, C. Proestos, E. Oz, E. Orhan, J. Kaur, M.R. Khan, T. Elobeid, Green synthesis of copper nanoparticles from Nigella sativa seed extract and evaluation of their antibacterial and antiobesity activity, Int. J. Food Sci. Technol. (2023), https://doi.org/10.1111/ijfs.16359.
[152] S. Khan, Z.M. Almarhoon, J. Bakht, Y.N. Mabkhot, A. Rauf, A.A. Shad, Single-step Acer pentapomicum-mediated green synthesis of silver nanoparticles and their potential antimicrobial and antioxidant activities, J. Nanomater. 2022 (2022) 1–10, https://doi.org/10.1155/2022/3783420.
[153] Y. Kocak, G. Oto, I. Meydan, H. Seckin, T. Gur, A. Aygun, F. Sen, Assessment of therapeutic potential of silver nanoparticles synthesized by Ferula Pseudalliacea rech. F. plant, Inorg. Chem. Commun. 140 (2022) 109417, https://doi.org/10.1016/j.inoche.2022.109417.
[154] A. Bergal, G.H. Matar, M. Andaç, Olive and green tea leaf extracts mediated green synthesis of silver nanoparticles (AgNPs): comparison investigation on characterizations and antibacterial activity, Bionanoscience 12 (2) (2022) 307–321, https://doi.org/10.1007/s12668-022-00958-2.
[155] A. Kyzioł, S. Łukasiewicz, V. Sebastian, P. Kuśtrowski, M. Kozieł, D. Majda, A. Cierniak, Towards plant-mediated chemistry–Au nanoparticles obtained using aqueous extract of Rosa damascena and their biological activity in vitro, J. Inorg. Biochem. 214 (2021) 111300, https://doi.org/10.1016/j.jinorgbio.2020.111300.
[156] S. Sundararaman, M. Karthikeyan, J. Aravind kumar, P. Deivasigamani, M. R. Soosai, A. Ramaraja, S. Sahana, B.M. Thamer, M.H. El-Newehy, M. Rajasimman, Facile synthesis of iron nanoparticles from Camellia sinensis leaves catalysed for biodiesel synthesis from Azolla filiculoides, Sci. Rep. 14 (1) (2024) 12818, https://doi.org/10.1038/s41598-024-61113-3.
[157] Å.P. Matos, E. Novelli, G. Tribuzi, Use of algae as food ingredient: sensory acceptance and commercial products, Front. Food Sci. Technol. 2 (2022), https://doi.org/10.3389/frfst.2022.989801.
[158] M.C. Mendes, S. Navalho, A. Ferreira, C. Paulino, D. Figueiredo, D. Silva, F. Gao, F. Gama, G. Bombo, R. Jacinto, S.S. Aveiro, P.S.C. Schulze, A.T. Goncalves, H. Pereira, L. Gouveia, R.F. Patarra, M.H. Abreu, J.L. Silva, J. Navalho, J.C. S. Varela, L.G. Speranza, Algae as food in Europe: an overview of species diversity and their application, Foods 11 (13) (2022), https://doi.org/10.3390/foods11131871.
[159] A.K. Patel, F. Albarico, P.K. Perumal, A.P. Vadrale, C.T. Nian, H.T.B. Chau, C. Anwar, H. Wani, A. Pal, R. Saini, L.H. Ha, B. Senthilkumar, Y.S. Tsang, C. W. Chen, C.D. Dong, R.R. Singhania, Algae as an emerging source of bioactive pigments, Bioresour. Technol. 351 (2022) 126910, https://doi.org/10.1016/j.biortech.2022.126910.
[160] E. Zanchetta, E. Damergi, B. Patel, T. Borgmeyer, H. Pick, A. Pulgarin, C. Ludwig, Algal cellulose, production and potential use in plastics: challenges and opportunities, Algal Res. 56 (2021), https://doi.org/10.1016/j.algal.2021.102288.
[161] A. Ahmad, F. Banat, H. Alsafar, S.W. Hasan, Algae biotechnology for industrial wastewater treatment, bioenergy production, and high-value bioproducts, Sci. Total Environ. 806 (Pt 2) (2022) 150585, https://doi.org/10.1016/j.scitotenv.2021.150585.
[162] S. Li, P.L. Show, H.H. Ngo, S.H. Ho, Algae-mediated antibiotic wastewater treatment: a critical review, Environ. Sci. Ecotechnol. 9 (2022) 100145, https://doi.org/10.1016/j.ese.2022.100145.
[163] E.E. Ammar, A.A.A. Aioub, A.E. Elesawy, A.M. Karkour, M.S. Mouhamed, A. A. Amer, N.A. El-Shershaby, Algae as bio-fertilizers: between current situation and future prospective, Saudi J. Biol. Sci. 29 (5) (2022) 3083–3096, https://doi.org/10.1016/j.sjbs.2022.03.020.
[164] D. Fawcett, J.J. Verduin, M. Shah, S.B. Sharma, G.E.J. Poinern, A review of current research into the biogenic synthesis of metal and metal oxide nanoparticles via marine algae and seagrasses, J. Nanosci. 2017 (2017) 1–15, https://doi.org/10.1155/2017/8013850.
[165] P. Khanna, A. Kaur, D. Goyal, Algae-based metallic nanoparticles: synthesis, characterization and applications, J. Microbiol Methods 163 (2019) 105656, https://doi.org/10.1016/j.mimet.2019.105656.
[166] A. Les, L. Popescu, D. Creanga, D.-O. Dorohoi, L. Sacarescu, Study of gallic acid antioxidant molecule in interaction with solvents, aiming its utilization as a stabilizer of magnetic nanoparticles in suspensions, Mol. Cryst. Liq. Cryst. 762 (1) (2023) 1–12, https://doi.org/10.1080/15421406.2022.2066789.
[167] H.-s Kim, Y.S. Seo, K. Kim, J.W. Han, Y. Park, S. Cho, Concentration effect of reducing agents on green synthesis of gold nanoparticles: size, morphology, and growth mechanism, Nanoscale Res. Lett. 11 (2016) 1–9, https://doi.org/10.1186/s11671-016-1393-x.
[168] J. Pekkoh, K. Ruangrit, T. Kaewkod, Y. Tragoolpua, S. Hoijang, L. Srisombat, A. Wichapein, W. Pathom-Aree, Y. Kato, G. Wang, S. Srinuanpan, Innovative eco-friendly microwave-assisted rapid biosynthesis of Ag/AgCl-NPs coated with algae bloom extract as multi-functional biomaterials with non-toxic effects on normal human cells, Nanomaterials 13 (14) (2023), https://doi.org/10.3390/nano13142141.
[169] R. Vinayagam, V. Nagendran, L.C. Goveas, M.K. Narasimhan, T. Varadavenkatesan, N. Chandrasekar, R. Selvaraj, Structural characterization of marine macroalgae derived silver nanoparticles and their colorimetric sensing of hydrogen peroxide, Mater. Chem. Phys. 313 (2024), https://doi.org/10.1016/j.matchemphys.2023.128787.

[170] T.A. Roseline, M.P. Sudhakar, A. Kulanthaiyesu, Synthesis of silver nanoparticle composites using Calliblepharis fimbriata aqueous extract, phytochemical stimulation, and controlling bacterial blight disease in rice, ACS Agric. Sci. Technol. 1 (6) (2021) 702–718, https://doi.org/10.1021/acsagscitech.1c00189.
[171] S. Thanigaivel, S. Vickram, V. Saranya, H. Ali, S. Alarifi, J. Kumar Reddy Modigunta, K. Anbarasu, R. Lakshmipathy, K. Rohini, Seaweed polysaccharide mediated synthesis of silver nanoparticles and its enhanced disease resistance in Oreochromis mossambicus, J. King Saud. Univ. - Sci. 34 (2) (2022), https://doi.org/10.1016/j.jksus.2021.101771.
[172] H.E. Lashgarian, M. Karkhane, A.K. Alhameedawi, A. Marzban, Phyco-mediated synthesis of Ag/AgCl nanoparticles using ethanol extract of a marine green algae, delile with biological activity, Biointerface Res Appl. 11 (6) (2021) 14545–14554, https://doi.org/10.33263/Briac116.1454514554.
[173] S. Dixit, N. Vishnoi, N.M. Tripathi, D.P. Singh, Y.K. Sharma, Biosynthesis of nanostructured silver by green algae and evaluation of its microbicidal property against pathogenic microbes, Environ. Sustain. 5 (2) (2022) 197–206, https://doi.org/10.1007/s42398-022-00223-y.
[174] B. Cardoso, G. Nobrega, M. Machado, R.A. Lima, Green synthesis of copper ferrite-based nanofluids using Chlorella vulgaris for heat transfer enhancement, J. Mol. Liq. (2025) 127498.
[175] J. Flieger, W. Franus, R. Panek, M. Szymanska-Chargot, W. Flieger, M. Flieger, P. Kolodziej, Green synthesis of silver nanoparticles using natural extracts with proven antioxidant activity, Molecules 26 (16) (2021), https://doi.org/10.3390/molecules26164986.
[176] W.C. Song, B. Kim, S.Y. Park, G. Park, J.-W. Oh, Biosynthesis of silver and gold nanoparticles using Sargassum horneri extract as catalyst for industrial dye degradation, Arab. J. Chem. 15 (9) (2022), https://doi.org/10.1016/j.arabjc.2022.104056.
[177] R. Thiurunavukkarau, S. Shanmugam, K. Subramanian, P. Pandi, G. Muralitharan, M. Arokiarajan, K. Kasinathan, A. Sivaraj, R. Kalyanasundaram, S.Y. AlOmar, V. Shanmugam, Silver nanoparticles synthesized from the seaweed Sargassum polycystum and screening for their biological potential, Sci. Rep. 12 (1) (2022) 14757, https://doi.org/10.1038/s41598-022-18379-2.
[178] C.T.D. Raj, K. Muthukumar, H.U. Dahms, R.A. James, S. Kandaswamy, Structural characterization, antioxidant and anti-uropathogenic potential of biogenic silver nanoparticles using brown seaweed Turbinaria ornata, Front Microbiol 14 (2023) 1072043, https://doi.org/10.3389/fmicb.2023.1072043.
[179] A.D. Solanki, I.C. Patel, Sargassum tenerrimum-mediated green synthesis of silver nanoparticles along with antimicrobial activity, Appl. Nanosci. 13 (6) (2022) 4415–4425, https://doi.org/10.1007/s13204-022-02709-x.
[180] S. Thanigaivel, J. Thomas, A.S. Vickram, K. Anbarasu, R. Karunakaran, J. Palanivelu, P.S. Srikumar, Efficacy of encapsulated biogenic silver nanoparticles and its disease resistance against Vibrio harveyi through oral administration in Macrobrachium rosenbergii, Saudi J. Biol. Sci. 28 (12) (2021) 7281–7289, https://doi.org/10.1016/j.sjbs.2021.08.037.
[181] S. Ulagesan, T.J. Nam, Y.H. Choi, Cytotoxicity against human breast carcinoma cells of silver nanoparticles biosynthesized using Capsosiphon fulvescens extract, Bioprocess Biosyst. Eng. 44 (4) (2021) 901–911, https://doi.org/10.1007/s00449-020-02498-z.
[182] S. Dogmaz, L. Cavas, Biohydrogen production via green silver nanoparticles synthesized through biomass of Ulva lactuca bloom, Bioresour. Technol. 379 (2023) 129028, https://doi.org/10.1016/j.biortech.2023.129028.
[183] H.A. Badr, S.A. Sayed, M. Obiedallah, Eco-friendly synthesis of silver nanoparticles using Eisenia bicyclis seaweed, their antimicrobial and anticancer activities, Lett. Appl. Microbiol 76 (2) (2023), https://doi.org/10.1093/lambio/ovad002.
[184] M. Govindaraj, M. Suresh, T. Palaniyandi, S. Viswanathan, M.R.A. Wahab, G. Baskar, H. Surendran, M. Ravi, A. Sivaji, Bio-fabrication of gold nanoparticles from brown seaweeds for anticancer activity against glioblastoma through invitro and molecular docking approaches, J. Mol. Struct. 1281 (2023), https://doi.org/10.1016/j.molstruc.2023.135178.
[185] M. Kamal, N. Abdel-Raouf, H. Sonbol, H. Abdel-Tawab, M.S. Abdelhameed, O. Hammouda, K.N.M. Elsayed, In vitro assessment of antimicrobial, anti-inflammatory, and schistolarvicidal activity of macroalgae-based gold nanoparticles, Front. Mar. Sci. 9 (2022), https://doi.org/10.3389/fmars.2022.1075832.
[186] S.M. Abd El-Aziz, A.A. Sleem, M.I.A. Abdel Maksoud, Comparative study of the antioxidant, toxicity, anti-inflammatory, and wound healing activities of both Digenea simplex polysaccharides and their corresponding (ZnO–Au) bimetallic nanoparticles, Cellulose 30 (1) (2022) 303–321, https://doi.org/10.1007/s10570-022-04878-y.
[187] S.Y. Park, K. Park, H.M. Kang, W.C. Song, J.W. Oh, Y.W. Choi, G. Park, Induction of browning in white adipocytes: Fucoidan characterization and gold nanoparticle synthesis from Undaria pinnatifida Sporophyll extract, Mar. Drugs 21 (12) (2023), https://doi.org/10.3390/md21120603.
[188] S. Rajeshkumar, M.H. Sherif, C. Malarkodi, M. Ponnanikajamideen, M.V. Arasu, N.A. Al-Dhabi, S.M. Roopan, Cytotoxicity behaviour of response surface model optimized gold nanoparticles by utilizing fucoidan extracted from padina tetrastromatica, J. Mol. Struct. 1228 (2021), https://doi.org/10.1016/j.molstruc.2020.129440.
[189] U. Žvab, D.S. Kukulin, M. Fanetti, M. Valant, Bioremediation of copper polluted wastewater-like nutrient media and simultaneous synthesis of stable copper nanoparticles by a viable green alga, J. Water Process Eng. 42 (2021), https://doi.org/10.1016/j.jwpe.2021.102123.
[190] S.A. Alsalamah, M.I. Alghonaim, A.M. Mohammad, T.M. Abdel Ghany, Algal biomass extract as mediator for copper oxide nanoparticle synthesis: applications in control of fungal, bacterial growth, and photocatalytic degradations of dyes, BioResources 18 (4) (2023) 7474–7489, https://doi.org/10.15376/biores.18.4.7474-7489.
[191] T. Balaji, C.M. Manushankar, K.A. Al-Ghanim, C. Kamaraj, D. Thirumurugan, S. Thanigaivel, M. Nicoletti, N. Sachivkina, M. Govindarajan, Padina boergesenii-mediated copper oxide nanoparticles synthesis, with their antibacterial and anticancer potential, Biomedicines 11 (8) (2023), https://doi.org/10.3390/biomedicines11082285.
[192] B.S. S, S. Pitchiah, V. Suresh, P. Ramasamy, Biosynthesis of copper nanoparticles from seaweed Ulva lactuca and their in vitro antioxidative potential, Cureus 15 (11) (2023) e48985, https://doi.org/10.7759/cureus.48985.
[193] F. Caf, Biogenic synthesis of iron oxide nanoparticle using Padina pavonica extract: application for photocatalytic degradation of congo red dye, neurotoxicity and antioxidant activity, Turk. J. Fish. Aquat. Sci. 23 (2) (2022), https://doi.org/10.4194/trjfas21398.
[194] T. Palaniyandi, G. Baskar, B. V, S. Viswanathan, M.R. Abdul Wahab, M. K. Govindaraj, A. Sivaji, B.K. Rajendran, S. Kaliamoorthy, Biosynthesis of iron nanoparticles using brown algae Spatoglossum asperum and its antioxidant and anticancer activities through in vitro and in silico studies, Part. Sci. Technol. 41 (7) (2023) 916–929. ⟨https://doi.org/10.1080/02726351.2022.2159900⟩.
[195] S. Bhukal, A. Sharma, Rishi Divya, S. Kumar, B. Deepak, K. Pal, S. Mona, Spirulina based iron oxide nanoparticles for adsorptive removal of crystal violet dye, Top. Catal. 65 (19-20) (2022) 1675–1685, https://doi.org/10.1007/s11244-022-01640-3.
[196] A.T. Mansour, A.E. Alprol, M. Khedawy, K.M. Abualnaja, T.A. Shalaby, G. Rayan, K.M.A. Ramadan, M. Ashour, Green synthesis of zinc oxide nanoparticles using red seaweed for the elimination of organic toxic dye from an aqueous solution, Materials 15 (15) (2022), https://doi.org/10.3390/ma15155169.
[197] G.S. Thirumoorthy, O. Balasubramaniam, P. Kumaresan, P. Muthusamy, K. Subramani, Tetraselmis indica mediated green synthesis of zinc oxide (ZnO) nanoparticles and evaluating its antibacterial, antioxidant, and hemolytic activity, BioNanoScience 11 (1) (2021) 172–181, https://doi.org/10.1007/s12668-020-00817-y.
[198] V. Marunganathan, M.S.K. Kumar, Z.A. Kari, J. Giri, M.R. Shaik, B. Shaik, A. Guru, Marine-derived kappa-carrageenan-coated zinc oxide nanoparticles for targeted drug delivery and apoptosis induction in oral cancer, Mol. Biol. Rep. 51 (1) (2024) 89, https://doi.org/10.1007/s11033-023-09146-1.
[199] L. Shu Hua, S.C.B. Gopinath, P. Anbu, A.R.W. Yaakub, Cobalt nanoparticle production using algal extract: a nanocarrier for antimicrobial potential, Mater. Express 13 (4) (2023) 679–687, https://doi.org/10.1166/mex.2023.2392.
[200] N.E. Sunny, A. Kaviya, P. Saravanan, R. Rajeshkannan, M. Rajasimman, S. V. Kumar, In vitro and in silico molecular docking analysis of green synthesized tin oxide nanoparticles using brown algae species of Padina gymnospora and Turbinaria ornata, Biomass Convers. Biorefin. (2022), https://doi.org/10.1007/s13399-022-03253-y.
[201] W. Salem, F.N. El-Deen, K. Ebnalwaleed, M. Badry, A.A.H.A. Latef, UV-induced antibacterial activity of green-synthesized TiO2 nanoparticles for the potential reuse of raw surface and underground water, J. Plant Growth Regul. 41 (3) (2021) 1344–1358, https://doi.org/10.1007/s00344-021-10391-6.
[202] W.M. Alarif, Y.A. Shaban, M.I. Orif, M.A. Ghandourah, A.J. Turki, H.S. Alorfi, H. R.Z. Tadros, Green synthesis of TiO(2) nanoparticles using natural marine extracts for antifouling activity, Mar. Drugs 21 (2) (2023), https://doi.org/10.3390/md21020062.
[203] S.A. Benson, Ultrastructure of bacteria. Principles of Medical Biology, Elsevier, 1998, pp. 1–14, https://doi.org/10.1016/S1569-2582(97)80138-9.
[204] K. Khosravi-Darani, A. da Cruz, M. Mozafari, Z. Abdi, N. Ahmadi, Biosynthesis of metal nanoparticles by probiotic bacteria, Lett. Appl. NanoBioSci. 8 (3) (2019) 619–626, https://doi.org/10.33263/LIANBS83.619626.
[205] W. Margolin, Sculpting the bacterial cell, Curr. Biol. 19 (17) (2009) R812–R822, https://doi.org/10.1016/j.cub.2009.06.033.
[206] D. Singhi, P. Srivastava, Role of bacterial cytoskeleton and other apparatuses in cell communication, Front. Mol. Biosci. 7 (2020) 158, https://doi.org/10.3389/fmolb.2020.00158.
[207] H. Wu, H. Cui, C. Fu, R. Li, F. Qi, Z. Liu, G. Yang, K. Xiao, M. Qiao, Unveiling the crucial role of soil microorganisms in carbon cycling: a review, Sci. Total Environ. (2023) 168627, https://doi.org/10.1016/j.scitotenv.2023.168627.
[208] C.M. Ferreira, H.M. Soares, E.V. Soares, Promising bacterial genera for agricultural practices: an insight on plant growth-promoting properties and microbial safety aspects, Sci. Total Environ. 682 (2019) 779–799, https://doi.org/10.1016/j.scitotenv.2019.04.225.
[209] X. Li, H. Xu, Z.-S. Chen, G. Chen, Biosynthesis of nanoparticles by microorganisms and their applications, J. Nanomater. 2011 (2011) 1–16, https://doi.org/10.1155/2011/270974.
[210] S. Iravani, Bacteria in nanoparticle synthesis: current status and future prospects, Int. Sch. Res. Not. 2014 (2014), https://doi.org/10.1155/2014/359316.
[211] S. Tsekhmistrenko, V. Bityutskyy, O. Tsekhmistrenko, L. Horalskyi, N. Tymoshok, M. Spivak, Bacterial synthesis of nanoparticles: a green approach, Biosyst. Divers. 28 (1) (2020) 9–17, https://doi.org/10.15421/012002.
[212] N.I. Hulkoti, T. Taranath, Biosynthesis of nanoparticles using microbes—a review, Colloids Surf. B Biointerfaces 121 (2014) 474–483, https://doi.org/10.1016/j.colsurfb.2014.05.027.
[213] A.K. Sidhu, N. Verma, P. Kaushal, Role of biogenic capping agents in the synthesis of metallic nanoparticles and evaluation of their therapeutic potential, Front. Nanotechnol. 3 (2022) 801620, https://doi.org/10.1186/s12951-020-00704-4.
[214] R. Javed, M. Zia, S. Naz, S.O. Aisida, Nu Ain, Q. Ao, Role of capping agents in the application of nanoparticles in biomedicine and environmental remediation:

recent trends and future prospects, J. Nanobiotechnol. 18 (2020) 1–15, https://doi.org/10.1186/s12951-020-00704-4.
[215] C.E. Escárcega-González, J.A. Garza-Cervantes, A. Vázquez-Rodríguez, J. R. Morones-Ramírez, Bacterial exopolysaccharides as reducing and/or stabilizing agents during synthesis of metal nanoparticles with biomedical applications, Int. J. Polym. Sci. 2018 (2018), https://doi.org/10.1155/2018/7045852.
[216] A.E.-R.R. El-Shanshoury, S.E. ElSilk, M.E. Ebeid, Extracellular biosynthesis of silver nanoparticles using Escherichia coli ATCC 8739, Bacillus subtilis ATCC 6633, and Streptococcus thermophilus ESh1 and their antimicrobial activities, Int. Sch. Res. Not. 2011 (2011), https://doi.org/10.5402/2011/385480.
[217] N. Krumov, I. Perner-Nochta, S. Oder, V. Gotcheva, A. Angelov, C. Posten, Production of inorganic nanoparticles by microorganisms, Chem. Eng. Technol.: Ind. Chem. -Plant Equip. Process Eng. Biotechnol. 32 (7) (2009) 1026–1035, https://doi.org/10.1002/ceat.200900046.
[218] H. Bahrulolum, S. Nooraei, N. Javanshir, H. Tarrahimofrad, V.S. Mirbagheri, A. J. Easton, G. Ahmadian, Green synthesis of metal nanoparticles using microorganisms and their application in the agrifood sector, J. Nanobiotechnol. 19 (2021) 1–26, https://doi.org/10.1186/s12951-021-00834-3.
[219] D. Lahiri, M. Nag, H.I. Sheikh, T. Sarkar, H.A. Edinur, S. Pati, R.R. Ray, Microbiologically-synthesized nanoparticles and their role in silencing the biofilm signaling cascade, Front. Microbiol. 12 (2021) 636588, https://doi.org/10.3389/fmicb.2021.636588.
[220] Q.A. Al-Maliki, W.R. Taj-Aldeen, Antibacterial and antibiofilm activity of bacteria mediated synthesized Fe3O4 nanoparticles using Bacillus Coagulans, J. Nanostruct. 11 (4) (2021) 782–789, https://doi.org/10.22052/JNS.2021.04.015.
[221] M.S. John, J.A. Nagoth, M. Zannotti, R. Giovannetti, A. Mancini, K.P. Ramasamy, C. Miceli, S. Pucciarelli, Biogenic synthesis of copper nanoparticles using bacterial strains isolated from an Antarctic consortium associated to a psychrophilic marine ciliate: characterization and potential application as antimicrobial agents, Mar. Drugs 19 (5) (2021) 263, https://doi.org/10.3390/md19050263.
[222] M.S. John, J.A. Nagoth, K.P. Ramasamy, A. Mancini, G. Giuli, C. Miceli, S. Pucciarelli, Synthesis of bioactive silver nanoparticles using new bacterial strains from an Antarctic consortium, Mar. Drugs 20 (9) (2022) 558, https://doi.org/10.3390/md20090558.
[223] M.A. Huq, A.A. Khan, J.M. Alshehri, M.S. Rahman, S.R. Balusamy, S. Akter, Bacterial mediated green synthesis of silver nanoparticles and their antibacterial and antifungal activities against drug-resistant pathogens, R. Soc. Open Sci. 10 (10) (2023) 230796, https://doi.org/10.1098/rsos.230796.
[224] R. Esmail, A. Afshar, M. Morteza, A. Abolfazl, E. Akhondi, Synthesis of silver nanoparticles with high efficiency and stability by culture supernatant of Bacillus ROM6 isolated from Zarshouran gold mine and evaluating its antibacterial effects, BMC Microbiol. 22 (1) (2022) 97, https://doi.org/10.1186/s12866-022-02490-5.
[225] Y.M. Kwon, E.-S. Cho, K.W. Kim, D. Chung, S.S. Bae, W.-J. Yu, J.Y.H. Kim, G. Choi, Synthesis of silver nanoparticles using Aggregatimonas sangjinii F202Z8T and their biological characterization, Microorganisms 11 (12) (2023) 2975, https://doi.org/10.3390/microorganisms11122975.
[226] D. Chung, J. Jung, J.Y.H. Kim, K.W. Kim, Y.M. Kwon, Aggregatimonas sangjinii gen. nov., sp. nov., a novel silver nanoparticle synthesizing bacterium belonging to the family Flavobacteriaceae, Antonie Van. Leeuwenhoek 115 (2) (2022) 325–335, https://doi.org/10.1007/s10482-021-01700-w.
[227] N. Pallath, B. Francis, S. Devanesan, N. Asemi, M.S. AlSalhi, S. Natarajan, Synthesis of silver nanoparticles from marine bacteria and evaluation of antimicrobial, antifungal and cytotoxic effects, J. King Saud. Univ. -Sci. 36 (2) (2024) 103073, https://doi.org/10.1016/j.jksus.2023.103073.
[228] M.M.N. El-Dein, Z.A. Baka, M.I. Abou-Dobara, A.K. El-Sayed, M.M. El-Zahed, Extracellular biosynthesis, optimization, characterization and antimicrobial potential of Escherichia coli D8 silver nanoparticles, J. Microbiol., Biotechnol. Food Sci. 10 (4) (2021) 648–656, https://doi.org/10.15414/jmbfs.2021.10.4.648-656.
[229] C. Pernas-Pleite, A.M. Conejo-Martínez, I. Marín, J.P. Abad, Green extracellular synthesis of silver nanoparticles by Pseudomonas alloputida, their growth and biofilm-formation inhibitory activities and synergic behavior with three classical antibiotics, Molecules 27 (21) (2022) 7589, https://doi.org/10.3390/molecules27217589.
[230] T. Monowar, M.S. Rahman, S.J. Bhore, K.V. Sathasivam, Endophytic bacteria enterobacter hormaechei fabricated silver nanoparticles and their antimicrobial activity, Pharmaceutics 13 (4) (2021), https://doi.org/10.3390/pharmaceutics13040511.
[231] Q. Li, T. Feng, H. Li, Z. Wang, X. Wei, J. Liu, Green synthesis of silver nanoparticles using endophytic bacterium Bacillus zanthoxyli GBE11 and their antimicrobial activity, Biomass Convers. Biorefin. (2022) 1–13, https://doi.org/10.1007/s13399-022-03266-7.
[232] S. Sudarsan, M. Kumar Shankar, A. Kumar Belagal Motatis, S. Shankar, D. Krishnappa, C.D. Mohan, K.S. Rangappa, V.K. Gupta, C.N. Siddaiah, Green synthesis of silver nanoparticles by Cytobacillus firmus isolated from the stem bark of Terminalia arjuna and their antimicrobial activity, Biomolecules 11 (2) (2021) 259, https://doi.org/10.3390/biom11020259.
[233] H. Ren Loi, S. Abbasiliasi, P. Bothi Raja, M. Shamzi Mohamed, W.-N. Tan, H. Suan Ng, J. Chi-Wei Lan, J. Shun Tan, Biosynthesis of silver nanoparticles using nitrate reductase produced by Lactobacillus plantarum CAM 4: characterization and in vitro evaluation of its antimicrobial efficiency, J. Mol. Liq. 376 (2023), https://doi.org/10.1016/j.molliq.2023.121476.
[234] E.M. Afolayan, S.L. Afegbua, S.A. Ado, Characterization and antibacterial activity of silver nanoparticles synthesized by soil-dwelling Bacillus thuringiensis against drug-resistant bacteria, Biologia 78 (8) (2023) 2283–2292, https://doi.org/10.1007/s11756-023-01381-y.
[235] L.V. Tan, T. Tran, V.D. Thi, Biosynthesis of silver nanoparticles from Bacillus licheniformis TT01 isolated from quail manure collected in Vietnam, Processes 9 (4) (2021), https://doi.org/10.3390/pr9040584.
[236] R. Shunmugam, S.R. Balusamy, V. Kumar, S. Menon, T. Lakshmi, H. Perumalsamy, Biosynthesis of gold nanoparticles using marine microbe (Vibrio alginolyticus) and its anticancer and antioxidant analysis, J. King Saud. Univ. Sci. 33 (1) (2021) 101260, https://doi.org/10.1016/j.jksus.2020.101260.
[237] M.S. Kuyukina, M.V. Makarova, I.B. Ivshina, K.P. Kazymov, B.M. Osovetsky, Biosynthesis and characterization of gold nanoparticles produced using Rhodococcus actinobacteria at elevated chloroauric acid concentrations, Int. J. Mol. Sci. 23 (21) (2022) 12939, https://doi.org/10.3390/ijms232112939.
[238] S. Wei, Q. Zheng, Biosynthesis and characterization of zinc sulphide nanoparticles produced by the bacterium Lysinibacillus sp. SH74, Ceram. Int. 50 (2) (2024) 2637–2642, https://doi.org/10.1016/j.ceramint.2023.10.246.
[239] A. Sivakumar, V. Suresh, S. Sethuraman, P. Sivaperumal, Biosynthesis of zinc nanoparticles from actinobacterium streptomyces species and their biological potential, Cureus 16(2 (2024) e54124, https://doi.org/10.7759/cureus.54124.
[240] A.M. Abdo, A. Fouda, A.M. Eid, N.M. Fahmy, A.M. Elsayed, A.M.A. Khalil, O. M. Alzahrani, A.F. Ahmed, A.M. Soliman, Green synthesis of zinc oxide nanoparticles (ZnO-NPs) by Pseudomonas aeruginosa and their activity against pathogenic microbes and common house mosquito, Culex pipiens, Materials 14 (22) (2021), https://doi.org/10.3390/ma14226983.
[241] S. Rajeshkumar, S. Jayakodi, M. Tharani, N.S. Alharbi, M. Thiruvengadam, Antimicrobial activity of probiotic bacteria-mediated cadmium oxide nanoparticles against fish pathogens, Microb. Pathog. (2024) 106602, https://doi.org/10.1016/j.micpath.2024.106602.
[242] I.A. Beleneva, U.V. Kharchenko, A.D. Kukhlevsky, A.V. Boroda, N.V. Izotov, A. S. Gnedenkov, V.S. Egorkin, Biogenic synthesis of selenium and tellurium nanoparticles by marine bacteria and their biological activity, World J. Microbiol Biotechnol. 38 (11) (2022) 188, https://doi.org/10.1007/s11274-022-03374-6.
[243] I. Ghiuta, C. Croitoru, J. Kost, R. Wenkert, D. Munteanu, Bacteria-mediated synthesis of silver and silver chloride nanoparticles and their antimicrobial activity, Appl. Sci. 11 (7) (2021) 3134, https://doi.org/10.3390/app11073134.
[244] A.F. Hassan, R.R. Hateet, M.A. Al-Shakban, Biosynthesis and antibacterial activity of gold oxide nanoparticles by nocardia asteroids isolated from soil, J. Nanostruct. 13 (2) (2023) 417–430, https://doi.org/10.22052/JNS.2023.02.012.
[245] O.G. Ozdal, Green synthesis of Ag, Se, and Ag(2)Se nanoparticles by Pseudomonas aeruginosa: characterization and their biological and photocatalytic applications, Folia Microbiol (Praha) 69 (3) (2024) 625–638, https://doi.org/10.1007/s12223-023-01100-9.
[246] M.A. Ashour, B.T. Abd-Elhalim, Biosynthesis and biocompatibility evaluation of zinc oxide nanoparticles prepared using Priestia megaterium bacteria, Sci. Rep. 14 (1) (2024) 4147, https://doi.org/10.1038/s41598-024-54460-8.
[247] E. Żymańczyk-Duda, M. Brzezińska-Rodak, M. Klimek-Ochab, M. Duda, A. Zerka, Yeast as a versatile tool in biotechnology, Yeast Ind. Appl. 1 (2017) 3–40, https://doi.org/10.5772/intechopen.70130.
[248] L. Breeden, K. Nasmyth, Similarity between cell-cycle genes of budding yeast and fission yeast and the Notch gene of Drosophila, Nature 329 (6140) (1987) 651–654, https://doi.org/10.1038/329651a0.
[249] M.K. Balasubramanian, E. Bi, M. Glotzer, Comparative analysis of cytokinesis in budding yeast, fission yeast and animal cells, Curr. Biol. 14 (18) (2004) R806–R818.
[250] A. Halász, R. Lásztity, Use of Yeast Biomass in Food Production, Routledge, 2017.
[251] H. Feng, S.-y Liu, X.-b Huang, R. Ren, Y. Zhou, C.-p Song, D.-h Qian, Green biosynthesis of CdS nanoparticles using yeast cells for fluorescence detection of nucleic acids and electrochemical detection of hydrogen peroxide, Int. J. Electrochem. Sci. 12 (1) (2017) 618–628, https://doi.org/10.20964/2017.01.57.
[252] A. Boroumand Moghaddam, F. Namvar, M. Moniri, P. Md. Tahir, S. Azizi, R. Mohamad, Nanoparticles biosynthesized by fungi and yeast: a review of their preparation, properties, and medical applications, Molecules 20 (9) (2015) 16540–16565, https://doi.org/10.3390/molecules200916540.
[253] M. Gajbhiye, J. Kesharwani, A. Ingle, A. Gade, M. Rai, Fungus-mediated synthesis of silver nanoparticles and their activity against pathogenic fungi in combination with fluconazole, Nanomed.: Nanotechnol., Biol. Med. 5 (4) (2009) 382–386, https://doi.org/10.1016/j.nano.2009.06.005.
[254] B.K. Salunke, S.S. Sawant, S.-I. Lee, B.S. Kim, Comparative study of MnO 2 nanoparticle synthesis by marine bacterium Saccharophagus degradans and yeast Saccharomyces cerevisiae, Appl. Microbiol. Biotechnol. 99 (2015) 5419–5427, https://doi.org/10.1007/s00253-015-6559-4.
[255] P. Perego, S.B. Howell, Molecular mechanisms controlling sensitivity to toxic metal ions in yeast, Toxicol. Appl. Pharmacol. 147 (2) (1997) 312–318, https://doi.org/10.1006/taap.1997.8271.
[256] D. Kumar, L. Karthik, G. Kumar, K. Roa, Biosynthesis of silver nanoparticles from marine yeast and their antimicrobial activity against multidrug resistant pathogens, Pharmacologyonline 3 (2011) 1100–1111.
[257] A. Roychoudhury, Yeast-mediated green synthesis of nanoparticles for biological applications, Indian J. Pharm. Biol. Res 8 (03) (2020) 26–31, https://doi.org/10.30750/ijpbr.8.3.4.
[258] X. Zhang, S. Yan, R. Tyagi, R. Surampalli, Synthesis of nanoparticles by microorganisms and their application in enhancing microbiological reaction rates, Chemosphere 82 (4) (2011) 489–494, https://doi.org/10.1016/j.chemosphere.2010.10.023.

[259] K.N. Thakkar, S.S. Mhatre, R.Y. Parikh, Biological synthesis of metallic nanoparticles, Nanomed.: Nanotechnol., Biol. Med. 6 (2) (2010) 257–262, https://doi.org/10.1016/j.nano.2009.07.002.
[260] D. Liu, L. Ding, J. Sun, N. Boussetta, E. Vorobiev, Yeast cell disruption strategies for recovery of intracellular bio-active compounds—a review, Innov. Food Sci. Emerg. Technol. 36 (2016) 181–192, https://doi.org/10.1016/j.ifset.2016.06.017.
[261] M. Shu, F. He, Z. Li, X. Zhu, Y. Ma, Z. Zhou, Z. Yang, F. Gao, M. Zeng, Biosynthesis and antibacterial activity of silver nanoparticles using yeast extract as reducing and capping agents, Nanoscale Res. Lett. 15 (2020) 1–9, https://doi.org/10.1186/s11671-019-3244-z.
[262] S. He, Z. Guo, Y. Zhang, S. Zhang, J. Wang, N. Gu, Biosynthesis of gold nanoparticles using the bacteria Rhodopseudomonas capsulata, Mater. Lett. 61 (18) (2007) 3984–3987, https://doi.org/10.1016/j.matlet.2007.01.018.
[263] M. Kowshik, N. Deshmukh, W. Vogel, J. Urban, S.K. Kulkarni, K. Paknikar, Microbial synthesis of semiconductor CdS nanoparticles, their characterization, and their use in the fabrication of an ideal diode, Biotechnol. Bioeng. 78 (5) (2002) 583–588, https://doi.org/10.1002/bit.10233.
[264] N. Krumov, S. Oder, I. Perner-Nochta, A. Angelov, C. Posten, Accumulation of CdS nanoparticles by yeasts in a fed-batch bioprocess, J. Biotechnol. 132 (4) (2007) 481–486, https://doi.org/10.1016/j.jbiotec.2007.08.016.
[265] T. Voeikova, E. Kozhukhova, O. Zhuravliova, V. Retivov, E. Chigorina, V. Kuligin, V. Debabov, Microbial synthesis of cadmium sulfide nanoparticles: influence of bacteria of various species on the characteristics of biogenic nanoparticles, Nanotechnol. Russ. 15 (2020) 182–190, https://doi.org/10.1134/S1995078020020202.
[266] A.F. El-Baz, N.M. Sorour, Y.M. Shetaia, Trichosporon jirovecii–mediated synthesis of cadmium sulfide nanoparticles, J. Basic Microbiol. 56 (5) (2016) 520–530, https://doi.org/10.1002/jobm.201500275.
[267] Z. Lin, J. Wu, R. Xue, Y. Yang, Spectroscopic characterization of Au3+ biosorption by waste biomass of Saccharomyces cerevisiae, Spectrochim. Acta Part A: Mol. Biomol. Spectrosc. 61 (4) (2005) 761–765, https://doi.org/10.1016/j.saa.2004.03.029.
[268] H.-A. Lim, A. Mishra, S.-I. Yun, Effect of pH on the extra cellular synthesis of gold and silver nanoparticles by Saccharomyces cerevisae, J. Nanosci. Nanotechnol. 11 (1) (2011) 518–522, https://doi.org/10.1166/jnn.2011.3266.
[269] P. Pimprikar, S. Joshi, A. Kumar, S. Zinjarde, S. Kulkarni, Influence of biomass and gold salt concentration on nanoparticle synthesis by the tropical marine yeast Yarrowia lipolytica NCIM 3589, Colloids Surf. B Biointerfaces 74 (1) (2009) 309–316, https://doi.org/10.1016/j.colsurfb.2009.07.040.
[270] M. Gericke, A. Pinches, Microbial production of gold nanoparticles, Gold. Bull. 39 (2006) 22–28.
[271] X. Zhang, Y. Qu, W. Shen, J. Wang, H. Li, Z. Zhang, S. Li, J. Zhou, Biogenic synthesis of gold nanoparticles by yeast Magnusiomyces ingens LH-F1 for catalytic reduction of nitrophenols, Colloids Surf. A Physicochem. Eng. Asp. 497 (2016) 280–285, https://doi.org/10.1016/j.colsurfa.2016.02.033.
[272] S. Lian, C.S. Diko, Y. Yan, Z. Li, H. Zhang, Q. Ma, Y. Qu, Characterization of biogenic selenium nanoparticles derived from cell-free extracts of a novel yeast Magnusiomyces ingens, 3 Biotech 9 (2019) 1–8, https://doi.org/10.1007/s13205-019-1748-y.
[273] M. Ashengroph, S. Tozandehjani, Optimized resting cell method for green synthesis of selenium nanoparticles from a new Rhodotorula mucilaginosa strain, Process Biochem. 116 (2022) 197–205, https://doi.org/10.1016/j.procbio.2022.03.014.
[274] A.M. El-Khawaga, M.A. Elsayed, M. Gobara, A.A. Soliman, A.H. Hashem, A. A. Zaher, M. Mohsen, S.S. Salem, Green synthesized ZnO nanoparticles by Saccharomyces cerevisiae and their antibacterial activity and photocatalytic degradation, Biomass Convers. Biorefin. (2023) 1–12, https://doi.org/10.1007/s13399-023-04827-0.
[275] A. Boroumand Moghaddam, M. Moniri, S. Azizi, R. Abdul Rahim, A. Bin Ariff, W. Zuhainis Saad, F. Namvar, M. Navaderi, R. Mohamad, Biosynthesis of ZnO nanoparticles by a new Pichia kudriavzevii yeast strain and evaluation of their antimicrobial and antioxidant activities, Molecules 22 (6) (2017) 872, https://doi.org/10.3390/molecules22060872.
[276] K. Roy, C. Sarkar, C. Ghosh, Photocatalytic activity of biogenic silver nanoparticles synthesized using yeast (Saccharomyces cerevisiae) extract, Appl. Nanosci. 5 (2015) 953–959, https://doi.org/10.1007/s13204-014-0392-4.
[277] I. Olobayotan, B. Akin-Osanaiye, Biosynthesis of silver nanoparticles using baker's yeast, Saccharomyces cerevisiae and its antibacterial activities, Microbiol. Soc. (2019).
[278] O. Skrotska, Y. Kharchenko, Y. Laziuka, A. Marynin, M. Kharchuk, Biosynthesis and characterictics of silver nanoparticles obtained using Saccharomyces cerevisiae M437, 2021.
[279] M. Kowshik, S. Ashtaputre, S. Kharrazi, W. Vogel, J. Urban, S.K. Kulkarni, K. M. Paknikar, Extracellular synthesis of silver nanoparticles by a silver-tolerant yeast strain MKY3, Nanotechnology 14 (1) (2002) 95, https://doi.org/10.1088/0957-4484/14/1/321.
[280] M. Eugenio, N. Müller, S. Frases, R. Almeida-Paes, L.M.T. Lima, L. Lemgruber, M. Farina, W. de Souza, C. Sant'Anna, Yeast-derived biosynthesis of silver/silver chloride nanoparticles and their antiproliferative activity against bacteria, RSC Adv. 6 (12) (2016) 9893–9904, https://doi.org/10.1039/C5RA22727E.
[281] X. Liu, J.-L. Chen, W.-Y. Yang, Y.-C. Qian, J.-Y. Pan, C.-N. Zhu, L. Liu, W.-B. Ou, H.-X. Zhao, D.-P. Zhang, Biosynthesis of silver nanoparticles with antimicrobial and anticancer properties using two novel yeasts, Sci. Rep. 11 (1) (2021) 15795, https://doi.org/10.1038/s41598-021-95262-6.
[282] M. Apte, D. Sambre, S. Gaikawad, S. Joshi, A. Bankar, A.R. Kumar, S. Zinjarde, Psychrotrophic yeast Yarrowia lipolytica NCYC 789 mediates the synthesis of antimicrobial silver nanoparticles via cell-associated melanin, Amb. Express 3 (2013) 1–8, https://doi.org/10.1186/2191-0855-3-32.
[283] S.D. Katharine, J. Aadhil, M. Saxena, P. Radha, Sustainable biosynthesis of silver nanoparticles and their application to recover" single cell oil" from Yarrowia Lipolytica for biodiesel synthesis, Bionanoscience 12 (3) (2022) 890–900, https://doi.org/10.1007/s12668-022-00985-z.
[284] A.A. Hassabo, E.I. Ibrahim, B.A. Ali, H.E. Emam, Anticancer effects of biosynthesized Cu2O nanoparticles using marine yeast, Biocatal. Agric. Biotechnol. 39 (2022) 102261, https://doi.org/10.1016/j.bcab.2021.102261.
[285] M. Sriramulu, S. Sumathi, Biosynthesis of palladium nanoparticles using Saccharomyces cerevisiae extract and its photocatalytic degradation behaviour, Adv. Nat. Sci.: Nanosci. Nanotechnol. 9 (2) (2018) 025018, https://doi.org/10.1088/2043-6254/aac506.
[286] F. Asghari-Paskiabi, M. Imani, H. Rafii-Tabar, M. Razzaghi-Abyaneh, Physicochemical properties, antifungal activity and cytotoxicity of selenium sulfide nanoparticles green synthesized by Saccharomyces cerevisiae, Biochem. Biophys. Res. Commun. 516 (4) (2019) 1078–1084, https://doi.org/10.1016/j.bbrc.2019.07.007.
[287] S. Faramarzi, Y. Anzabi, H. Jafarizadeh-Malmiri, Nanobiotechnology approach in intracellular selenium nanoparticle synthesis using Saccharomyces cerevisiae—fabrication and characterization, Arch. Microbiol. 202 (5) (2020) 1203–1209, https://doi.org/10.1007/s00203-020-01831-0.
[288] S.S. Salem, Baker's yeast-mediated silver nanoparticles: characterisation and antimicrobial biogenic tool for suppressing pathogenic microbes, BioNanoScience 12 (4) (2022) 1220–1229, https://doi.org/10.1007/s12668-022-01026-5.
[289] H.A. Ammar, A.A.A. El Aty, S.A. El Awdan, Extracellular myco-synthesis of nano-silver using the fermentable yeasts Pichia kudriavzevii HA-NY2 and Saccharomyces uvarum HA-NY3, and their effective biomedical applications, Bioprocess Biosyst. Eng. 44 (2021) 841–854, https://doi.org/10.1007/s00449-020-02494-3.
[290] R. Chauhan, A. Reddy, J. Abraham, Biosynthesis of silver and zinc oxide nanoparticles using Pichia fermentans JA2 and their antimicrobial property, Appl. Nanosci. 5 (2015) 63–71, https://doi.org/10.1007/s13204-014-0292-7.
[291] C.T. Ingold, The biology of fungi, Springer Science & Business Media, 2012 https://doi.org/10.1007/978-94-011-1496-7.
[292] K. Vahabi, G.A. Mansoori, S. Karimi, Biosynthesis of silver nanoparticles by fungus Trichoderma reesei (a route for large-scale production of AgNPs), Insci. J. 1 (1) (2011) 65–79, https://doi.org/10.5640/insc.010165.
[293] N. Durán, P.D. Marcato, M. Durán, A. Yadav, A. Gade, M. Rai, Mechanistic aspects in the biogenic synthesis of extracellular metal nanoparticles by peptides, bacteria, fungi, and plants, Appl. Microbiol. Biotechnol. 90 (2011) 1609–1624, https://doi.org/10.1007/s00253-011-3249-8.
[294] A. Ingle, A. Gade, S. Pierrat, C. Sonnichsen, M. Rai, Mycosynthesis of silver nanoparticles using the fungus Fusarium acuminatum and its activity against some human pathogenic bacteria, Curr. Nanosci. 4 (2) (2008) 141–144, https://doi.org/10.2174/157341308784340804.
[295] P. Mukherjee, M. Roy, B. Mandal, G. Dey, P. Mukherjee, J. Ghatak, A. Tyagi, S. Kale, Green synthesis of highly stabilized nanocrystalline silver particles by a non-pathogenic and agriculturally important fungus T. asperellum, Nanotechnology 19 (7) (2008) 075103, https://doi.org/10.1088/0957-4484/19/7/075103.
[296] T. Sakurai, K. Kataoka, Basic and applied features of multicopper oxidases, CueO, bilirubin oxidase, and laccase, Chem. Rec. 7 (4) (2007) 220–229, https://doi.org/10.1002/tcr.20125.
[297] P. Aza, S. Camarero, Fungal laccases: fundamentals, engineering and classification update, Biomolecules 13 (12) (2023) 1716, https://doi.org/10.3390/biom13121716.
[298] M. Šebesta, H. Vojtková, V. Cyprichová, A.P. Ingle, M. Urík, M. Kolenčík, Mycosynthesis of metal-containing nanoparticles—fungal metal resistance and mechanisms of synthesis, Int. J. Mol. Sci. 23 (22) (2022) 14084, https://doi.org/10.3390/ijms232214084.
[299] A. Lateef, E.B. Gueguim-Kana, N. Dasgupta, S. Ranjan, Microbial Nanobiotechnology, Springer, 2021, https://doi.org/10.1007/978-981-33-4777-9.
[300] P.L. Kashyap, S. Kumar, A.K. Srivastava, A.K. Sharma, Myconanotechnology in agriculture: a perspective, World J. Microbiol. Biotechnol. 29 (2013) 191–207, https://doi.org/10.1007/s11274-012-1171-6.
[301] R.R. Nayak, N. Pradhan, D. Behera, K.M. Pradhan, S. Mishra, L.B. Sukla, B. K. Mishra, Green synthesis of silver nanoparticle by Penicillium purpurogenum NPMF: the process and optimization, J. Nanopart. Res. 13 (8) (2011) 3129–3137, https://doi.org/10.1007/s11051-010-0208-8.
[302] S.A. Kumar, A.A. Ansary, A. Ahmad, M. Khan, Extracellular biosynthesis of CdSe quantum dots by the fungus, Fusarium oxysporum, J. Biomed. Nanotechnol. 3 (2) (2007) 190–194, https://doi.org/10.1166/jbn.2007.027.
[303] L.S. Devi, S. Joshi, Ultrastructures of silver nanoparticles biosynthesized using endophytic fungi, J. Microsc. Ultrastruct. 3 (1) (2015) 29–37, https://doi.org/10.1016/j.jmau.2014.10.004.
[304] G. Li, D. He, Y. Qian, B. Guan, S. Gao, Y. Cui, K. Yokoyama, L. Wang, Fungus-mediated green synthesis of silver nanoparticles using Aspergillus terreus, Int. J. Mol. Sci. 13 (1) (2011) 466–476, https://doi.org/10.3390/ijms13010466.
[305] Y. San, M. Chan, M. Don, S. Selatan, Instantaneous biosynthesis of silver nanoparticles by selected macro fungi, Aust. J. Basic Appl. Sci. 6 (2012) 86–88.
[306] M. Sastry, A. Ahmad, M.I. Khan, R. Kumar, Biosynthesis of metal nanoparticles using fungi and actinomycete, Curr. Sci. (2003) 162–170.

[307] G.S. Dhillon, S.K. Brar, S. Kaur, M. Verma, Green approach for nanoparticle biosynthesis by fungi: current trends and applications, Crit. Rev. Biotechnol. 32 (1) (2012) 49–73, https://doi.org/10.3109/07388551.2010.550568.
[308] S. Machado, R. Pereira, R.M.O. Sousa, Nanobiopesticides: are they the future of phytosanitary treatments in modern agriculture? Sci. Total Environ. (2023) 166401 https://doi.org/10.1016/j.scitotenv.2023.166401.
[309] R. Bihal, J.M. Al-Khayri, A.N. Banu, N. Kudesia, F.K. Ahmed, R. Sarkar, A. Arora, K.A. Abd-Elsalam, Entomopathogenic fungi: an eco-friendly synthesis of sustainable nanoparticles and their nanopesticide properties, Microorganisms 11 (6) (2023) 1617, https://doi.org/10.3390/microorganisms11061617.
[310] A.M. Elgorban, S. Aref, S. Seham, K. Elhindi, A. Bahkali, S. Sayed, M. Manal, Extracellular synthesis of silver nanoparticles using Aspergillus versicolor and evaluation of their activity on plant pathogenic fungi, Mycosphere 7 (6) (2016) 844–852, https://doi.org/0.5943/mycosphere/7/6/15.
[311] M. Yadav, K. Behera, Y.-H. Chang, F.-C. Chiu, Cellulose nanocrystal reinforced chitosan based UV barrier composite films for sustainable packaging, Polymers 12 (1) (2020) 202, https://doi.org/10.3390/polym12010202.
[312] A. Kausar, S. Hussain, T. Javed, S. Zafar, S. Anwar, S. Hussain, N. Zahra, M. Saqib, Zinc oxide nanoparticles as potential hallmarks for enhancing drought stress tolerance in wheat seedlings, Plant Physiol. Biochem. 195 (2023) 341–350, https://doi.org/10.1016/j.plaphy.2023.01.014.
[313] H. Sonawane, D. Shelke, M. Chambhare, N. Dixit, S. Math, S. Sen, S.N. Borah, N. F. Islam, S.J. Joshi, B. Yousaf, Fungi-derived agriculturally important nanoparticles and their application in crop stress management–prospects and environmental risks, Environ. Res. 212 (2022) 113543, https://doi.org/10.1016/j.envres.2022.113543.
[314] G. Shukla, S.S. Gaurav, A. Singh, Synthesis of mycogenic zinc oxide nanoparticles and preliminary determination of its efficacy as a larvicide against white grubs (Holotrichia sp.), Int. Nano Lett. 10 (2) (2020) 131–139, https://doi.org/10.1007/s40089-020-00302-0.
[315] K. Natesan, P. Ponmurugan, B.M. Gnanamangai, V. Manigandan, S.P.J. Joy, C. Jayakumar, G. Amsaveni, Biosynthesis of silica and copper nanoparticles from Trichoderma, Streptomyces and Pseudomonas spp. evaluated against collar canker and red root-rot disease of tea plants, Arch. Phytopathol. Plant Prot. 54 (1-2) (2021) 56–85, https://doi.org/10.1080/03235408.2020.1817258.
[316] M. Guilger-Casagrande, Rd Lima, Synthesis of silver nanoparticles mediated by fungi: a review, Front. Bioeng. Biotechnol. 7 (2019) 287, https://doi.org/10.3389/fbioe.2019.00287.
[317] F. Fatima, S.R. Verma, N. Pathak, P. Bajpai, Extracellular mycosynthesis of silver nanoparticles and their microbicidal activity, J. Glob. Antimicrob. Resist. 7 (2016) 88–92, https://doi.org/10.1016/j.jgar.2016.07.013.
[318] V.F. Consolo, A. Torres-Nicolini, V.A. Alvarez, Mycosinthetized Ag, CuO and ZnO nanoparticles from a promising Trichoderma harzianum strain and their antifungal potential against important phytopathogens, Sci. Rep. 10 (1) (2020) 20499, https://doi.org/10.1038/s41598-020-77294-6.
[319] A.H. Hashem, A.M. Abdelaziz, A.A. Askar, H.M. Fouda, A.M. Khalil, K.A. Abd-Elsalam, M.M. Khaleil, Bacillus megaterium-mediated synthesis of selenium nanoparticles and their antifungal activity against Rhizoctonia solani in faba bean plants, J. Fungi 7 (3) (2021) 195, https://doi.org/10.3390/jof7030195.
[320] T.S. Santos, C. de Souza Varize, E. Sanchez-Lopez, S.A. Jain, E.B. Souto, P. Severino, Md.C. Mendonça, Entomopathogenic fungi-mediated AgNPs: synthesis and insecticidal effect against Plutella xylostella (Lepidoptera: Plutellidae), Materials 15 (21) (2022) 7596, https://doi.org/10.3390/ma15217596.
[321] S.A. Zaki, S.A. Ouf, F.M. Albarakaty, M.M. Habeb, A.A. Aly, K.A. Abd-Elsalam, Trichoderma harzianum-mediated ZnO nanoparticles: a green tool for controlling soil-borne pathogens in cotton, J. Fungi 7 (11) (2021) 952, https://doi.org/10.3390/jof7110952.
[322] S.A. Zaki, S.A. Ouf, K.A. Abd-Elsalam, A.A. Asran, M.M. Hassan, A. Kalia, F. M. Albarakaty, Trichogenic silver-based nanoparticles for suppression of fungi involved in damping-off of cotton seedlings, Microorganisms 10 (2) (2022) 344, https://doi.org/10.3390/microorganisms10020344.
[323] M. Amr, S.H. Abu-Hussien, R. Ismail, A. Aboubakr, R. Wael, M. Yasser, B. Hemdan, S.M. El-Sayed, A. Bakry, N.M. Ebeed, Utilization of biosynthesized silver nanoparticles from Agaricus bisporus extract for food safety application: synthesis, characterization, antimicrobial efficacy, and toxicological assessment, Sci. Rep. 13 (1) (2023) 15048, https://doi.org/10.1038/s41598-023-42103-3.
[324] S.M. Husseiny, T.A. Salah, H.A. Anter, Biosynthesis of size controlled silver nanoparticles by Fusarium oxysporum, their antibacterial and antitumor activities, Beni-Suef Univ. J. Basic Appl. Sci. 4 (3) (2015) 225–231, https://doi.org/10.1016/j.bjbas.2015.07.004.
[325] M. Balakumaran, R. Ramachandran, P. Kalaichelvan, Exploitation of endophytic fungus, Guignardia mangiferae for extracellular synthesis of silver nanoparticles and their in vitro biological activities, Microbiol. Res. 178 (2015) 9–17, https://doi.org/10.1016/j.micres.2015.05.009.
[326] M. Wypij, M. Rai, L.F. Zemljič, M. Bračič, S. Hribernik, P. Golińska, Pullulan-based films impregnated with silver nanoparticles from the Fusarium culmorum strain JTW1 for potential applications in the food industry and medicine, Front. Bioeng. Biotechnol. 11 (2023), https://doi.org/10.3389/fbioe.2023.1241739.
[327] R. Tripathi, R.K. Gupta, P. Singh, A.S. Bhadwal, A. Shrivastav, N. Kumar, B. Shrivastav, Ultra-sensitive detection of mercury (II) ions in water sample using gold nanoparticles synthesized by Trichoderma harzianum and their mechanistic approach, Sens. Actuators B: Chem. 204 (2014) 637–646, https://doi.org/10.1016/j.snb.2014.08.015.
[328] M.M. Abo Elsoud, E. El Kady, Current trends in fungal biosynthesis of chitin and chitosan, Bull. Natl. Res. Cent. 43 (1) (2019) 1–12, https://doi.org/10.1186/s42269-019-0105-y.
[329] Y. Araki, E. Ito, A pathway of chitosan formation in Mucor rouxii, Eur. J. Biochem. 55 (1) (1975), https://doi.org/10.1016/0006-291X(74)90657-3.
[330] T. Kaur, M. Bala, G. Kumar, A. Vyas, Biosynthesis of zinc oxide nanoparticles via endophyte Trichoderma viride and evaluation of their antimicrobial and antioxidant properties, Arch. Microbiol. 204 (10) (2022) 620, https://doi.org/10.1007/s00203-022-03218-9.
[331] A.N.M. Muzahid, Y. Araf, N.U. Mahmud, A. Sarker, F. Akter, M.T.I. Chowdhury, M.J. Shiddiky, H. Sohrawardy, M. Chakraborty, T. Islam, Potentials of mycosynthesized nanomaterials for efficient remediation of environmental contaminants. Fungal Cell Factories for Sustainable Nanomaterials Productions and Agricultural Applications, Elsevier, 2023, pp. 693–724, https://doi.org/10.1016/B978-0-323-99922-9.00015-5.
[332] N. Pariona, A.I. Mtz-Enriquez, D. Sánchez-Rangel, G. Carrión, F. Paraguay-Delgado, G. Rosas-Saito, Green-synthesized copper nanoparticles as a potential antifungal against plant pathogens, RSC Adv. 9 (33) (2019) 18835–18843, https://doi.org/10.1039/C9RA03110C.
[333] S. Hassan, Karaila G.K, P. Singh, R. Meenatchi, A.S. Venkateswaran, T. Ahmed, S. Bansal, R. Kamalraj, G.S. Kiran, J. Selvin, Implications of fungal nanotechnology for sustainable agriculture-applications and future perspectives, Biocatal. Agric. Biotechnol. (2024) 103110, https://doi.org/10.1016/j.bcab.2024.103110.
[334] V. Saisruthi, J.A. Kumar, N.T.M. Rosana, K.L.V. Joseph, S.J. Rubavathy, Bio-fabricated TiO2 nanoparticles: a comprehensive insight into its antimicrobial, anticancer, and environmental applications, Environ. Qual. Manag. 34 (2) (2024) e22359, https://doi.org/10.1002/tqem.22359.
[335] L. Nehru, G.D. Kandasamy, V. Sekar, M.A. Alshehri, C. Panneerselvam, A. Alasmari, P. Kathirvel, Green synthesis of ZnO-NPs using endophytic fungal extract of Xylaria arbuscula from Blumea axillaris and its biological applications, Artif. Cells, Nanomed., Biotechnol. 51 (1) (2023) 318–333, https://doi.org/10.1080/21691401.2023.2232654.
[336] R.P. Velamakanni, R. Gothalwal, R.S. Velamakanni, S.R. Ayinampudi, P. Vuppugalla, R. Merugu, Fungi-Mediated Green Synthesis of Nanoparticles and Their Renewable Energy Applications. Green Nano Solution for Bioenergy Production Enhancement, Springer, 2022, pp. 201–224, https://doi.org/10.1007/978-981-16-9356-4_8.
[337] P. Mathur, S. Saini, E. Paul, C. Sharma, P. Mehtani, Endophytic fungi mediated synthesis of iron nanoparticles: characterization and application in methylene blue decolorization, Curr. Res. Green. Sustain. Chem. 4 (2021) 100053, https://doi.org/10.1016/j.crgsc.2020.100053.
[338] P. Clarance, B. Luvankar, J. Sales, A. Khusro, P. Agastian, J.-C. Tack, M.M. Al Khulaifi, H.A. Al-Shwaiman, A.M. Elgorban, A. Syed, Green synthesis and characterization of gold nanoparticles using endophytic fungi Fusarium solani and its in-vitro anticancer and biomedical applications, Saudi J. Biol. Sci. 27 (2) (2020) 706–712, https://doi.org/10.1016/j.sjbs.2019.12.026.
[339] O. Gemishev, M. Panayotova, G. Gicheva, N. Mintcheva, Green synthesis of stable spherical monodisperse silver nanoparticles using a cell-free extract of Trichoderma reesei, Materials 15 (2) (2022) 481, https://doi.org/10.3390/ma15020481.
[340] M. Farzana Fathima, A. Usha Raja Nanthini, F.S. Al-Khattaf, A.A. Hatamleh, S. B. Kabir, Mycosynthesis of noble metal nanoparticle using Laetiporus versisporus mushroom and analysis of antioxidant activity, J. Nanomater. 2022 (2022), https://doi.org/10.1155/2022/8086803.
[341] S.E.-D. Hassan, A. Fouda, E. Saied, M.M. Farag, A.M. Eid, M.G. Barghoth, M. A. Awad, M.F. Hamza, M.F. Awad, Rhizopus Oryzae-mediated green synthesis of magnesium oxide nanoparticles (MgO-NPs): a promising tool for antimicrobial, mosquitocidal action, and tanning effluent treatment, J. Fungi 7 (5) (2021) 372, https://doi.org/10.3390/jof7050372.
[342] E. Saied, A.E. Mekky, A.A. Al-Askar, A.F. Hagag, A.A. El-bana, M. Ashraf, A. Walid, T. Nour, M.M. Fawzi, A.A. Arishi, Aspergillus terreus-mediated selenium nanoparticles and their antimicrobial and photocatalytic activities, Crystals 13 (3) (2023) 450, https://doi.org/10.3390/cryst13030450.
[343] K. Andrade-Zavaleta, Y. Chacon-Laiza, D. Asmat-Campos, N. Raquel-Checca, Green synthesis of superparamagnetic iron oxide nanoparticles with Eucalyptus globulus extract and their application in the removal of heavy metals from agricultural soil, Molecules 27 (4) (2022) 1367, https://doi.org/10.3390/molecules27041367.
[344] O. Długosz, J. Chwastowski, M. Banach, Hawthorn berries extract for the green synthesis of copper and silver nanoparticles, Chem. Pap. 74 (2020) 239–252, https://doi.org/10.1007/s11696-019-00873-z.
[345] G. Nandhini, R. Suriyaprabha, W. Maria Sheela Pauline, V. Rajendran, W. K. Aicher, O.K. Awitor, Influence of solvents on the changes in structure, purity, and in vitro characteristics of green-synthesized ZnO nanoparticles from Costus igneus, Appl. Nanosci. 8 (2018) 1353–1360, https://doi.org/10.1007/s13204-018-0810-0.
[346] Y. Rufai, S. Chandren, N. Basar, Influence of solvents' polarity on the physicochemical properties and photocatalytic activity of titania synthesized using deinbollia Pinnata leaves, Front. Chem. 8 (2020) 597980, https://doi.org/10.3389/fchem.2020.597980.
[347] M. Tesfaye, Y. Gonfa, G. Tadesse, T. Temesgen, S. Periyasamy, Green synthesis of silver nanoparticles using Vernonia amygdalina plant extract and its antimicrobial activities, Heliyon 9 (6) (2023), https://doi.org/10.1016/j.heliyon.2023.e17356.

[348] S.R. Chowdhury, P.S. Roy, S.K. Bhattacharya, Green synthesis and characterization of polyvinyl alcohol stabilized palladium nanoparticles: effect of solvent on diameter and catalytic activity, Adv. Nat. Sci. Nanosci. Nanotechnol. 8 (2) (2017) 025002, https://doi.org/10.1088/2043-6254/aa690e.
[349] N. Sharma, S.K. Gautam, A. Adhikari, B. Bhakta Neupane, Himalayan lichen biomass for green synthesis of silver nanocolloids: growth kinetics, effect of pH and metal sensing, R. Soc. Open Sci. 11 (3) (2024) 231633, https://doi.org/10.1098/rsos.231633.
[350] C.A. Mbachu, A.K. Babayemi, T.C. Egbosiuba, J.I. Ike, I.J. Ani, S. Mustapha, Green synthesis of iron oxide nanoparticles by Taguchi design of experiment method for effective adsorption of methylene blue and methyl orange from textile wastewater, Results Eng. 19 (2023) 101198, https://doi.org/10.1016/j.rineng.2023.101198.
[351] M. Vanin dos Santos Lima, G. Beloni de Melo, L. Gracher Teixeira, C. Grella Miranda, P.H. Hermes de Araújo, C. Sayer, R. Porto Ineu, F.V. Leimann, O. Hess Gonçalves, Green synthesis of silver nanoparticles using Ilex paraguariensis extracts: antimicrobial activity and acetilcolinesterase modulation in rat brain tissue, Green. Chem. Lett. Rev. 15 (1) (2022) 128–138, https://doi.org/10.1080/17518253.2021.2024896.
[352] N.S. Al-Radadi, Ephedra mediated green synthesis of gold nanoparticles (AuNPs) and evaluation of its antioxidant, antipyretic, anti-asthmatic, and antimicrobial properties, Arab. J. Chem. 16 (1) (2023) 104353, https://doi.org/10.1016/j.arabjc.2022.104353.
[353] N.S. Al-Radadi, Facile one-step green synthesis of gold nanoparticles (AuNp) using licorice root extract: Antimicrobial and anticancer study against HepG2 cell line, Arab. J. Chem. 14 (2) (2021) 102956, https://doi.org/10.1016/j.arabjc.2020.102956.
[354] M. Younas, M.H. Rasool, M. Khurshid, A. Khan, M.Z. Nawaz, I. Ahmad, M. N. Lakhan, Moringa oleifera leaf extract mediated green synthesis of silver nanoparticles and their antibacterial effect against selected gram-negative strains, Biochem. Syst. Ecol. 107 (2023) 104605, https://doi.org/10.1016/j.bse.2023.104605.
[355] A. Alnehia, A.-B. Al-Odayni, A. Al-Sharabi, A. Al-Hammadi, W.S. Saeed, Pomegranate peel extract-mediated green synthesis of ZnO-NPs: extract concentration-dependent structure, optical, and antibacterial activity, J. Chem. 2022 (2022) 1–11, https://doi.org/10.1155/2022/9647793.
[356] N.T.H. Nam, N.M. Dat, N.D. Hai, N.T. Dat, H. An, P.N.P. Hung, N.T. Truong, N. T. Son, M.T. Phong, N.H. Hieu, Green synthesis of silver@ graphene oxide nanocomposite for antibacterial, cytotoxicity assessment, and hydrogen peroxide electro-sensing, N. J. Chem. 47 (17) (2023) 8090–8101, https://doi.org/10.1039/D3NJ00618B.
[357] S. Seshadri, K. Saranya, M. Kowshik, Green synthesis of lead sulfide nanoparticles by the lead resistant marine yeast, Rhodosporidium diobovatum, Biotechnol. Prog. 27 (5) (2011), https://doi.org/10.1002/btpr.651.
[358] S.C. Kumari, P.N. Padma, A facile, green approach for enhanced synthesis of silver nanoparticles by Weissella confusa produced dextran, 2020.
[359] V. Mihailović, N. Srećković, Z.P. Nedić, S. Dimitrijević, M. Matić, A. Obradović, D. Selaković, G. Rosić, J.S. Katanić Stanković, Green synthesis of silver nanoparticles using Salvia verticillata and Filipendula ulmaria extracts: optimization of synthesis, biological activities, and catalytic properties, Molecules 28 (2) (2023) 808, https://doi.org/10.3390/molecules28020808.
[360] S. Bhullar, N. Goyal, S. Gupta, A recipe for optimizing TiO2 nanoparticles for drug delivery applications, OpenNano 8 (2022) 100096, https://doi.org/10.1016/j.onano.2022.100096.
[361] M. Alavi, N. Karimi, I. Salimikia, Phytosynthesis of zinc oxide nanoparticles and its antibacterial, antiquorum sensing, antimotility, and antioxidant capacities against multidrug resistant bacteria, J. Ind. Eng. Chem. 72 (2019) 457–473, https://doi.org/10.1016/j.jiec.2019.01.002.
[362] S. Chouhan, S. Guleria, Green synthesis of AgNPs using Cannabis sativa leaf extract: Characterization, antibacterial, anti-yeast and α-amylase inhibitory activity, Mater. Sci. Energy Technol. 3 (2020) 536–544, https://doi.org/10.1016/j.mset.2020.05.004.
[363] G. Arya, R.M. Kumari, N. Sharma, N. Gupta, A. Kumar, S. Chatterjee, S. Nimesh, Catalytic, antibacterial and antibiofilm efficacy of biosynthesised silver nanoparticles using Prosopis juliflora leaf extract along with their wound healing potential, J. Photochem. Photobiol. B Biol. 190 (2019) 50–58, https://doi.org/10.1016/j.jphotobiol.2018.11.005.
[364] Y.H. Gonfa, A.A. Gelagle, B. Hailegnaw, S.A. Kabeto, G.A. Workeneh, F. B. Tessema, M.G. Tadesse, S.M. Wabaidur, K.A. Dahlous, S. Abou Fayssal, Optimization, characterization, and biological applications of silver nanoparticles synthesized using essential oil of aerial part of Laggera tomentosa, Sustainability 15 (1) (2023) 797, https://doi.org/10.3390/su15010797.
[365] K. Prasad, A.K. Jha, Biosynthesis of CdS nanoparticles: an improved green and rapid procedure, J. Colloid Interface Sci. 342 (1) (2010) 68–72, https://doi.org/10.1016/j.jcis.2009.10.003.
[366] K. Zomorodian, S. Pourshahid, A. Sadatsharifi, P. Mehryar, K. Pakshir, M. J. Rahimi, A. Arabi Monfared, Biosynthesis and characterization of silver nanoparticles by Aspergillus species, BioMed. Res. Int. 2016 (2016), https://doi.org/10.1155/2016/5435397.
[367] M. Baymiller, F. Huang, S. Rogelj, Rapid one-step synthesis of gold nanoparticles using the ubiquitous coenzyme NADH, Matters (2017), https://doi.org/10.19185/matters.201705000007.
[368] Y. Nangia, N. Wangoo, N. Goyal, G. Shekhawat, C.R. Suri, A novel bacterial isolate Stenotrophomonas maltophilia as living factory for synthesis of gold nanoparticles, Microb. Cell Factor. 8 (2009) 1–7, https://doi.org/10.1186/1475-2859-8-39.
[369] S. Jain, M.S. Mehata, Medicinal plant leaf extract and pure flavonoid mediated green synthesis of silver nanoparticles and their enhanced antibacterial property, Sci. Rep. 7 (1) (2017) 15867, https://doi.org/10.1038/s41598-017-15724-8.
[370] U. Habeeba, N. Raghavendra, Green synthesis and antioxidant potency of silver nanoparticles using arecanut seed extract, Nano-Struct. Nano-Objects 38 (2024) 101118, https://doi.org/10.1016/j.nanoso.2024.101118.
[371] X. Maimaiti, A.P. Bassey, X. Liu, Y. Zhu, L. Fan, N. Rahman, R. Luo, F. Wang, Y. Wang, Green synthesis of silver nanoparticles using Houttuynia cordata Thunb rhizome extracts and their antibacterial potential against common foodborne pathogens, Int. J. Food Sci. Technol. (2024), https://doi.org/10.1111/ijfs.17074.
[372] Q. Ni, T. Zhu, W. Wang, D. Guo, Y. Li, T. Chen, X. Zhang, Green synthesis of narrow-size silver nanoparticles using Ginkgo biloba leaves: condition optimization, characterization, and antibacterial and cytotoxic activities, Int. J. Mol. Sci. 25 (3) (2024) 1913, https://doi.org/10.3390/ijms25031913.
[373] F.M. Mohammadi, N. Ghasemi, Influence of temperature and concentration on biosynthesis and characterization of zinc oxide nanoparticles using cherry extract, J. Nanostruct. Chem. 8 (1) (2018) 93–102, https://doi.org/10.1007/s40097-018-0257-6.
[374] M.I. Khan, M.N. Akhtar, N. Ashraf, J. Najeeb, H. Munir, T.I. Awan, M.B. Tahir, M. R. Kabli, Green synthesis of magnesium oxide nanoparticles using Dalbergia sissoo extract for photocatalytic activity and antibacterial efficacy, Appl. Nanosci. 10 (2020) 2351–2364, https://doi.org/10.1007/s13204-020-01414-x.
[375] P. Phanjom, G. Ahmed, Effect of different physicochemical conditions on the synthesis of silver nanoparticles using fungal cell filtrate of Aspergillus oryzae (MTCC No. 1846) and their antibacterial effect, Adv. Nat. Sci. Nanosci. Nanotechnol. 8 (4) (2017) 045016, https://doi.org/10.1088/2043-6254/aa92bc.
[376] A. Shahzad, H. Saeed, M. Iqtedar, S.Z. Hussain, A. Kaleem, R. Abdullah, S. Sharif, S. Naz, F. Saleem, A. Aihetasham, Size-controlled production of silver nanoparticles by Aspergillus fumigatus BTCB10: likely antibacterial and cytotoxic effects, J. Nanomater. 2019 (2019), https://doi.org/10.1155/2019/5168698.
[377] N.P. Shetti, S.J. Malode, D.S. Nayak, G.B. Bagihalli, S.S. Kalanur, R.S. Malladi, C. V. Reddy, T.M. Aminabhavi, K.R. Reddy, Fabrication of ZnO nanoparticles modified sensor for electrochemical oxidation of methdilazine, Appl. Surf. Sci. 496 (2019) 143656, https://doi.org/10.1016/j.apsusc.2019.143656.
[378] M.S. Jameel, A.A. Aziz, M.A. Dheyab, Green synthesis: proposed mechanism and factors influencing the synthesis of platinum nanoparticles, Green. Process. Synth. 9 (1) (2020) 386–398, https://doi.org/10.1515/gps-2020-0041.
[379] N. Karim, N. Rubinsin, M. Burukan, S. Kamarudin, Sustainable route of synthesis platinum nanoparticles using orange peel extract, Int. J. Green. Energy 16 (15) (2019) 1518–1526, https://doi.org/10.1080/15435075.2019.1671422.
[380] J. Jeevanandam, Y.S. Chan, M.K. Danquah, Cytotoxicity and insulin resistance reversal ability of biofunctional phytosynthesized MgO nanoparticles, 3 Biotech 10 (11) (2020) 489, https://doi.org/10.1007/s13205-020-02480-2.
[381] T.U.D. Thi, T.T. Nguyen, Y.D. Thi, K.H.T. Thi, B.T. Phan, K.N. Pham, Green synthesis of ZnO nanoparticles using orange fruit peel extract for antibacterial activities, RSC Adv. 10 (40) (2020) 23899–23907, https://doi.org/10.1039/D0RA04926C.
[382] B. Gherbi, S.E. Laouini, S. Meneceur, A. Bouafia, H. Hemmami, M.L. Tedjani, G. Thiripuranathar, A. Barhoum, F. Menaa, Effect of pH value on the bandgap energy and particles size for biosynthesis of ZnO nanoparticles: efficiency for photocatalytic adsorption of methyl orange, Sustainability 14 (18) (2022) 11300, https://doi.org/10.3390/su141811300.
[383] V. Manikandan, P. Jayanthi, A. Priyadharsan, E. Vijayaprathap, P. Anbarasan, P. Velmurugan, Green synthesis of pH-responsive Al2O3 nanoparticles: application to rapid removal of nitrate ions with enhanced antibacterial activity, J. Photochem. Photobiol. A: Chem. 371 (2019) 205–215, https://doi.org/10.1016/j.jphotochem.2018.11.009.
[384] A. Kaler, S. Jain, U.C. Banerjee, Green and rapid synthesis of anticancerous silver nanoparticles by Saccharomyces boulardii and insight into mechanism of nanoparticle synthesis, BioMed. Res. Int. 2013 (2013), https://doi.org/10.1155/2013/872940.
[385] E. Priyadarshini, N. Pradhan, L.B. Sukla, P.K. Panda, Controlled synthesis of gold nanoparticles using Aspergillus terreus IF0 and its antibacterial potential against Gram negative pathogenic bacteria, J. Nanotechnol. 2014 (2014) 1–9, https://doi.org/10.1155/2014/653198.
[386] S. Nouren, I. Bibi, A. Kausar, M. Sultan, H.N. Bhatti, Y. Safa, S. Sadaf, N. Alwadai, M. Iqbal, Green synthesis of CuO nanoparticles using Jasmin sambac extract: conditions optimization and photocatalytic degradation of Methylene Blue dye, J. King Saud. Univ. -Sci. 36 (3) (2024) 103089, https://doi.org/10.1016/j.jksus.2024.103089.
[387] M. Hamk, F.A. Akçay, A. Avcı, Green synthesis of zinc oxide nanoparticles using Bacillus subtilis ZBP4 and their antibacterial potential against foodborne pathogens, Prep. Biochem. Biotechnol. 53 (3) (2023) 255–264, https://doi.org/10.1080/10826068.2022.2076243.
[388] M. Darroudi, M.B. Ahmad, R. Zamiri, A.K. Zak, A.H. Abdullah, N.A. Ibrahim, Time-dependent effect in green synthesis of silver nanoparticles, Int. J. Nanomed. (2011) 677–681, https://doi.org/10.2147/IJN.S17669.
[389] N. Manosalva, G. Tortella, M. Cristina Diez, H. Schalchli, A.B. Seabra, N. Durán, O. Rubilar, Green synthesis of silver nanoparticles: effect of synthesis reaction parameters on antimicrobial activity, World J. Microbiol. Biotechnol. 35 (2019) 1–9, https://doi.org/10.1007/s11274-019-2664-3.
[390] V. Karade, T. Dongale, S.C. Sahoo, P. Kollu, A. Chougale, P. Patil, P. Patil, Effect of reaction time on structural and magnetic properties of green-synthesized magnetic nanoparticles, J. Phys. Chem. Solids 120 (2018) 161–166, https://doi.org/10.1016/j.jpcs.2018.04.040.

[391] Z. Ren, H. Li, J. Li, J. Cai, L. Zhong, Y. Ma, Y. Pang, Green synthesis of reduced graphene oxide/chitosan/gold nanoparticles composites and their catalytic activity for reduction of 4-nitrophenol, Int. J. Biol. Macromol. 229 (2023) 732–745, https://doi.org/10.1016/j.ijbiomac.2022.12.282.
[392] D. Philip, C. Unni, S.A. Aromal, V. Vidhu, Murraya koenigii leaf-assisted rapid green synthesis of silver and gold nanoparticles, Spectrochim. Acta Part A: Mol. Biomol. Spectrosc. 78 (2) (2011) 899–904, https://doi.org/10.1016/j.saa.2010.12.060.
[393] D. Philip, Rapid green synthesis of spherical gold nanoparticles using Mangifera indica leaf, Spectrochim. Acta Part A: Mol. Biomol. Spectrosc. 77 (4) (2010) 807–810, https://doi.org/10.1016/j.saa.2010.08.008.
[394] B. Mohapatra, S. Kuriakose, S. Mohapatra, Rapid green synthesis of silver nanoparticles and nanorods using Piper nigrum extract, J. Alloy. Compd. 637 (2015) 119–126, https://doi.org/10.1016/j.jallcom.2015.02.206.
[395] S. Basu, P. Maji, J. Ganguly, Rapid green synthesis of silver nanoparticles by aqueous extract of seeds of Nyctanthes arbor-tristis, Appl. Nanosci. 6 (2016) 1–5, https://doi.org/10.1007/s13204-015-0407-9.
[396] S. Sadhasivam, V. Vinayagam, M. Balasubramaniyan, Recent advancement in biogenic synthesis of iron nanoparticles, J. Mol. Struct. 1217 (2020) 128372, https://doi.org/10.1016/j.molstruc.2020.128372.
[397] N. Korkmaz, Y. Ceylan, A. Hamid, A. Karadağ, A.S. Bülbül, M.N. Aftab, Ö. Çevik, F. Şen, Biogenic silver nanoparticles synthesized via Mimusops elengi fruit extract, a study on antibiofilm, antibacterial, and anticancer activities, J. Drug Deliv. Sci. Technol. 59 (2020) 101864, https://doi.org/10.1016/j.jddst.2020.101864.
[398] E. Sreelekha, B. George, A. Shyam, N. Sajina, B. Mathew, A comparative study on the synthesis, characterization, and antioxidant activity of green and chemically synthesized silver nanoparticles, BioNanoScience 11 (2021) 489–496, https://doi.org/10.1007/s12668-021-00824-7.
[399] H. Zhang, S. Chen, X. Jia, Y. Huang, R. Ji, L. Zhao, Comparation of the phytotoxicity between chemically and green synthesized silver nanoparticles, Sci. Total Environ. 752 (2021) 142264, https://doi.org/10.1016/j.scitotenv.2020.142264.
[400] F. Abdullah, N.A. Bakar, M.A. Bakar, Comparative study of chemically synthesized and low temperature bio-inspired Musa acuminata peel extract mediated zinc oxide nanoparticles for enhanced visible-photocatalytic degradation of organic contaminants in wastewater treatment, J. Hazard. Mater. 406 (2021) 124779, https://doi.org/10.1016/j.jhazmat.2020.124779.
[401] T.S. Aldeen, H.E.A. Mohamed, M. Maaza, ZnO nanoparticles prepared via a green synthesis approach: physical properties, photocatalytic and antibacterial activity, J. Phys. Chem. Solids 160 (2022) 110313, https://doi.org/10.1016/j.jpcs.2021.110313.
[402] M. Aravind, M. Amalanathan, M.S.M. Mary, Synthesis of TiO 2 nanoparticles by chemical and green synthesis methods and their multifaceted properties, SN Appl. Sci. 3 (2021) 1–10, https://doi.org/10.1007/s42452-021-04281-5.
[403] M. Dusinska, J. Tulinska, N. El Yamani, M. Kuricova, A. Liskova, E. Rollerova, E. Rundén-Pran, B. Smolkova, Immunotoxicity, genotoxicity and epigenetic toxicity of nanomaterials: new strategies for toxicity testing? Food Chem. Toxicol. 109 (2017) 797–811, https://doi.org/10.1016/j.fct.2017.08.030.
[404] R.P. Pandey, J. Vidic, R. Mukherjee, C.-M. Chang, Experimental methods for the biological evaluation of nanoparticle-based drug delivery risks, Pharmaceutics 15 (2) (2023) 612, https://doi.org/10.3390/pharmaceutics15020612.
[405] V. Kumar, N. Sharma, S. Maitra, In vitro and in vivo toxicity assessment of nanoparticles, Int. Nano Lett. 7 (4) (2017) 243–256, https://doi.org/10.1007/s40089-017-0221-3.
[406] M. Gharbavi, M. Mousavi, M. Pour-Karim, M. Tavakolizadeh, A. Sharafi, Biogenic and facile synthesis of selenium nanoparticles using Vaccinium arctostaphylos L. fruit extract and anticancer activity against in vitro model of breast cancer, Cell Biol. Int. 46 (10) (2022) 1612–1624, https://doi.org/10.1002/cbin.11852.
[407] I.S. Tamanna, R. Gayathri, K. Sankaran, V.P. Veeraraghavan, A.P. Francis, Eco-friendly synthesis of selenium nanoparticles using orthosiphon stamineus leaf extract and its biocompatibility studies, BioNanoScience 14 (1) (2024) 37–44, https://doi.org/10.1007/s12668-023-01277-w.
[408] S. Anjum, K. Nawaz, B. Ahmad, C. Hano, B.H. Abbasi, Green synthesis of biocompatible core–shell (Au–Ag) and hybrid (Au–ZnO and Ag–ZnO) bimetallic nanoparticles and evaluation of their potential antibacterial, antidiabetic, antiglycation and anticancer activities, RSC Adv. 12 (37) (2022) 23845–23859, https://doi.org/10.1039/D2RA03196E.
[409] S. Khare, R.K. Singh, O. Prakash, Green synthesis, characterization and biocompatibility evaluation of silver nanoparticles using radish seeds, Results Chem. 4 (2022) 100447, https://doi.org/10.1016/j.rechem.2022.100447.
[410] K.M. Mahmud, M.M. Hossain, S.A. Polash, M. Takikawa, M.S. Shakil, M.F. Uddin, M. Alam, M.M. Ali Khan Shawan, T. Saha, S. Takeoka, Investigation of antimicrobial activity and biocompatibility of biogenic silver nanoparticles synthesized using Syzigyum cymosum Extract, ACS Omega 7 (31) (2022) 27216–27229, https://doi.org/10.1021/acsomega.2c01922.
[411] M.J.H. Dowlath, S.A. Musthafa, S.M. Khalith, S. Varjani, S.K. Karuppannan, G. M. Ramanujam, A.M. Arunachalam, K.D. Arunachalam, M. Chandrasekaran, S. W. Chang, Comparison of characteristics and biocompatibility of green synthesized iron oxide nanoparticles with chemical synthesized nanoparticles, Environ. Res. 201 (2021) 111585, https://doi.org/10.1016/j.envres.2021.111585.
[412] C. López-Badillo, M. Hernández-González, F. Hernández-Centeno, I. Olivas-Armendáriz, C. Rodríguez-González, E. Múzquiz-Ramos, J. López-Cuevas, H. López-De la Peña, Antibacterial activity and in vitro cytotoxicity studies of Ag-doped CaO nanoparticles, Mater. Lett. 283 (2021) 128741, https://doi.org/10.1016/j.matlet.2020.128741.
[413] H.M. Abdelmigid, N.A. Hussien, A.A. Alyamani, M.M. Morsi, N.M. AlSufyani, H. A. Kadi, Green synthesis of zinc oxide nanoparticles using pomegranate fruit peel and solid coffee grounds vs. chemical method of synthesis, with their biocompatibility and antibacterial properties investigation, Molecules 27 (4) (2022) 1236, https://doi.org/10.3390/molecules27041236.
[414] K.E. Ibrahim, M.G. Al-Mutary, A.O. Bakhiet, H.A. Khan, Histopathology of the liver, kidney, and spleen of mice exposed to gold nanoparticles, Molecules 23 (8) (2018) 1848, https://doi.org/10.3390/molecules23081848.
[415] A. Sani, C. Cao, D. Cui, Toxicity of gold nanoparticles (AuNPs): a review, Biochem. Biophys. Rep. 26 (2021) 100991, https://doi.org/10.1016/j.bbrep.2021.100991.
[416] D. Veeragoni, S. Deshpande, H.K. Rachamalla, A. Ande, S. Misra, S.R. Mutheneni, In vitro and in vivo anticancer and genotoxicity profiles of green synthesized and chemically synthesized silver nanoparticles, ACS Appl. Bio Mater. 5 (5) (2022) 2324–2339, https://doi.org/10.1021/acsabm.2c00149.
[417] F.S. Aljohani, M.T. Hamed, B.A. Bakr, Y.H. Shahin, M.M. Abu-Serie, A.K. Awaad, H. El-Kady, B.H. Elwakil, In vivo bio-distribution and acute toxicity evaluation of greenly synthesized ultra-small gold nanoparticles with different biological activities, Sci. Rep. 12 (1) (2022) 6269, https://doi.org/10.1038/s41598-022-10251-7.
[418] F. Raoof, A. Munawar, M. Ahmad, S.F.A. Rizvi, Z. Ali, A.B. Shahid, Multifunctional iron oxide nanocarriers synthesis for drug delivery, diagnostic imaging, and biodistribution study, Appl. Biochem. Biotechnol. 195 (7) (2023) 4469–4484, https://doi.org/10.1007/s12010-023-04345-9.
[419] R.K. Vasappa, D.S. Mohan, S. Mutalik, M.B. Krishnaswamy, A.K.H. Srinivasalu, M. Suryanarayana, V.S. Muddappa, In vivo toxicity and biodistribution of intravenously administered antibiotic-functionalized gold nanoparticles, Gold. Bull. 56 (4) (2023) 209–220, https://doi.org/10.1007/s13404-024-00343-9.
[420] T. Asefa, Z. Tao, Biocompatibility of mesoporous silica nanoparticles, Chem. Res. Toxicol. 25 (11) (2012) 2265–2284, https://doi.org/10.1021/tx300166u.
[421] S.K. Misra, H.-H. Chang, P. Mukherjee, S. Tiwari, A. Ohoka, D. Pan, Regulating biocompatibility of carbon spheres via defined nanoscale chemistry and a careful selection of surface functionalities, Sci. Rep. 5 (1) (2015) 14986, https://doi.org/10.1038/srep14986.
[422] T.R. Kyriakides, A. Raj, T.H. Tseng, H. Xiao, R. Nguyen, F.S. Mohammed, S. Halder, M. Xu, M.J. Wu, S. Bao, Biocompatibility of nanomaterials and their immunological properties, Biomed. Mater. 16 (4) (2021) 042005, https://doi.org/10.1088/1748-605X/abe5fa.
[423] H.-M.D. Wang, P. Thakur, A. Thakur, Biocompatibility, bio-clearance, and toxicology. Integrated Nanomaterials and Their Applications, Springer, 2023, pp. 201–221, https://doi.org/10.1007/978-981-99-6105-4_10.
[424] P. Li, X.J. Gao, X. Gao, Theoretical Investigation on the Oxidoreductase-Mimicking Activity of Carbon-Based Nanozyme. Nanozymes: Design, Synthesis, and Applications, ACS Publications, 2022, pp. 67–89, https://doi.org/10.1021/bk-2022-1422.ch003.
[425] Z. Yue, X. Zhang, Q. Yu, L. Liu, X. Zhou, Cytochrome P450-dependent reactive oxygen species (ROS) production contributes to Mn 3O 4 nanoparticle-caused liver injury, RSC Adv. 8 (65) (2018) 37307–37314, https://doi.org/10.1039/C8RA05633A.
[426] S. Alarifi, D. Ali, S. Alkahtani, Oxidative stress-induced DNA damage by manganese dioxide nanoparticles in human neuronal cells, BioMed. Res. Int. 2017 (1) (2017) 5478790, https://doi.org/10.1155/2017/5478790.
[427] X. Jiang, P. Gray, M. Patel, J. Zheng, J.-J. Yin, Crossover between anti-and pro-oxidant activities of different manganese oxide nanoparticles and their biological implications, J. Mater. Chem. B 8 (6) (2020) 1191–1201, https://doi.org/10.1039/C9TB02524C.
[428] S.E. Cornwell, S.O. Okocha, E. Ferrari, Multivariate analysis of protein–nanoparticle binding data reveals a selective effect of nanoparticle material on the formation of soft corona, Nanomaterials 13 (21) (2023) 2901, https://doi.org/10.3390/nano13212901.
[429] F. Fu, D. Crespy, K. Landfester, S. Jiang, In situ characterization techniques of protein corona around nanomaterials, Chem. Soc. Rev. (2024), https://doi.org/10.1039/D4CS00507D.
[430] E. Rahimi, A. Imani, D. Kim, M. Rahimi, L. Fedrizzi, A. Mol, E. Asselin, S. Pané, M. Lekka, Physicochemical changes of apoferritin protein during biodegradation of magnetic metal oxide nanoparticles, ACS Appl. Mater. Interfaces 16 (39) (2024) 53299–53310, https://doi.org/10.1021/acsami.4c12269.
[431] S. Lopatko, V. Chayka, The main ways for metal nanoparticles degradation, Sci. J. 'Biol. Syst.: Theory Innov. /Biolog. Sist.: Teor. Ìnnov. 13 (2022), https://doi.org/10.31548/biologiya13(3-4).2022.061.
[432] J.K. Pandey, P. Bobde, R.K. Patel, S. Manna, Disposal and Recycling Strategies for Nano-engineered Materials, Elsevier, 2023.
[433] H.R. El-Seedi, M.S. Omara, A.H. Omar, M.M. Elakshar, Y.M. Shoukhba, H. Duman, S. Karav, A.K. Rashwan, A.H. El-Seedi, H.A. Altaleb, Updated review of metal nanoparticles fabricated by green chemistry using natural extracts: biosynthesis, mechanisms, and applications, Bioengineering 11 (11) (2024) 1095, https://doi.org/10.3390/bioengineering11111095.
[434] J. Jeyaraj, V. Baskaralingam, T. Stalin, I. Muthuvel, Mechanistic vision on polypropylene microplastics degradation by solar radiation using TiO2 nanoparticle as photocatalyst, Environ. Res. 233 (2023) 116366, https://doi.org/10.1016/j.envres.2023.116366.
[435] A. Sanli, C. Elibol, A. Aydınoğlu, Biocompatibility of polymers. Handbook of Polymers in Medicine, Elsevier, 2023, pp. 87–142.

[436] M.N. Javed, S.A.K. Bangash, M. Abbas, S. Ahmed, A. Kaplan, S. Iqbal, S. Wahab, Potential and challenges in green synthesis of nanoparticles: a review, Xi' Shiyou Daxue Xuebao (Ziran Kexue Ban.)/J. Xi' Shiyou Univ. 19 (2023) 1155–1165.
[437] S. Ying, Z. Guan, P.C. Ofoegbu, P. Clubb, C. Rico, F. He, J. Hong, Green synthesis of nanoparticles: current developments and limitations, Environ. Technol. Innov. 26 (2022) 102336, https://doi.org/10.1016/j.eti.2022.102336.
[438] K. Yu, B. Chai, T. Zhuo, Q. Tang, X. Gao, J. Wang, L. He, X. Lei, B. Chen, Hydrostatic pressure drives microbe-mediated biodegradation of microplastics in surface sediments of deep reservoirs: novel findings from hydrostatic pressure simulation experiments, Water Res. 242 (2023) 120185, https://doi.org/10.1016/j.watres.2023.120185.
[439] D.A. Patiño-Ruiz, S.I. Meramo-Hurtado, An.D. González-Delgado, A. Herrera, Environmental sustainability evaluation of iron oxide nanoparticles synthesized via green synthesis and the coprecipitation method: a comparative life cycle assessment study, ACS Omega 6 (19) (2021) 12410–12423. ⟨https://doi.org/10.1021/acsomega.0c05246⟩.
[440] K.B. Narayanan, N. Sakthivel, Biological synthesis of metal nanoparticles by microbes, Adv. Colloid Interface Sci. 156 (1-2) (2010) 1–13, https://doi.org/10.1016/j.cis.2010.02.001.
[441] A.G. Atanasov, S.B. Zotchev, V.M. Dirsch, C.T. Supuran, Natural products in drug discovery: advances and opportunities, Nat. Rev. Drug Discov. 20 (3) (2021) 200–216, https://doi.org/10.1038/s41573-020-00114-z.
[442] N. Baig, I. Kammakakam, W. Falath, Nanomaterials: a review of synthesis methods, properties, recent progress, and challenges, Mater. Adv. 2 (6) (2021) 1821–1871, https://doi.org/10.1039/D0MA00807A.
[443] L.X. Yip, J. Wang, Y. Xue, K. Xing, C. Sevencan, K. Ariga, D.T. Leong, Cell-derived nanomaterials for biomedical applications, Sci. Technol. Adv. Mater. (just-accepted) (2024) 2315013, https://doi.org/10.1080/14686996.2024.2315013.
[444] F. Xu, Y. Li, X. Zhao, G. Liu, B. Pang, N. Liao, H. Li, J. Shi, Diversity of fungus-mediated synthesis of gold nanoparticles: properties, mechanisms, challenges, and solving methods, Crit. Rev. Biotechnol. (2023) 1–17, https://doi.org/10.1080/07388551.2023.2225131.
[445] S.A. Yadav, G. Suvathika, M.A. Alghuthaymi, K.A. Abd-Elsalam, Fungal-derived nanoparticles for the control of plant pathogens and pests, Fungal Cell Factor. Sustain. Nanomater. Prod. Agric. Appl. (2023) 755–784, https://doi.org/10.1016/B978-0-323-99922-9.00009-X.
[446] A. Bubyrev, A. Tsarkova, Z. Kaskova, Optimization of fungal luciferin synthesis, Russ. J. Bioorg. Chem. 45 (2019) 183–185, https://doi.org/10.1134/S106816201902002X.
[447] L.E. Walls, J.L. Martinez, E.A. del Rio Chanona, L. Rios-Solis, Definitive screening accelerates Taxol biosynthetic pathway optimization and scale up in Saccharomyces cerevisiae cell factories, Biotechnol. J. 17 (1) (2022) 2100414, https://doi.org/10.1002/biot.202100414.
[448] F. Cao, M.-K. Zhang, X. Yang, C.-X. Xu, J.-T. Cheng, Q.-W. Zhao, R. Wu, R. Sheng, X.-M. Mao, A target and efficient synthetic strategy for structural and bioactivity optimization of a fungal natural product, Eur. J. Med. Chem. 229 (2022) 114067, https://doi.org/10.1016/j.ejmech.2021.114067.